

**DOCTORAL THESIS**

# The Permeability of Mitochondrial Outer Membrane and Metabolic Plasticity in Colorectal Cancer

Laura Truu

TALLINN UNIVERSITY OF TECHNOLOGY  
DOCTORAL THESIS  
19/2024

# **The Permeability of Mitochondrial Outer Membrane and Metabolic Plasticity in Colorectal Cancer**

LAURA TRUU



TALLINN UNIVERSITY OF TECHNOLOGY  
School of Science  
Department of Chemistry and Biotechnology

National Institute Of Chemical Physics And Biophysics  
Laboratory of Chemical Biology

This dissertation was accepted for the defence of the degree of Doctor of Philosophy in Gene Technology on 05/04/2024

**Supervisor:** Tuuli Käämbre, PhD  
Laboratory of Chemical Biology  
National Institute of Chemical Physics and Biophysics  
Tallinn, Estonia

**Opponents:** Mari Nygård, MD, PhD  
Cancer Registry of Norway  
National Institute of Public Health  
Oslo, Norway

Ago Rincken, PhD  
Chair of Bioorganic Chemistry, Institute of Chemistry  
University of Tartu  
Tartu, Estonia

**Defence of the thesis:** 21/05/2024, Tallinn

**Declaration:**

Hereby I declare that this doctoral thesis, my original investigation and achievement, submitted for the doctoral degree at Tallinn University of Technology has not been submitted for doctoral or equivalent academic degree.

Laura Truu

-----  
signature



European Union  
European Regional  
Development Fund



Investing  
in your future

Copyright: Laura Truu, 2024  
ISSN 2585-6898 (publication)  
ISBN 978-9916-80-134-5 (publication)  
ISSN 2585-6901 (PDF)  
ISBN 978-9916-80-135-2 (PDF)  
DOI <https://doi.org/10.23658/taltech.19/2024>  
Printed by Koopia Niini & Rauam

Truu, L. (2024). *The Permeability of Mitochondrial Outer Membrane and Metabolic Plasticity in Colorectal Cancer* [TalTech Press]. <https://doi.org/10.23658/taltech.19/2024>

TALLINNA TEHNIKAÜLIKOOL  
DOKTORITÖÖ  
19/2024

# Mitokondrite välismembraani läbitavus ja metaboolne plastilisus käärsoolevähis

LAURA TRUU





# Contents

List of publications .....	7
Author's contribution to the publications .....	8
Introduction .....	9
Abbreviations .....	10
1. Review of literature .....	11
1.1. The definition and etiology of colon polyps and colorectal cancer .....	11
1.2. The incidence and survival of colorectal cancer worldwide and in Estonia .....	11
1.3. Prognosis and treatment.....	12
1.4. Metabolic plasticity of cancer cells .....	13
1.5. Glycolysis and Warburg effect in cancer cells .....	13
1.6. The role of MOM in metabolic reprogramming.....	14
1.7. Michaelis-Menten kinetics as the classical and simple method for investigating the permeability of the mitochondrial outer membrane.....	15
1.8. Energy transfer pathways .....	17
1.9. The role of free tubulin isotypes in the metabolic regulation of cancer .....	18
1.10. The complex regulation of the mitochondrial outer membrane.....	19
2. Materials and methods.....	21
3. Results and discussion .....	22
3.1. ADP-regulated mitochondrial respiration in human colorectal cancer (Publication I) .....	22
3.2. The heterogeneity of colon tissue (Publication I).....	23
3.3. Mitochondrial $V_{max}$ as a biomarker for cancer aggressiveness (Publication I) .....	24
3.4. Mitochondrial Respiration in CRC and Polyps: ADP Regulation and <i>KRAS/BRAF</i> Mutation (Publication III).....	25
3.5. The low oxidative capacity of mitochondria in colon lesions (Publication III).....	27
3.6. Effect of CRC location (Publication III) .....	28
3.7. Overview of sample types exhibiting diverse $K_m$ values (Publications I, II and III) ...	29
3.8. The potential role of $\beta$ II-tubulin in aerobic glycolysis (Publication II).....	29
Conclusions .....	35
List of figures .....	36
List of tables .....	37
References .....	38
Acknowledgements.....	46

Abstract.....	47
Lühikokkuvõte.....	49
Appendix 1 .....	51
Appendix 2 .....	69
Appendix 3 .....	87
<i>Curriculum vitae</i> .....	103
Elulookirjeldus.....	106

## List of publications

- I Koit, A., I. Shevchuk, L. Ounpuu, A. Klepinin, V. Chekulayev, N. Timohhina, K. Tepp, M. Puurand, **L. Truu**, K. Heck, V. Valvere, R. Guzun and T. Kaambre (2017). "Mitochondrial Respiration in Human Colorectal and Breast Cancer Clinical Material Is Regulated Differently." *Oxid Med Cell Longev* 2017: 1372640.
- II Klepinin, A., L. Ounpuu, K. Mado, **L. Truu**, V. Chekulayev, M. Puurand, I. Shevchuk, K. Tepp, A. Planken and T. Kaambre (2018). "The complexity of mitochondrial outer membrane permeability and VDAC regulation by associated proteins." *J Bioenerg Biomembr* 50(5): 339-354.
- III E. Rebane-Klemm\*, **L. Truu\***, L. Reinsalu, M. Puurand, I. Shevchuk, V. Chekulayev, N. Timohhina, K. Tepp, J. Bogovskaja, V. Afanasjev, K. Suurmaa, V. Valvere and T. Kaambre (2020). "Mitochondrial Respiration in KRAS and BRAF Mutated Colorectal Tumors and Polyps." *Cancers (Basel)* 12(4).

\* equal contribution



## **Author's contribution to the publications**

- I The author processed human clinical materials, participated in conducting high-resolution respirometry studies, and in the process of writing the original draft of the manuscript.
- II The author processed cell culture samples and participated in conducting high-resolution respirometry and immunofluorescence studies, as well as in analysing data.
- III The author conceptualized the experiment, performed formal analysis and investigation, developed the methodology, composed the original draft, and reviewed the final manuscript.

## Introduction

In this doctoral thesis, we delve into metabolic reprogramming in colorectal cancer (CRC). This field has garnered increasing attention due to its potential impact on cancer prognosis and treatment strategies. The choice to investigate this area stems from the rising prevalence and mortality rates associated with CRC, alongside the urgent need to understand its underlying molecular mechanisms.

The thesis mainly utilizes high-resolution respirometry, immunofluorescence, western blot, mutation analysis, and a comprehensive review of current literature and clinical data. The critical aspect of the methodology is the use of high-resolution respirometry to analyse the role of oxidative phosphorylation (OXPHOS) in adenosine triphosphate (ATP) synthesis in the studied samples. By evaluating the ADP-dependent respiration rate in permeabilized tissue samples, we can ascertain two crucial parameters of OXPHOS: the maximal exogenous ADP-activated respiration rate ( $V_{\max}$ ), and the apparent affinity of mitochondria for exogenous ADP, denoted as the apparent Michaelis-Menten constant ( $K_m(\text{ADP})$ ). Consequently, this study investigates and elucidates the metabolic reprogramming occurring in colorectal polyps, cell line models and CRC tissues. This approach not only enhances our understanding of CRC at a molecular level but also may contribute to developing more effective diagnostic and therapeutic methods.

Clinical material provides a unique and realistic perspective of CRC, offering a closer representation of the disease in its natural physiological state. This approach also augments our understanding of CRC at a molecular level and enhances the potential for developing more effective diagnostic and therapeutic methods.

## Abbreviations

ADP	Adenosine diphosphate
AK	Adenylate kinase
AMP	Adenosine monophosphate
ANT	Adenine nucleotide translocator
ATP	Adenosine triphosphate
<i>BRAF</i>	Proto-oncogene B-Raf oncogene
Caco2	Human colorectal adenocarcinoma cells
CAT	Carboxyatractyloside
CK	Creatine kinase
CM	Cardiomyocytes
CRC	Colorectal cancer
CytoC	Cytochrome C
dN2a	Differentiated N2a cells
GLUT1	Glucose transporter 1
HK	Hexokinase
HL-1	Murine sarcoma cells
IMS	Intermembrane space
$K_m$	Michaelis-Menten constant
<i>KRAS</i>	Kirsten rat sarcoma virus oncogene
MI	Mitochondrial interactosome
MIM	Mitochondrial inner membrane
MOM	Mitochondrial outer membrane
MtCK	Mitochondrial creatine kinase
N2a	NEURO 2a cells
NADH	Reduced nicotinamide adenine dinucleotide
OXPHOS	Oxidative phosphorylation
PCr	Phosphocreatine
Pi	Inorganic phosphate
SEM	Standard error of the mean
SSLs	Sessile serrated lesions
TCA	Tricarboxylic acid cycle
<i>TUBB</i>	Tubulin beta gene
uN2a	Undifferentiated N2a cells
VDAC	Voltage-dependent anion channel
$V_{max}$	Maximal respiration rate
$V_o$	Rate of basal respiration

# 1. Review of literature

## 1.1. The definition and etiology of colon polyps and colorectal cancer

Colorectal cancer (CRC) is a diverse malignant tumour caused by uncontrolled growth of mutated cells in the large colon or rectum with different subtypes characterized by distinct molecular and pathological features. In most cases of sporadic CRC, the disease progresses gradually from non-cancerous polyps to malignant tumours (*Figure 1*). While the majority of colorectal polyps are harmless, some can transform into invasive adenocarcinomas with malignant properties, and most CRC cases develop from precancerous adenomatous and serrated polyps. Around 70% of sporadic CRCs originate from adenomatous polyps. In comparison, 25% to 30% arise from sessile serrated lesions (SSLs) following the SSL-to-carcinoma pathway, although the specific mechanisms behind this transformation are not yet fully understood. Well-established risk factors for conventional adenomas and CRC include advancing age, male gender, having a family history of the disease, being overweight or inactive, and consuming red meat. On the other hand, white race, tobacco, and alcohol use are significant risk factors for serrated polyps, which have a different set of risk factors compared to conventional adenomas. Additionally, a history of abdominopelvic radiation, acromegaly, hereditary hemochromatosis, or prior ureterosigmoidostomy also increases the risk of CRC (Sninsky, Shore et al. 2022).

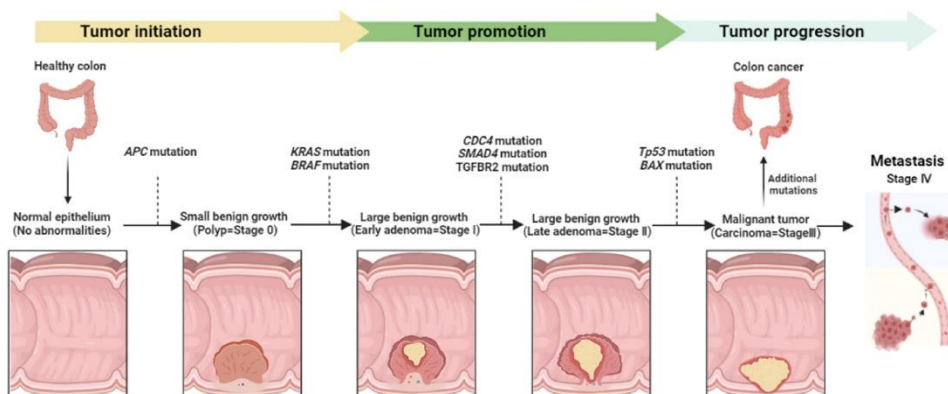


*Figure 1. The progression of colorectal cancer. The various stages, and the primary genetic alterations throughout the advancement of the tumour (Mahmod, Haif et al. 2022).*

## 1.2. The incidence and survival of colorectal cancer worldwide and in Estonia

Colorectal cancer also referred to as bowel cancer, ranks as the third most prevalent cancer globally and is the second most common cause of cancer-related deaths in Europe. It holds the 3rd position among cancers affecting men and the 2nd position among cancers affecting women. In the year 2020 alone, there were approximately 1,931,590 newly diagnosed cases of CRC, accounting for around 10% of all cancer cases worldwide. Additionally, CRC was responsible for 915,880 deaths, which constituted 9.2% of all cancer-related deaths (Globocan 2020).

According to the Estonian National Institute for Health Development, the incidence of CRC in Estonia has steadily risen over the past 30 years, with the number of affected individuals continuously increasing (Database 2020). Approximately 500,000 people are diagnosed with CRC in Europe each year. In Estonia, 972 new cases of CRC were diagnosed in 2018. Annually, over 400 people die from CRC in Estonia, with 495 deaths reported in 2019 (Development 2020).

However, when detected early, colorectal cancer is one of the most treatable forms of cancer, thus emphasizing the urgent need to develop more effective treatment strategies.

### 1.3. Prognosis and treatment

The implementation of colorectal cancer screening has played a significant role in reducing the occurrence and death rates of CRC in the past two decades. This has proven to be clinically valuable as it can prevent cancer-related illnesses, deaths, and excessive treatment expenses. By identifying significant abnormalities before they develop into cancerous growths and detecting early-stage cancer that has not spread beyond the bowel wall, we can increase the relatively low survival rate (Society 2008). The 5-year overall survival rate of individuals diagnosed with CRC is at 64%. Notably, patients with localized cancer (stages I, IIA, and IIB) exhibit a high 90% survival rate, while those with regional cancer (stages IIC and III) have a slightly lower rate at 71%. However, the survival rate sharply decreases to 14% for individuals with distant cancer (stage IV). In the case of rectal cancer, the 5-year cumulative prognosis is at 67%. Patients with localized cancer have an 89% survival rate, whereas those with regional cancer show a 70% survival rate. Unfortunately, the survival rate drops significantly to 15% for individuals diagnosed with distant cancer (stage IV) (Mattiuzzi, Sanchis-Gomar et al. 2019).

Currently, CRC screening focuses on the removal of adenomas and sessile serrated lesions, as well as the identification of early-stage disease. On the other hand, the survival rate drops significantly for those diagnosed with late-stage CRC, which involves the spread of cancer to distant organs. Treatment primarily focuses on relieving symptoms at this advanced stage, and the associated financial burdens are at their highest. Molecular alterations and response to chemotherapy can vary based on the location of the cancer within the colon or rectum. Tumours located in the proximal colon, distal colon, or rectum exhibit distinct molecular characteristics and may respond differently to chemotherapy (Shaukat, Kahi et al. 2021).

It has also been shown that the mutations in the *KRAS* and *BRAF* genes are significant influencers in the regulation of metabolic reprogramming across various cancers, including CRC (Hutton, Wang et al. 2016). They are thought to contribute to cancer development by driving the proliferation of cells with these initiating mutations (Shirasawa, Furuse et al. 1993). The *BRAF*V600E mutation in exon 15, codon 600, is linked to an unfavourable prognosis for CRC (Shirasawa, Furuse et al. 1993). Meanwhile, activating *KRAS* mutations in codon 12 and 13 of exon 2, which are prevalent in CRC (occurring in 30-50% of tumours), are associated with reduced survival rates and decreased responsiveness to chemotherapy (Phipps, Buchanan et al. 2013).

## 1.4. Metabolic plasticity of cancer cells

Tumour cells possess the ability to reconfigure metabolic processes, which plays a crucial role in disease advancement. This metabolic reprogramming allows tumour cells to adapt to the increased energy demands and fluctuating environmental conditions throughout the development of tumours (Goodpaster and Sparks 2017), while it exerts a profound influence on cell differentiation, the tumour microenvironment, and gene expression (Pavlova and Thompson 2016).

Metabolic reprogramming has been included as one of the hallmarks of cancer development (Hanahan and Weinberg 2000). Cancer cells encounter various physiological challenges during the process of metastasis, such as limited nutrient availability, hypoxia, and exposure to therapeutic agents. The crucial factor for the survival of tumour cells lies in their capability to adjust their metabolic activities to sustain energy production and fulfil biosynthetic requirements throughout the progression of the disease (McGuirk, Audet-Delage et al. 2020). Hence, cancer cells are compelled to fulfil the demands of accelerated growth and survival, while also possessing the capability to swiftly adapt to alterations in the tumour microenvironment. This molecular possibility, known as metabolic adaptability, relies on metabolic flexibility or plasticity and encompasses the ability to efficiently process substrates via multiple metabolic pathways while concurrently orchestrating the production of bioactive factors that actively contribute to the processes of oncogenic progression and therapeutic resistance (Fendt, Frezza et al. 2020).

## 1.5. Glycolysis and Warburg effect in cancer cells

Otto H. Warburg demonstrated in the 1920s that cancer cells, despite the presence of oxygen, primarily produce energy through glycolysis. The characteristic of this modified metabolism is the increased uptake of glucose and the conversion of glucose into lactate through fermentation, even when mitochondria are fully functional. This phenomenon is referred to as the “Warburg Effect” (Warburg, Wind et al. 1927).

This glycolytic phenotype has been found in a significant number of human tumours. However, the bioenergetic importance of oxidative phosphorylation and glycolysis varies according to histological type, growth stage, and vascularization (Vander Heiden, Cantley et al. 2009). The first type of cancer cells exhibits high glycolytic activity, the second type is characterized by deficient OXPHOS, and the third type shows enhanced OXPHOS. The existing evidence indicates that akin to normal cells, cancer cells concurrently undergo both aerobic and anaerobic glycolysis. The rates of glycolysis in cancer cells, as demonstrated in cell culture studies, are significantly elevated compared to non-tumour cells (Moreno-Sanchez, Marin-Hernandez et al. 2014). Current knowledge supports the observation of increased glucose consumption in colorectal cancer cells, leading to the utilization of glycolysis even in the presence of oxygen (Warburg and Dickens 1930, Warburg 1956, Izuishi, Yamamoto et al. 2012). However, it has been shown that OXPHOS serves as the primary source of ATP rather than glycolysis in these malignancies. Cancer cells are classified based on their metabolic remodelling pattern, balancing glycolysis and OXPHOS (Bellance, Pabst et al. 2012).

CRC has been regarded as a purely hypoxic tumour of the Warburg phenotype for many years, where normal colonocytes use OXPHOS as the primary energy source. Short-chain fatty acids undergo  $\beta$ -oxidation to form acetyl-CoA, which enters into the tricarboxylic acid (TCA) cycle to yield citrate, NADH, and finally ATP. However, CRC cells

cannot utilize butyrate as an energy source, which might refer to the truncated TCA cycle (Donohoe, Garge et al. 2011).

Consequently, it becomes evident that the bioenergetic profiles of tumours exhibit significant heterogeneity, which underscores the need for personalized treatment strategies that are specifically tailored to address the unique metabolic characteristics of each tumour.

## **1.6. The role of MOM in metabolic reprogramming**

For adenosine triphosphate (ATP) synthesis in the matrix by ATPase, adenosine diphosphate (ADP) from the cytosol needs to be conveyed across both mitochondrial membranes. The key facilitators of this adenine nucleotide exchange between the matrix and the cytosol include the adenine nucleotide translocator (ANT) on the mitochondrial inner membrane (MIM) and the voltage-dependent anion channel (VDAC) on the mitochondrial outer membrane (MOM). The flux of ATP, ADP, and inorganic phosphate (Pi) through the MOM is facilitated via the VDAC. Consequently, the regulation of OXPHOS is predominantly coordinated through the control of VDAC since the closure of this channel would limit the substrate supply for respiration and would stop the exchange of ADP and Pi for ATP during OXPHOS (Wallace 1999, Lemasters and Holmuhamedov 2006).

Research involving permeabilized muscle fibers has shown that cellular respiration and ATP synthesis are governed by a protein complex referred to as the Mitochondrial Interactosome (MI) (Guzun, Kaambre et al. 2015). MI is a multiprotein transmembrane complex that, among others, consists of VDAC, ATP synthasome, adenylate kinase (AK), hexokinase (HK), and mitochondrial creatine kinases (MtCK), which regulate the permeability of MOM for adenine nucleotides. The regulation of adenine nucleotides within VDAC is evident through the determination of the apparent affinity of mitochondria for exogenous ADP ( $K_m(\text{ADP})$ ), achieved via high-resolution respirometry on permeabilized cells and tissues and not in isolated mitochondria (Kay, Li et al. 1997, Puurand, Tepp et al. 2018). This indicates that the metabolic plasticity of cancer cells is linked to regulating VDAC permeability with respect to ADP.

Studies have demonstrated that VDAC is a crucial regulator determining the balance between the OXPHOS and glycolysis in cancerous cells (Carre, Andre et al. 2002, Maldonado 2017). This finding suggests that targeting VDAC could be a promising approach for developing a new generation of cancer therapies. The mitochondrial VDAC not only plays a significant role in maintaining high OXPHOS rates but also contributes to the activation of apoptotic pathways (Shoshan-Barmatz, Israelson et al. 2006, Shoshan-Barmatz, Zakar et al. 2009, Shoshan-Barmatz, Krelin et al. 2017).

There is limited scientific research on CRC pathogenesis, particularly concerning the critical processes of maintaining energy homeostasis and mitochondrial bioenergetic function. A novel and highly effective approach could involve manipulating the energy metabolism of cancer cells, enabling the selective identification of malignant tumours (Gogvadze, Orrenius et al. 2009). Intracellular ATP levels may be a crucial determinant of chemoresistance in CRC cells (Zhou, Tozzi et al. 2012), and mitochondria may play a supportive or even initiating role in the metastasis of cancer cells (Amoedo, Rodrigues et al. 2014). Evidently, the glycolytic pathway and associated genes play an important role in CRC tumorigenesis, yet further research is needed to understand their molecular mechanisms. The malignant transformation of cells results in reprogramming various signalling and metabolic pathways, particularly those related to energy metabolism.

Targeting the energy metabolism of tumour-initiating and cancer cells has been suggested as a promising and specific approach for eliminating malignant tumours (Moreno-Sanchez, Rodriguez-Enriquez et al. 2007, Gogvadze, Orrenius et al. 2009, Lamb, Bonuccelli et al. 2015).

### **1.7. Michaelis-Menten kinetics as the classical and simple method for investigating the permeability of the mitochondrial outer membrane**

High-resolution respirometry can be used to assess the metabolic plasticity. The relationship between ATP synthesis (mitochondrial oxygen consumption) and ADP concentration adheres to Michaelis-Menten kinetics (*Figure 2*). This enables the assessment of the apparent Michaelis-Menten constant for ADP ( $K_m(\text{ADP})$ ) in various tissues, cancers, and cell cultures. Measured in permeabilized cells and tissues,  $K_m(\text{ADP})$  represents the mitochondria's affinity for exogenous ADP and defines the permeability of the MOM via the VDAC for adenine nucleotides (Saks, Belikova et al. 1991, Kuznetsov, Tiivel et al. 1996) (*Figure 3b*).

The permeabilization technique facilitates the examination of mitochondrial function within cells in their native environment, preserving the connections between cytoskeletal structures and the MOM without necessitating the separation of these organelles. Treatment with agents that form complexes with cholesterol, such as digitonin, saponin, or filipin, interact with cholesterol molecules, which are prevalent in the plasma membrane (the polar heads of cholesterol and phospholipids associate). This interaction leads to a loss of membrane integrity (permeabilization), eliminating the barrier between the intracellular space and surrounding medium. As a result, the cytosol and its solutes are washed away, aligning the composition of the intracellular environment with the experimental incubation medium. The cholesterol levels in internal organelles or membrane structures like mitochondria or the sarcoplasmic reticulum are significantly lower, and the concentration of the cholesterol-complex-forming agent used for the permeabilization of the outer cell membrane does not disrupt these structures, enabling the investigation of mitochondria (Kuznetsov, Veksler et al. 2008).

$$V = \frac{V_{max} \times [S]}{K_m + [S]}$$

*Figure 2. The Michaelis–Menten equation.  $V$  shows the initial reaction velocity,  $V_{max}$  is the maximum reaction velocity (the rate where the enzyme is saturated with substrate),  $[S]$  is the substrate concentration and  $K_m$  is the Michaelis constant, which is the substrate concentration at which the reaction velocity is half of  $V_{max}$  (Michaelis and Menten 1913).*



Cell-specific differences in  $K_m(\text{ADP})$  are likely a result of the unique structural and functional organization of energy metabolism. For instance, cells with a low  $K_m(\text{ADP})$  value ( $\sim 10 \mu\text{M}$ ), such as glycolytic muscle cells, experience fewer structural and functional constraints on ADP/ATP movement through the MOM when compared to oxidative muscles with a  $K_m(\text{ADP})$  value around  $300 \mu\text{M}$  (Kuznetsov, Tiivel et al. 1996). Therefore, using the analogy of muscles, the  $K_m(\text{ADP})$  value serves as an indicative parameter for describing the primary setting of energy metabolism arrangement. According to the model proposed by Saks V. et al, the proportion of mitochondria with low oxidative capacity in the tissue can be inferred from the  $K_m(\text{ADP})$  value (Saks, Veksler et al. 1998).

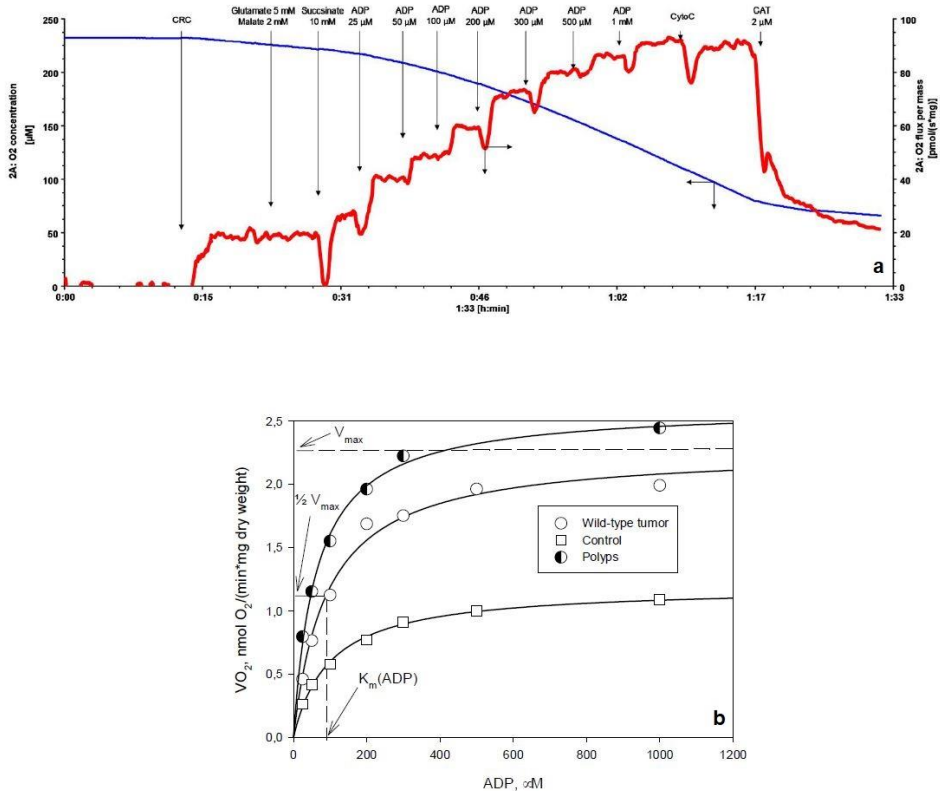


*Figure 3. Michaelis-Menten kinetics and mitochondrial respiration. Michaelis-Menten kinetics can be applied to study ADP-dependent respiration in biopsy and postoperational materials from human colorectal cancer and polyps. (a) Presentative traces show oxygen consumption rates activated by adenosine diphosphate (ADP) in permeabilized tissue from colorectal cancer. CytoC is cytochrome C (to confirm the integrity of the MOM); CAT is carboxyatractyloside (to confirm the integrity of the MIM). (b)  $K_m(\text{ADP})$  and  $V_{\max}$  values can be determined through non-linear regression using the Michaelis-Menten equation (Publication III).*

In addition to  $K_m(\text{ADP})$ , the maximal ADP-dependent oxygen consumption ( $V_{\max}$ ) is a defining characteristic of metabolic plasticity and is correlated with mitochondrial density in the tissue.  $V_{\max}$  values are higher in CRC compared to normal colon tissue (Kaldma, Klepinin et al. 2014), indicating robust metabolic activity. However, further studies are required to confirm the extent to which high  $V_{\max}$  values correlate with tumour aggressiveness.

## 1.8. Energy transfer pathways

The cellular phosphotransfer system is a complex network of enzymes crucial for intracellular energy transfer and signalling processes. This system plays a vital role in cellular energy metabolism and regulation, particularly in facilitating efficient energy transfer and distribution, thereby ensuring cellular economy and energetic homeostasis (Dzeja and Terzic 2003). The key elements of the system are AK, CK, and HK. CK and AK enzymes are involved in cancer cell proliferation (Klepinin, Chekulayev et al. 2014, Ounpuu, Klepinin et al. 2017).

AKs play the key role in facilitating AMP metabolic signalling and optimizing the ATP supply. Efficient high-energy phosphoryl exchange between the mitochondria and cytosol is enabled by the position of the AK2 in the mitochondrial intermembrane and cristae space. Two AK isoforms, AK3 and AK4, are situated in the mitochondrial matrix and participate in the control of the mitochondrial Krebs cycle and OXPHOS. (Dzeja and Terzic 2009).

Both essential phosphotransfer enzymes AK2 and MtCK are located in the intermembrane/cristae space in mitochondria (Saks, Dzeja et al. 2006, Dzeja and Terzic 2009). AK2 and MtCK mediate metabolic signalling, while facilitating the export of ATP from mitochondria and receiving feedback signals from the cytosol, including ADP, AMP, and creatine (Dzeja, Zeleznikar et al. 1998, Dzeja and Terzic 2009). In 2016, Fujisawa with colleagues proposed a mechanism through which AK4 regulates mitochondrial respiration in cancer cells. The mechanism stated that AK4 expression is elevated under hypoxic conditions, leading to the formation of a complex with HK2, VDAC, and adenine nucleotide translocase (ANT), promoting increased ADP recycling. The efficiently recycled ADP within the mitochondrion is then converted into ATP by ATP synthase. This ATP, in turn, serves as a substrate for HK2, amplifying glycolytic activity in cancer cells (Pedersen 2007, Fujisawa, Terai et al. 2016).

Hexokinases, which are evolutionarily preserved enzymes, facilitate the virtually irreversible initial stage of the glycolytic pathway. In this process, glucose is phosphorylated to glucose-6-phosphate, simultaneously accompanied by the de-phosphorylation of ATP. When attached to mitochondria, HK1 and HK2 enhance the survival of both healthy and cancerous cells, while also improving their efficiency in utilizing glucose (Mathupala, Ko et al. 2006). The upregulation of HK2 in cancer cells might indicate a shift in the metabolic activity within the cells as a strengthened connection between mitochondria and the process of glycolytic phosphotransfer (Han, Patten et al. 2019), leading to a possible unrestrained energy distribution across the cancer cells.

Numerous results have shown that in CRC (Kaldma, Klepinin et al. 2014), breast cancer (Kaambre, Chekulayev et al. 2012), neuroblastoma (Klepinin, Chekulayev et al. 2014), prostate cancer (Amamoto, Uchiumi et al. 2016), and embryonic stem cells (Ounpuu, Klepinin et al. 2017) the MtCK was downregulated. The decrease in the levels of MtCK in cancer cells was associated with the upregulation of adenylate kinase AK2 isoform in intermembrane space, which enhances the utilization of extra-mitochondrial AMP for OXPHOS (Kaambre, Chekulayev et al. 2012, Kaldma, Klepinin et al. 2014, Klepinin, Ounpuu et al. 2016, Ounpuu, Klepinin et al. 2017). It has also been shown that the intestinal cells can deactivate the CK circuit and activate the AK pathway, demonstrating metabolic plasticity (Klepinina, Klepinin et al. 2021).

## 1.9. The role of free tubulin isotypes in the metabolic regulation of cancer

Tubulin serves as the protein subunit of microtubules, forming dimers that can exist as either heterodimers (composed of  $\alpha$  and  $\beta$  subunits) or homodimers (consisting of either  $\alpha$  or  $\beta$  subunits) (Ludueña, Shooter et al. 1977). It has been shown in humans that there are 10  $\alpha$ -tubulin and nine  $\beta$ -tubulin genes within the tubulin gene family. Regarding gene expression, it has been noted that genes TUBB2A (II $\alpha$ ), TUBB2B (II $\beta$ ), TUBB3 (III $\beta$ ), and TUBB4 (IV $\alpha$ ) exhibit high expression levels in the brain. In contrast, TUBB2C (IV $\beta$ ) demonstrates elevated expression in the heart and skeletal muscles. Nevertheless, the contribution of the various isotypes to the total beta-tubulin content varies across tissues and displays a complex pattern (Findeisen, Mühlhausen et al. 2014). Notably, tumour cells are characterized by a significant increase in the expression of TUBB3 (III $\beta$ ), while the expression of TUBB6 (V) is markedly reduced in most tumours (Leandro-Garcia, Leskela et al. 2010). TUBB2B (II $\beta$ ) is often highly expressed in tumours while the corresponding normal cells express minimal or no  $\beta$ II (Yeh and Luduena 2004).

Tubulins fulfil diverse roles within a cell, serving structural functions when polymerized into microtubules and regulatory roles when they exist in unpolymerized tubulin (Rostovtseva, Gurnev et al. 2018). For example, microtubules shape the subcellular organization and movement of mitochondria in skeletal and cardiac muscle cells (Tepp, Mado et al. 2014). Nonetheless, the regulatory function of unpolymerized tubulin in bioenergetics might be associated with the modulation of VDAC permeability within the MOM (Puurand, Tepp et al. 2019). However, the function of tubulin in controlling the permeability of the MOM in cancerous cells remains uncertain.

Research involving VDAC reconstituted into planar lipid bilayers, along with model experiments using isolated mitochondria, has demonstrated that tubulin significantly reduces the permeability of VDAC for specific adenine nucleotides like ADP and ATP. This has led to the suggestion that this effect may be a key player in controlling mitochondrial function in both healthy and cancerous cells (Rostovtseva, Sheldon et al. 2008, Maldonado and Lemasters 2012)

Research has shown the presence of a supercomplex called the mitochondrial interactosome (MI). This complex includes the ATP synthasome, MtCK, VDAC, and tubulin and plays a crucial role in regulating mitochondrial respiration. Studies have indicated that in rat heart cardiomyocytes (CMs),  $\beta$ II-tubulin binds to VDAC, which regulates the permeability of this mitochondrial channel for adenine nucleotides. This process promotes the generation of phosphocreatine (PCr) through MtCK (Timohhina, Guzun et al. 2009, Guzun, Kaambre et al. 2015). Additionally, it has been observed that during carcinogenesis, the composition and structure of the MI can undergo significant reorganization due to substantial changes in the expression of its components (Chevrollier, Loiseau et al. 2011). It is proposed that  $\beta$ III-tubulin plays a role in governing cellular metabolism and enhancing the signalling response to glucose stress, thus promoting cell survival and reducing cell dependence on glycolytic metabolism. In cancer cells,  $\beta$ III-tubulin variants with particular post-translational modifications have been observed to be situated in mitochondrial membranes (Cicchillitti, Penci et al. 2008).

Further research is required to explore the connection between mitochondrial and cytosolic  $\beta$ II/ $\beta$ III-tubulin variants, their involvement in the development and advancement of malignancies, and their potential role in drug resistance.

## 1.10. The complex regulation of the mitochondrial outer membrane

Multiple models have been proposed for the regulation of MOM for the permeability of adenine nucleotides in colorectal cells, but we still do not have a clear understanding of this. Two proposed mechanisms govern the regulation of the MOM permeability in cancer cells. Firstly, as per the model suggested by Pedersen and colleagues, the interaction between VDAC and HK2 stands out as a primary pathway mediating the Warburg effect or aerobic glycolysis in cancer cells (Pedersen 2007, Mathupala, Ko et al. 2009). It has been established that the binding of HK2 to the VDAC channel maintains it in an open state (Majewski, Nogueira et al. 2004) enabling HK2 to utilize intra-mitochondrially generated ATP for the phosphorylation of glucose (Cesar Mde and Wilson 1998). This means that low  $K_m(\text{ADP})$  values can be expected. The possible model for the regulatory mechanisms governing MOM permeability to adenine nucleotides is proposed for both normal and CRC cells (Figure 4). VDAC serves as the channel facilitating the movement of adenine nucleotides into and out of mitochondria. In normal cells (Figure 4a), a minor fraction of HK is associated with VDAC, utilizing mitochondrial ATP for the phosphorylation of glucose. The resulting ADP is directed back to the mitochondrial matrix through VDAC and ANT for incorporation into OXPHOS. Tubulin binding further modulates VDAC permeability, making it less receptive to adenine nucleotides due to the interaction between beta-tubulin and VDAC. Consequently, cells are prompted to use CK and AK energy transfer networks for the intracellular distribution of high-energy phosphates. The MtCK, situated in the intermembrane space (IMS) of the mitochondria, is functionally connected to the ANT, thereby creating a dependency of OXPHOS on ADP produced from the MtCK reaction. The mitochondrial AK isoform AK2 utilizes AMP passing through VDAC and ATP passing through ANT to generate ADP, thereby stimulating OXPHOS. These energy transport systems establish a feedback loop between ATP consumption and synthesis. The role of tubulin in regulating VDAC permeability remains ambiguous, as the interaction of truncated VDAC with tubulin might be compromised (Pedersen 2007, Reinsalu, Puurand et al. 2021).

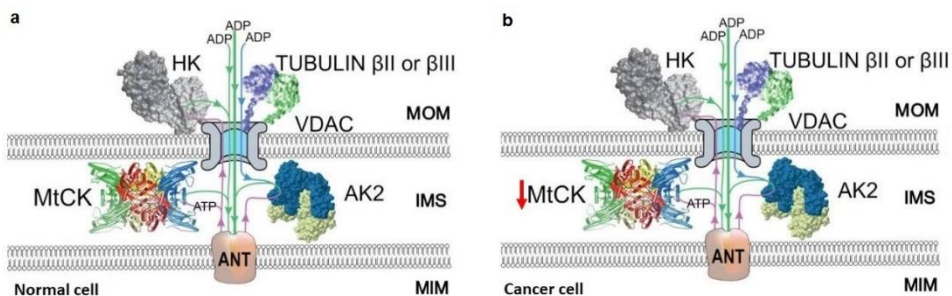


Figure 4. Regulatory mechanisms in normal cells and CRC. Possible model for the regulatory mechanisms governing the MOM permeability proposed for adenine nucleotides in both normal (a) and CRC cells (b). In cancer cells the mitochondrial MtCK might be downregulated or entirely absent. Voltage-dependent anion channel (VDAC); hexokinase (HK), adenine nucleotide translocase (ANT); oxidative phosphorylation (OXPHOS); creatine kinase (CK); adenylate kinase (AK); mitochondrial outer membrane (MOM); mitochondrial inner membrane (MIM); intermembrane space (IMS). Figure modified from (Reinsalu, Puurand et al. 2021).

The second mechanism, proposed by Maldonado and colleagues, reveals that in hepatocarcinoma cells, VDAC is obstructed by free tubulin, prompting malignant cells to transition to aerobic glycolysis (Maldonado, Patnaik et al. 2010). They have demonstrated that an increase in non-polymerized  $\alpha$ - $\beta$  heterodimer tubulin level in liver cancer cells results in an elevation of mitochondrial membrane potential, leading to the closure of VDAC. Our investigation into rat muscle tissues suggested that only non-polymerized  $\beta$ II-tubulin in heart and soleus muscles significantly influences the regulation of MOM permeability for ADP (Varikmaa, Bagur et al. 2014). Nevertheless, both studies underscore that the impact of free dimeric tubulin on VDAC permeability is dependent on the polymerized/dimeric tubulin ratio.

It has also been illustrated that multiple other proteins are able to interact with VDAC. For example, a VDAC binding protein erastin effectively prevented and reversed the loss of mitochondrial membrane potential following exposure to microtubule destabilizers in intact cells. It also acted against the tubulin-induced inhibition of VDAC in planar lipid bilayers (Maldonado, Sheldon et al. 2013). The disruption caused by erastin in the tubulin-VDAC interaction counteracts the Warburg metabolic effect, ultimately restoring oxidative mitochondrial metabolism. Furthermore, it has been observed in cardiac tissue that both desmin and  $\alpha$  $\beta$ -crystallin are localized at the mitochondria-associated membranes, where they engage with VDAC. The protection provided by overexpressed  $\alpha$  $\beta$ -crystallin involves keeping mitochondrial proteins at the needed levels, preventing unusual changes in the mitochondrial permeability transition pore, and maintaining the energy potential of the mitochondria (Diokmetzidou, Soumaka et al. 2016). These interactions between VDAC and other proteins are currently not fully understood and need further investigation.

## 2. Materials and methods

In this research, a range of techniques were employed, and for more comprehensive information on each, please refer to the accompanying publications (see appendixes).

- Clinical materials and patients – Publication I, II and III
- Preparation and permeabilization method for permeabilized tumour samples – Publication I and III
- Mitochondrial respiration / oxygraphic measurements – Publication I, II and III
- Immunofluorescence analysis – Publication II
- DNA extraction – Publication III
- *KRAS* and *BRAF* mutation analyses – Publication III

### 3. Results and discussion

#### 3.1. ADP-regulated mitochondrial respiration in human colorectal cancer (Publication I)

Most of our knowledge about how CRC changes its molecular metabolism comes from research on cell culture models, whereas few studies have used clinical samples. Additionally, the diverse conditions of cell culture introduce variations that can significantly impact the cellular metabolic profile. Thus, we wanted to see the dynamics of mitochondrial function within cells in their native environment, preserving the connections between cytoskeletal structures and the outer membranes of mitochondria. For this, we measured the apparent ( $K_m(\text{ADP})$ ) values and maximum respiration rates ( $V_{\max}$ ) for ADP in the human CRC and adjacent colon control tissues.

*Table 1. Apparent  $K_m$  and maximum respiration rate ( $V_{\max}$ ) values for CRC and the corresponding adjacent healthy tissues. Apparent  $K_m$  ( $K_m(\text{ADP})$ ) and maximum respiration rate ( $V_{\max}$ ) values were determined for ADP-dependent respiration in samples from CRC and the corresponding adjacent healthy tissues.  $V_{\max}$  values are expressed as  $\text{nMO}_2/\text{min}/\text{mg}$  dry tissue weight, excluding proton leak rates.  $K_m$  and  $V_{\max}$  values for ADP were derived from the respective titration curves by fitting experimental data to a non-linear regression equation based on a Michaelis–Menten model. The analysis included data from 35 patients (Publication I).*

Tissues	$K_m(\text{ADP}), \mu\text{M} \pm \text{SEM}$	$V_{\max} \pm \text{SEM}$
Human colorectal cancer tissue	$93.6 \pm 7.7$	$2.41 \pm 0.32$
Human adjacent colon control tissue	$256 \pm 34$	$0.71 \pm 0.23$

Table 1 from the publication I outlines the ADP-regulated mitochondrial respiration parameters calculated for permeabilized tissue samples. Here, it is observed that the  $K_m(\text{ADP})$  value for adjacent colon control tissue is 2,7 times greater than that for CRC tissue and the  $V_{\max}$  value for control tissue is 3,4 times lower than in the CRC tissue.

Discrepancies in the rates of  $V_{\max}$  in colon tissue samples correlate with variances identified in our previous study (Kaldma, Klepinin et al. 2014), indicating higher mitochondrial quantity in CRC cells with a 50% increase compared to healthy control tissue. According to numerous studies (Chance and Williams 1955, Saks, Kuznetsov et al. 1995, Saks, Veksler et al. 1998, Kuznetsov, Strobl et al. 2002), the  $K_m(\text{ADP})$  value for ADP in isolated mitochondria is shown to be minimal, approximately  $15 \mu\text{M}$ . Mitochondria from human colorectal cancer demonstrate an elevated affinity for exogenous ADP compared to normal colon tissues; however, this preference is still 6 times higher than the  $K_m(\text{ADP})$  for isolated mitochondria (Table 1) (Chance and Williams 1955). When comparing the results for cancer biopsies and the adjacent healthy tissue (Table 1; Figure 5a), we demonstrate that the glycolytic and OXPHOS activity in CRC has not changed. These results contradict the observations obtained from cell culture studies, particularly in human colorectal adenocarcinoma cells (Caco2), where the  $K_m(\text{ADP})$  was recorded at  $40 \mu\text{M}$ , highlighting a discrepancy between *in vitro* and *in vivo* data (Kaambre, Chekulayev et al. 2012, Chekulayev, Mado et al. 2015, Ounpuu, Truu et al. 2018). Despite using the same preparation method, the difference observed between cultured cells and clinical samples highlights distinctions in these two sample groups, emphasizing substantial differences in MOM permeability.

According to the findings from our laboratory, it is conceivable that a low  $K_m$  value for ADP may be a prevalent trait for cancer cells *in vitro*. However, in *in vivo* tumour samples, the modulation of MOM permeability appears to be more intricate, likely associated with the interplay between energy transfer pathways, alterations in the phosphorylation state of VDAC channels and modulation of the cytoskeleton or membrane potential arising from tumour formation. This underscores the limitations of cell culture studies and emphasizes the significance of utilizing clinical material to assess the mechanisms underlying cancer metabolic plasticity.

### 3.2. The heterogeneity of colon tissue (Publication I)

Permeabilized samples were subjected to increasing concentrations of ADP, and the rates of  $O_2$  consumption, normalized to  $V_{max}$ , were analysed in relation to the corresponding ADP concentration values using double reciprocal Lineweaver–Burk plots (Figure 5a and 5b) (Saks, Veksler et al. 1998). The outcomes of the Lineweaver–Burk analysis of the experimental data associated with ADP-regulated mitochondrial respiration in samples of CRC and healthy colon are depicted in Figure 5a. The  $V_{max}$  and  $K_m$  values were derived through the linearization method. As demonstrated by Saks and colleagues, a biphasic pattern in respiration regulation on the graph curve suggests the presence of two distinct populations of mitochondria with varying affinities for ADP. Our findings indicated such distinctions in healthy colon tissue but not in CRC tissue.

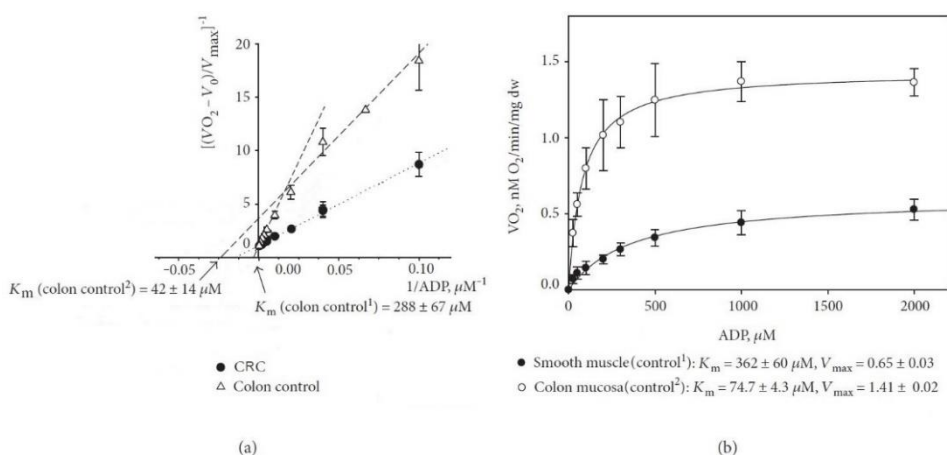


Figure 5. Analysis of the normalized respiration rate patterns for CRC. (a) Analysis of the normalized respiration rate patterns for CRC (dotted line) and samples from healthy colon tissues (dashed line) is depicted in double reciprocal Lineweaver–Burk plots. This data comes from an examination of 10 colorectal cancer patients. (b) ADP-dependent respiration in samples of healthy colon mucosa (as control<sup>2</sup>) and smooth muscle (as control<sup>1</sup>) tissues. This is presented in the form of a Michaelis–Menten curve, and the data is derived from 8 samples.  $V_o$  and  $V_{max}$  represent the rates of basal and maximal ADP-activated respiration, respectively (Publication I).

CRC tissue exhibits monophasic regulation in mitochondrial respiration, whereas in healthy colon tissue, a distinct pattern emerges with the identification of two mitochondrial populations possessing markedly different properties (Figure 5a). The first population of mitochondria is characterized by a lower  $K_m$  value ( $42 \pm 14 \mu\text{M}$ ), while the  $K_m(\text{ADP})$  value for the second mitochondrial population is nearly seven times higher



( $288 \pm 67 \mu\text{M}$ ). Subsequently, we isolated mucosal and smooth muscle sections from the colon samples for additional  $K_m$  measurements to discern their individual contributions. The  $K_m(\text{ADP})$  value for the mucosal part was determined to be  $74.7 \pm 4.3 \mu\text{M}$ , while for colon smooth muscle tissues, the corresponding value was  $362 \pm 60 \mu\text{M}$  (Figure 5b). Consequently, the results following the separation process elucidate the outcomes of the initial experiment, where the entire colon wall was analysed, revealing the presence of two distinct groups of mitochondria.

### 3.3. Mitochondrial $V_{\text{max}}$ as a biomarker for cancer aggressiveness (Publication I)

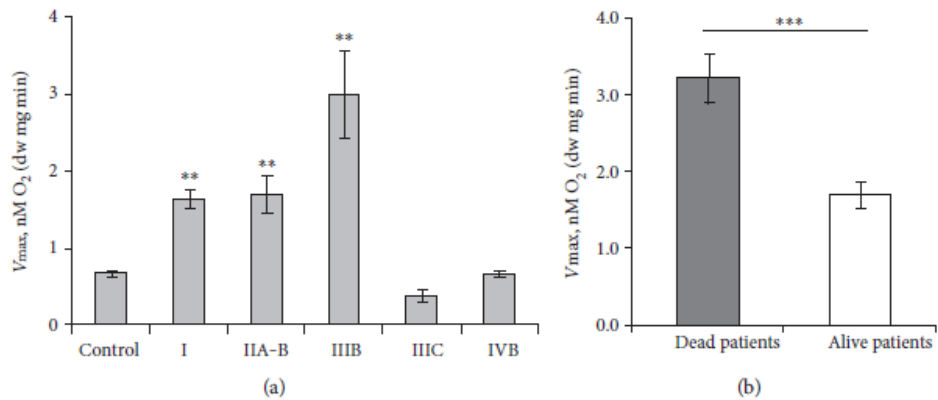


Figure 6. Comparison of the maximal mitochondrial respiration rate ( $V_{\text{max}}$ ) across different stages of CRC. (a) Comparison of the maximal mitochondrial respiration rate ( $V_{\text{max}}$ ) across different stages of CRC. Stage I includes data from 13 patients, IIA and IIB from 13 patients, IIIB from 4 patients, IIIC from 3 patients, and IVB from 1 patient. Control colon tissue data is collected from 34 patients and used as a reference for comparing  $V_{\text{max}}$ . The error bars represent standard error of the mean (SEM), and significant differences are indicated as \*\* ( $p < 0.005$ ). In part (b), the study looks at  $V_{\text{max}}$  in CRC patients in a follow-up context. Among 32 patients, 7 have unfortunately succumbed to CRC (with  $V_{\text{max}} = 3.19 \pm 0.34$ ), while 25 patients remain in remission (with  $V_{\text{max}} = 1.70 \pm 0.17$ ). Significant differences are indicated as \*\*\* ( $p < 0.001$ ) (Publication I).

We compared the disease stage with the average  $V_{\text{max}}$  value corresponding to each CRC stage (Figure 6a, Publication I). While an increase in  $V_{\text{max}}$  during initial stages shows significant differences in comparison to control samples, the decline in  $V_{\text{max}}$  for stages IIIC and IVB deviates from this upward trend. It becomes apparent that relying solely on the disease stage at the time of diagnosis is not a dependable indicator of aggressiveness, potentially sparking debates about the validity of such graphical representations. Consequently, we collected initial longitudinal data on patient progression within our CRC cohort. We validated that out of 32 eligible patients, seven had succumbed to the disease (median follow-up time of  $47.3 \pm 4.9$  months). The  $V_{\text{max}}$  values in patients who did not survive were significantly higher than those in the group that did not experience progression (Figure 6b). Hence, it can be argued, based on this observed similarity, that higher tumour respiratory parameters in deceased CRC patients indicated a more aggressive form of the disease.

### 3.4. Mitochondrial Respiration in CRC and Polyps: ADP Regulation and *KRAS/BRAF* Mutation (Publication III)

Furthermore, we explored the dynamics of ATP production through OXPHOS in human tissues across the progression from normal colon tissue to polyps and cancer. We aimed to elucidate the influence of *BRAF* and *KRAS* mutations on the process since the distinctiveness of cancer metabolism compared to normal cellular metabolism underscores a significant gap in understanding the interconnected relationships between cancer mitochondrial respiration and key oncogenic driver genes such as *KRAS* and *BRAF*. This emphasizes the necessity to explore and shed light on the associations between cellular respiration and these mutations, providing valuable insights into cancer biology.

Our approach involved employing high-resolution respirometry. This enabled the measurement of the maximal rate of ADP-activated respiration ( $V_{\max}$ ). Additionally, we determined  $K_m(\text{ADP})$  values for exogenously added ADP ( $K_m(\text{ADP})$ ) using permeabilized postoperative tissues, encompassing CRC, colon polyps, and normal colon tissue. These methodological steps laid the groundwork for our research results.

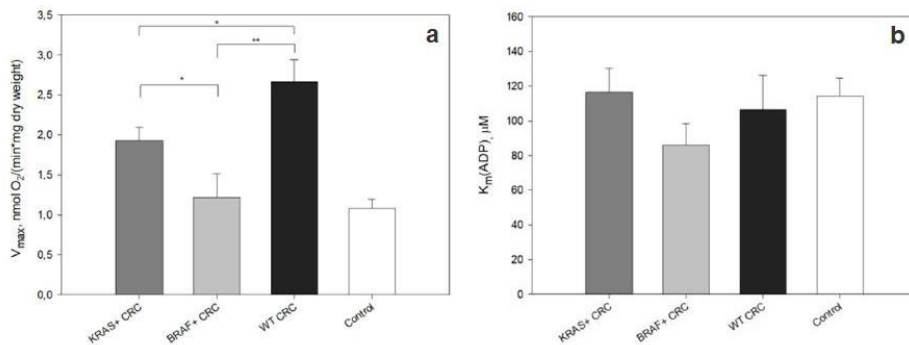


Figure 7. Regulation of mitochondrial respiration in tumours with *KRAS*+, *BRAF*+ mutations, wild-type tumours, and control tissues. (a) The analysis compares the maximal ADP-activated respiratory rate ( $V_{\max}$ ). (b) The comparison of apparent Michaelis–Menten constant ( $K_m(\text{ADP})$ ) values for ADP. *KRAS*+: tumours with *KRAS* mutations; *BRAF*+: tumours with *BRAF* mutations; WT: Wild type; CRC: Colorectal cancer; Control: Control tissue. \* Indicates statistical significance at  $p < 0.05$ , \*\* at  $p < 0.01$  (Publication III).

It is evident that among all the studied groups, tumours with wild-type characteristics exhibited the highest  $V_{\max}$ , whereas *BRAF* or *KRAS* mutated tumours displayed significantly lower values (Figure 7a). This observation underscores the involvement of oncogenic *KRAS* and *BRAF* in the metabolic reprogramming of colon mucosa. Additionally, notable differences in  $V_{\max}$  values were observed between *BRAF* mutated and *KRAS* mutated tumours (Figure 7a). Intriguingly, the  $V_{\max}$  of *BRAF* mutated tumours resembled that of control tissues. These results suggest a distinctive role of mutated *KRAS* and *BRAF* in influencing mitochondrial biogenesis and likely contributing to tissue differentiation.

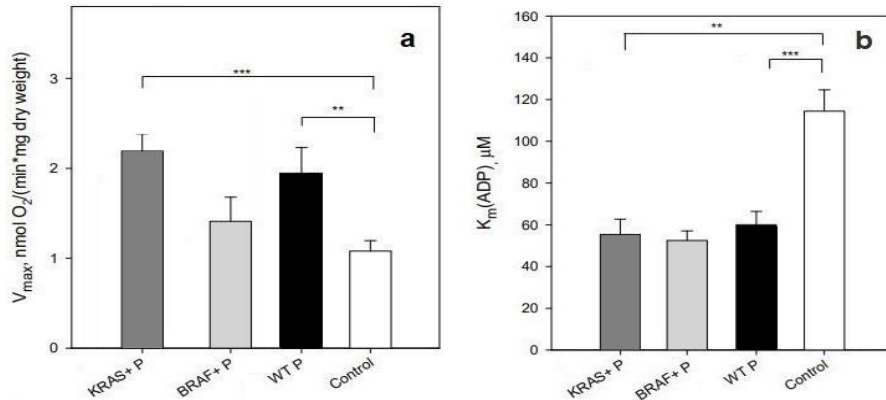


Figure 8. Regulation of mitochondrial respiration in polyps with *KRAS*+, *BRAF*+ mutations, wild-type polyps, and control tissues. (a) The analysis compares the maximal ADP-activated respiratory rate ( $V_{max}$ ). (b) The comparison of apparent Michaelis-Menten constant ( $K_m(ADP)$ ) values for ADP. KRAS+P: polyps with *KRAS* mutations; BRAF+P: polyps with *BRAF* mutations; WT: Wild type; Control: Control tissue. \*\* Indicates statistical significance at  $p < 0.01$ ; \*\*\*  $p < 0.001$  (Publication III).

In colorectal polyps, the  $V_{max}$  pattern closely mirrored that of the corresponding tumours. Respiration rates in polyps from both *KRAS* mutated and wild-type molecular groups exhibited significantly higher  $V_{max}$  values compared to the control tissue, where  $V_{max}$  values were  $2.19 \pm 0.19$  and  $1.95 \pm 0.28$  for the *KRAS* mutated and wild-type groups, respectively,  $p < 0.001$  and  $p = 0.004$  as compared to the control group (Figure 8a). Polyps harbouring the *BRAF* mutation displayed a tendency toward lower OXPHOS rates ( $V_{max} = 1.41 \pm 0.27$ ) compared to mutated *KRAS* and wild-type groups. Similar to the *BRAF* CRC group, polyps with mutated *BRAF* did not exhibit a difference from the control tissue (Figure 8a). Surprisingly, *KRAS* mutated polyps showed signs of stimulated mitochondrial biogenesis, hinting at a potential progression toward highly metastatic malignant tumours. This unexpected finding contrasts with previous associations of *KRAS* gene mutations with elevated glycolysis and reduced oxygen consumption in cell cultures, which was shown to be a combination of heightened expression of glucose transporter 1 (GLUT1) and HK2, along with mitochondrial dysfunction (Yun, Rago et al. 2009, Iwamoto, Kawada et al. 2014, Wang, Song et al. 2015). This implies that changes in mitochondrial biogenesis are an early occurrence, already manifesting in the pre-malignant stage.

To explore potential regulatory changes impacting OXPHOS in carcinogenesis, we assessed the apparent affinity of mitochondria for ADP. In all CRC and polyp groups, the respective  $K_m(ADP)$  values were calculated, and the recorded values (Figure 7) were determined to be 4 to 8 times higher than those observed in isolated mitochondria (15  $\mu M$ , as measured by Chance and Williams (Chance and Williams 1955)). From this, colon polyps and CRC displayed heightened rates of maximal ADP-activated respiration, indicating increased mitochondrial mass compared to normal colon tissue. This discovery also suggests the presence of limitations on the movement of ADP through mitochondrial membranes.

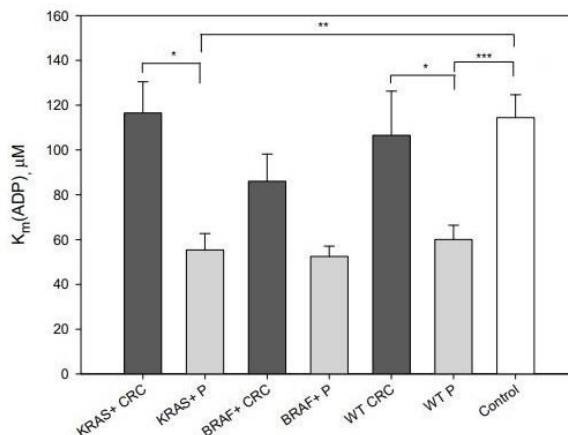


Figure 9. The apparent Michaelis-Menten constant ( $K_m(\text{ADP})$ ) values for ADP in colorectal polyps, CRC and control tissues. KRAS+—KRAS mutated; BRAF+—BRAF mutated; WT—wild type; CRC—colorectal cancer; P—polyps; Control—control tissue. \*  $p < 0.05$ ; \*\*  $p < 0.01$ ; \*\*\*  $p < 0.001$  (Publication III).

Therefore, the comparatively low  $K_m(\text{ADP})$  observed in colorectal polyps (approximately 50-60  $\mu\text{M}$ ) suggests a metabolic reprogramming favouring the glycolytic phenotype with functional OXPHOS, similar to the glycolytic muscle (Figure 8; Figure 9; Figure 7). Conversely, the elevated  $K_m(\text{ADP})$  values in CRC (approximately 100-120  $\mu\text{M}$ ) indicate a transition to the oxidative phosphorylation phenotype with heightened intracellular complexity, similar to the oxidative muscle (Figure 7; Figure 9).

### 3.5. The low oxidative capacity of mitochondria in colon lesions (Publication III)

To assess the percentage of mitochondria with regulated (oxidative) and unregulated (glycolytic) MOM permeability, we applied a mathematical model adapted for our tissue studies based on a previously proposed model (Saks, Veksler et al. 1998). Calculated from the  $K_m(\text{ADP})$  value as an inverse asymptotic dependence, the percentage of low oxidative capacity mitochondria indicates a metabolic shift to a glycolytic state in all colon polyps, excluding KRAS mutated and wild-type tumours when compared to control tissue (Table 2). Early changes in glycolytic markers have been observed in the premalignant colorectal mucosal field, suggesting the promotion of increased glycolysis (Cruz, Ledbetter et al. 2017).

The  $K_m(\text{ADP})$  values in polyp molecular groups were  $55.3 \pm 7.4 \mu\text{M}$ ,  $52.5 \pm 4.7 \mu\text{M}$ , and  $60.1 \pm 6.3 \mu\text{M}$  for KRAS mutated, BRAF mutated, and wild-type groups, respectively. These were lower than in control tissue (Figure 9), showing significant changes in the regulation of MOM permeability. Despite similar  $V_{\text{max}}$  values in KRAS mutated polyp and CRC groups, the difference in  $K_m(\text{ADP})$  between these groups was significant ( $p = 0.014$ ; Figure 9). Our findings, showcasing a relatively low  $K_m$  value for ADP in colorectal polyps, suggest an early metabolic reprogramming toward the glycolytic phenotype with functional oxidative phosphorylation.

Table 2. Modelled percentage of mitochondria with low oxidative capacity in tumours with KRAS, BRAF mutations, wild-type tumours (Publication III).

Sample	% of Low Oxidative Capacity of Mitochondrion
KRAS tumors	28.1
KRAS polyps	65.9
BRAF tumors	43.0
BRAF polyps	68.6
Wild-type tumors	32.4
Wild-type polyps	61.7
All controls	29.0

### 3.6. Effect of CRC location (Publication III)

Furthermore, we investigated whether the observed alterations in  $V_{max}$  and  $K_m(ADP)$  values correlate with tumour location. CRC is more frequently observed in the distal colon (left colon, from the splenic flexure to the rectum) than in the proximal side (right colon, from the cecum to the transverse colon) (Missiaglia, Jacobs et al. 2014). Prior studies have indicated variations in epidemiology, biology, histology, and microbial diversity between tumours arising from the left and right colon (Missiaglia, Jacobs et al. 2014, Drewes, Housseau et al. 2016). Our study compared all distal and proximal tumours revealed differences in  $K_m(ADP)$  but not in  $V_{max}$  values (Figure 10).

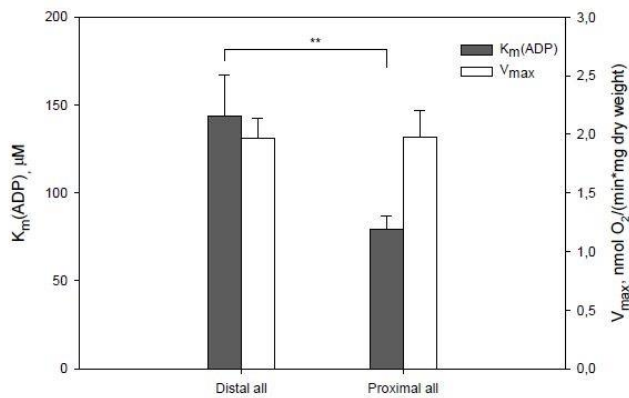


Figure 10. Comparison of maximal respiration ( $V_{max}$ ) and apparent Michaelis–Menten constant ( $K_m(ADP)$ ) values for ADP for both distal and proximal tumours. \*\* indicates a significant difference,  $p < 0.01$ . 20 distal and 24 proximal samples (Publication III).

### **3.7. Overview of sample types exhibiting diverse $K_m$ values (Publications I, II and III)**

The measured  $K_m(\text{ADP})$  values vary across different experimental materials: approximately 110  $\mu\text{M}$  for normal human colon mucosa (Rebane-Klemm, Truu et al. 2020), around 100  $\mu\text{M}$  for CRC tissue (Koit, Shevchuk et al. 2017, Rebane-Klemm, Truu et al. 2020), roughly 60  $\mu\text{M}$  for colon polyps ((Rebane-Klemm, Truu et al. 2020), about 40  $\mu\text{M}$  for the Caco2 cells (Ounpuu, Truu et al. 2018) and approximately 20-30  $\mu\text{M}$  for murine sarcoma cells (HL-1) and NEURO 2a (N2a) cell lines (Publication II) . These values suggest a shift in the control mechanisms regulating the permeability of VDAC and OXPHOS throughout the progression of malignancy. Thus, the regulation of the MOM permeability to adenine nucleotides in cancer tissues diverges from that in normal cells ((Koit, Shevchuk et al. 2017, Klepinin, Ounpuu et al. 2018). Notably,  $K_m(\text{ADP})$  values measured in cell cultures are markedly lower than those in tissue biopsies. They are similar to  $K_m(\text{ADP})$  values for isolated mitochondria at around 15  $\mu\text{M}$  (Chance and Williams 1955, Saks, Belikova et al. 1991). This indicates that the cell line models and colon polyp tissues experience fewer structural and functional constraints on ADP/ATP movement through the MOM, showing a metabolic shift towards aerobic glycolysis. Therefore, the  $K_m(\text{ADP})$  value serves as a crucial characteristic for describing metabolic plasticity.

### **3.8. The potential role of $\beta$ II-tubulin in aerobic glycolysis (Publication II)**

It has been shown that the VDAC in the MOM acts as the primary regulator, toggling between mitochondrial OXPHOS and glycolysis in malignant cells (Carre, Andre et al. 2002, Maldonado 2017). This discovery suggests that VDAC could serve as a promising target for a novel generation of cancer therapies.

The proteins regulating VDAC permeability for adenine nucleotides in colonocytes and their corresponding cancer cells remain unidentified. As previously mentioned, two potential mechanisms have been proposed for this regulation. Where the first proposes that the overexpression of mitochondria-bound HK2 in cancer cells promotes increased permeability of VDAC to adenine nucleotides, channelling ATP toward the glycolytic pathway, thereby facilitating aerobic glycolysis and initiating malignant metabolic reprogramming (Pedersen 2007). In the second model, the restriction of mitochondrial metabolism in cancer cells is proposed through the inhibition of VDAC by free tubulin (Maldonado, Patnaik et al. 2010). From this, we used cell line models to further understand whether unbound  $\beta$ II-tubulin may contend with HKs for attachment to VDAC within cancer cells. This competition is suggested to potentially play a role in modulating aerobic glycolysis in tumour cells.

It has been proposed that only non-polymerized  $\beta$ II-tubulin in the heart and soleus muscle play a crucial role in regulating the permeability of the MOM for ADP (Varikmaa, Bagur et al. 2014). It was indicated that the free dimeric tubulin affects VDAC permeability, but its impact is contingent on the polymerized/dimeric tubulin ratio. Thus, we wanted to show, in cancer cells, whether free  $\beta$ II-tubulin could compete with HK2 for binding sites on VDAC, thereby regulating aerobic glycolysis in tumour cells. The objective was to elucidate the involvement of free/polymerized  $\beta$ II-tubulin and HK2 in the regulation of energy transfer in malignancies.

In our investigation, we analysed the total  $\beta$  and  $\beta$ -II tubulin levels in HL-1 cells. The findings revealed that  $\beta$ -II tubulin makes up approximately half of the total  $\beta$ -tubulin content in these cells (*Figure 11a*). Interestingly, we found that the quantities of free

versus polymerized  $\beta$ -II tubulin are comparable to the total  $\beta$ -tubulin amount (Figure 11b). Using confocal microscopy, we observed that mitochondria within HL-1 cells exhibit a varied distribution: some are randomly dispersed, while others are anchored to  $\beta$ II-tubulin microfilaments and are predominantly located near the cell nucleus, a region characterized by higher energy requirements (Figure 13).

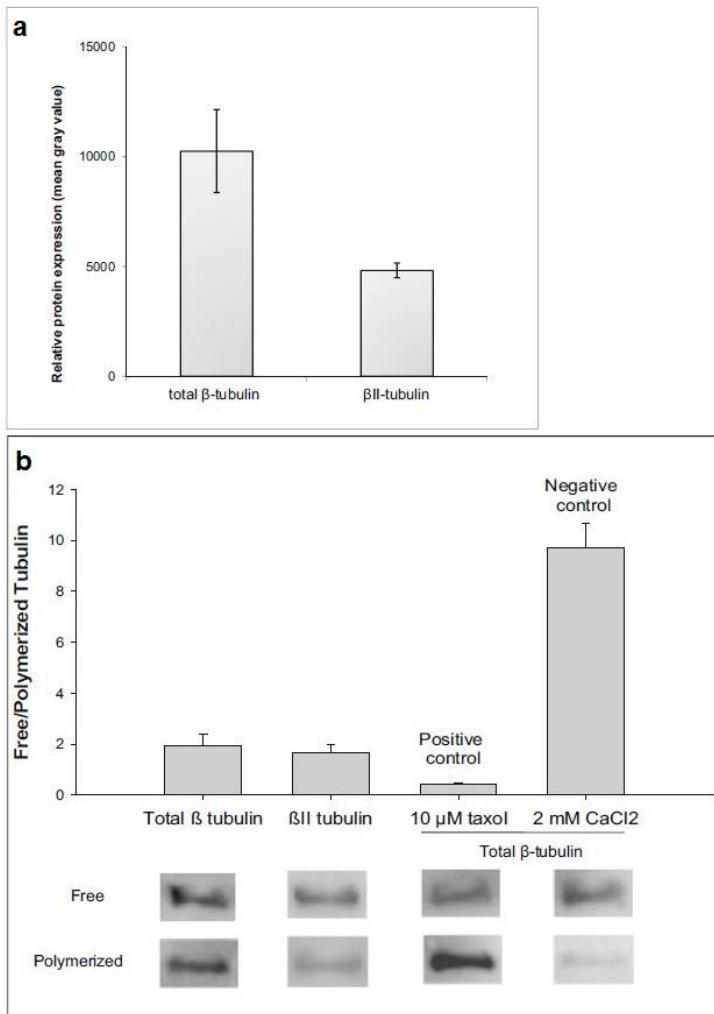


Figure 11. Western blot analysis for the presence of total  $\beta$  and  $\beta$ II-tubulin in HL-1 cells. (a) Densitometric quantification of the total  $\beta$  and  $\beta$ II-tubulin in the soluble and insoluble fractions of HL-1 cells. (b) Illustrative immunoblot test for free and polymerized total  $\beta$  and  $\beta$ II-tubulin in HL-1 cells. Error bars represent the mean  $\pm$  standard error from three separate experiments. \* $p < 0.05$  when compared to total  $\beta$ -tubulin in HL-1 cells; \*\* $p < 0.005$  when compared to  $\beta$ II-tubulin in HL-1 cells (Publication II).

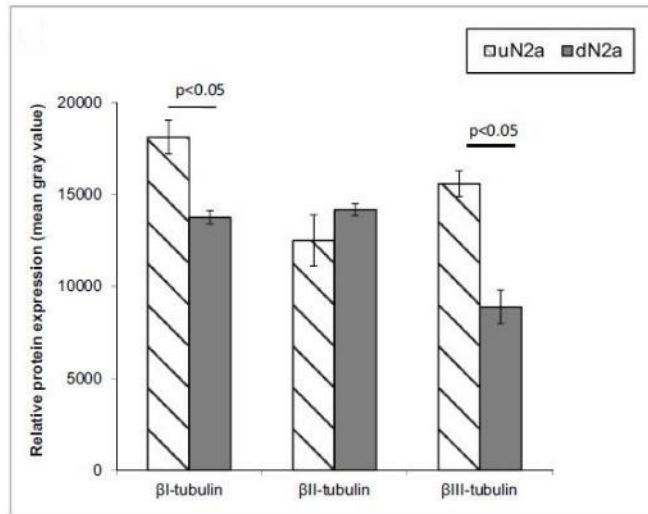


Figure 12. Western blot analysis for tubulin isoforms in N2a cells. (a) The expression levels of  $\beta$ I-,  $\beta$ II-, and  $\beta$ III-tubulin in both undifferentiated and retinoic acid (RA)-differentiated N2a cells. The error bars represent the mean  $\pm$  SE derived from five independent experiments (Publication II).

Given that  $\beta$ II-tubulin has been identified as a regulator of MOM permeability in brain synaptosomes (Monge, Beraud et al. 2008), our study extended to evaluating the  $\beta$ -tubulin isoforms in cancer cells of neurological origin. We cultured N2a cells in both differentiated and undifferentiated states to assess the variations in  $\beta$ -tubulin concentration and distribution during differentiation. Our findings indicated notable shifts in the  $\beta$ I- and  $\beta$ III-tubulin levels, while the amount of  $\beta$ II-tubulin stayed consistent (Figure 12).

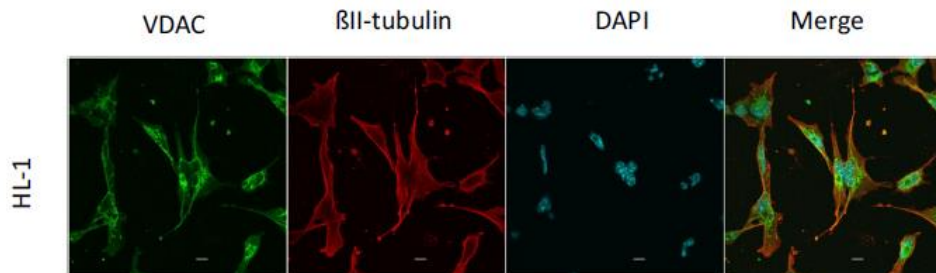
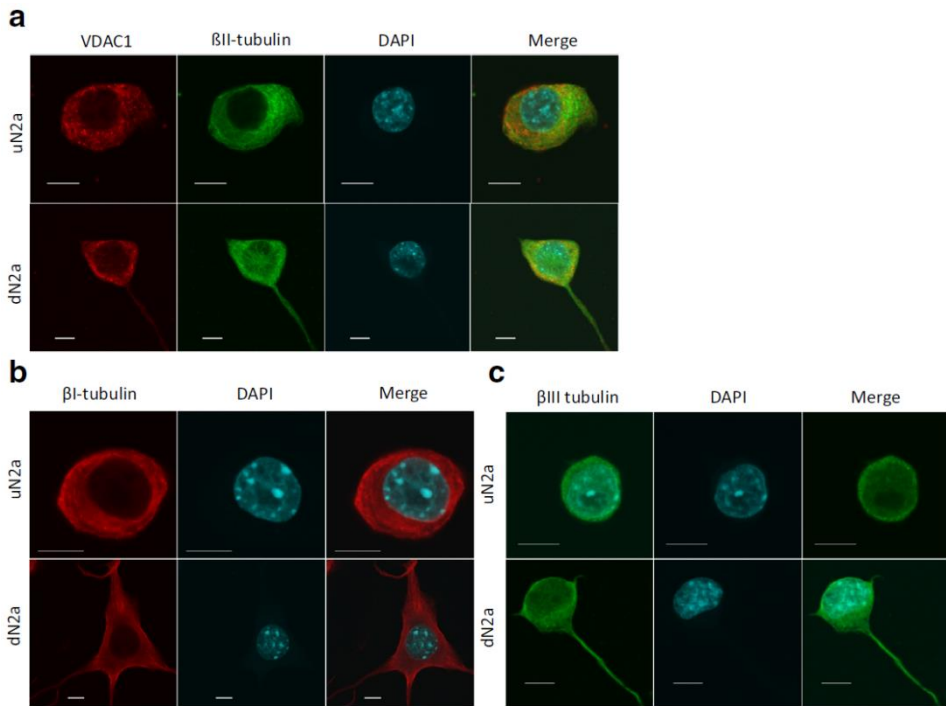


Figure 13. Confocal immunofluorescence imaging of the mitochondrial VDAC1 protein,  $\beta$ II-tubulin, the nucleus and their overlapping presence in HL-1 tumour cells. Cell nuclei were stained with DAPI (blue), VDAC1 protein (green),  $\beta$ II-tubulin (red), the scale bars are set at 10  $\mu$ m (Publication II).

Immunofluorescence analysis further revealed that the differentiation process in N2a cells resulted in significant changes in the cellular distribution of the primary  $\beta$ -tubulin isoforms. In undifferentiated N2a (uN2a) cells,  $\beta$ I-,  $\beta$ II-, and  $\beta$ III-tubulins were mainly concentrated around the cell nucleus. Contrastingly, in retinoic acid-treated cells, portions of the isoforms of these  $\beta$ -tubulin formed filamentous structures spanning the entirety of the cell and extending into the neurites (Figure 14 a-c).





*Figure 14. Confocal immunofluorescence imaging of the mitochondrial VDAC1 protein, tubulin isoforms and the nucleus in N2a cells. (a) Visualised mitochondrial VDAC1 protein (red),  $\beta$ II-tubulin (green), and their colocalization in undifferentiated (uN2a) and retinoic acid-differentiated (dN2a) cells with confocal immunofluorescence imaging. The distribution of  $\beta$ I-tubulin isoforms (red) (panel b) and  $\beta$ III-tubulin isoforms (green) (panel c) in uN2a and dN2a cells was examined. Cell nuclei were stained with DAPI (blue); scale bars represent 10  $\mu$ m (Publication II).*

Our confocal microscopy analysis of immunostained preparations of both uN2a and dN2a cells revealed a similar degree of HK2–VDAC colocalization, showing a tight coupling between VDAC and HK2, indicating that these cells are prone to aerobic glycolysis (Figure 15).

*Table 3. The effect of taxol and colchicine treatment in uN2a, dN2a, and HL-1 cells. Taxol and colchicine treatment on mitochondrial affinity for externally added ADP in undifferentiated (uN2a), retinoic acid-differentiated (dN2a), and HL-1 tumour cells.\* significance towards untreated cells;  $p < 0.05$ . These cells were treated overnight (a) or for 20 minutes (b) with 10  $\mu\text{M}$  colchicine or 10  $\mu\text{M}$  taxol before respiratory studies (Publication II).*

Cells and their treatments	$K_m^{\text{ADP}}$ for ADP, $\mu\text{M} \pm \text{SEM}$ ; $n = 4^{(a)}$	$K_m^{\text{ADP}}$ for ADP, $\mu\text{M} \pm \text{SEM}$ ; $n = 4^{(b)}$
HL-1 cells, control	$16.7 \pm 2.2$	–
HL-1, colchicine	$16 \pm 2$	–
HL-1, taxol	$25 \pm 5^*$	–
uN2a cells, control	$20 \pm 2$	$31.7 \pm 3.9$
uN2a, colchicine	$15 \pm 2$	$24.6 \pm 3.7$
uN2a, taxol	$37 \pm 3^*$	$30.4 \pm 4.5$
dN2a, control	–	$11.0 \pm 0.5$
dN2a, colchicine	–	$12.3 \pm 1.7$
dN2a, taxol	–	$11.0 \pm 1.1$

Furthermore, we measured the  $K_m(\text{ADP})$  values after stabilizing microtubules with taxol or destabilizing them with colchicine. Taxol stabilizes assembled microtubules and inversely decreases free tubulin content, while colchicine increases free tubulin levels in cells by inhibiting microtubule polymerization (Maldonado, Patnaik et al. 2010). We did not see any impact on the MOM permeability for ADP in either N2a or HL-1 cells (Table 3).

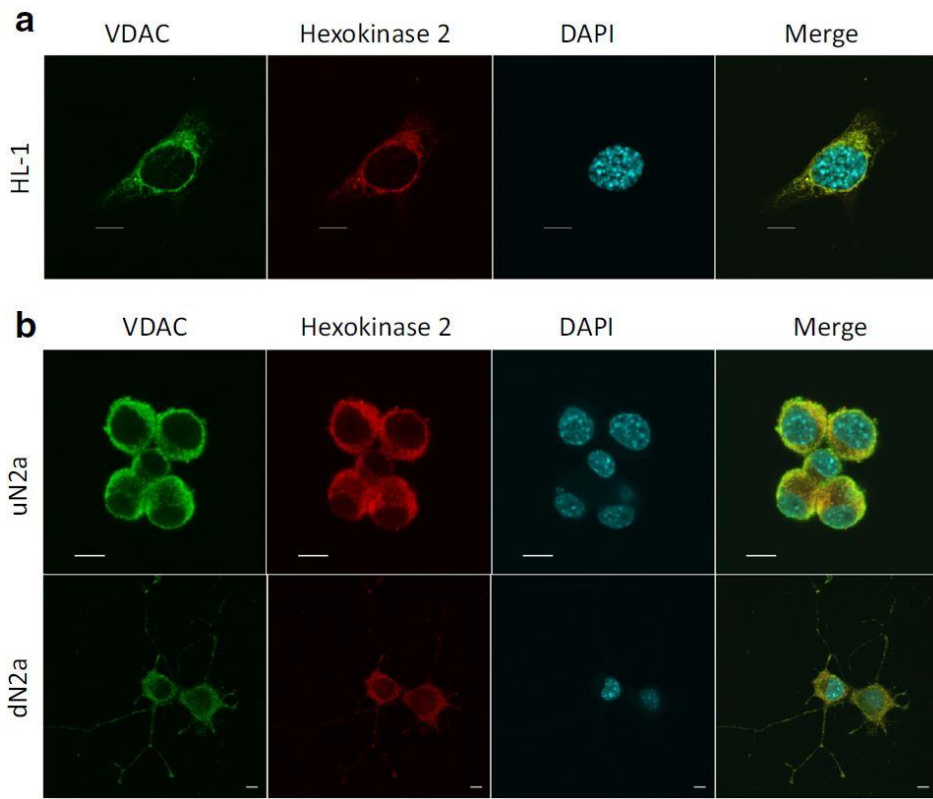


*Figure 15. Confocal immunofluorescence imaging of VDAC1 and HK2. (a) Imaging via confocal microscopy of VDAC1, HK2 and their colocalization in HL-1 cells. (b) The colocalization of VDAC1 and HK2 in both uN2a and dN2a. The cell nucleus is shown in blue (DAPI), HK2 in red, and VDAC1 in green; scale bars represent 10  $\mu$ M (Publication II).*

These observations conclude that  $\beta$ II-tubulin does not compete with HK for binding sites on VDAC in cancer cells. An intriguing possibility is the involvement of an alternate tubulin isoform, other than  $\beta$ II, in the regulation of MOM. In dN2a cells, compared to their undifferentiated counterparts, both  $\beta$ I- and  $\beta$ III-tubulin expressions are significantly reduced. Therefore,  $\beta$ III-tubulin emerges as a potential candidate for the regulatory protein of VDAC in neuroblastoma and other cancer cells.

The regulation of MOM permeability is a complex process that involves more than just the interaction between the VDAC channel and a single type of protein molecule. This study reveals that the presence of mitochondria-bound HK2 can influence the “Warburg effect” observed in murine neuroblastoma (NB) and cardiac sarcoma cells. We found that  $\beta$ II-tubulin has a limited role in regulating energy metabolism in sarcoma cells. Our findings also suggest that the binding sites within the MI for tubulin and HK differ in cancer cells. Additionally, alterations in MOM permeability for adenine nucleotides appear to be a distinctive trait of malignant tumours. While these findings are promising, they underscore the need for further research to fully understand the regulatory roles of different tubulin isoforms in VDAC function and cancer cell metabolism.

## Conclusions

The findings from this thesis showed a notable distinction in the metabolic profiles between clinical materials in the respiratory experiments:

- The  $V_{\max}$  value for colon control tissue is 3,4 times lower than in CRC tissue.
- Human CRC mitochondria exhibit higher  $K_m(\text{ADP})$  values than normal tissues, yet these values are still 6 times higher than those for isolated mitochondria.
- Deceased patients demonstrated significantly elevated  $V_{\max}$  values in comparison to patients who remained alive.

Significant differences were also seen in the respiration experiments on *KRAS/BRAF* mutated clinical materials of colon polyps and CRC:

- Wild-type tumours showed higher  $V_{\max}$  than *BRAF* or *KRAS* mutated tumours, indicating the role of these mutations in the metabolic shift to glycolysis in CRC.
- *KRAS* mutated polyps show signs of stimulated mitochondrial biogenesis, indicating early changes in the pre-malignant stage.
- $K_m(\text{ADP})$  values in CRC and colon polyps were 4-8 times higher than in isolated mitochondria, indicating limitations on ADP movement through mitochondrial membranes.
- Low  $K_m(\text{ADP})$  in colorectal polyps suggests early metabolic reprogramming toward a glycolytic phenotype with functional oxidative phosphorylation.

The experiments for MOM permeability in cell line models gave the following results:

- $\beta$ II-tubulin does not regulate MOM permeability for adenine nucleotides in N2a or HL-1 cell models, nor compete with HK for VDAC binding sites in cancer cells.
- Tight coupling between VDAC and HK2 in cancer cells was demonstrated.

## List of figures

Figure 1. The progression of colorectal cancer. ....	11
Figure 2. The Michaelis–Menten equation. ....	15
Figure 3. Michaelis-Menten kinetics and mitochondrial respiration. ....	16
Figure 4. Regulatory mechanisms in normal cells and CRC.....	19
Figure 5. Analysis of the normalized respiration rate patterns for CRC.....	23
Figure 6. Comparison of the maximal mitochondrial respiration rate ( $V_{max}$ ) across different stages of CRC.....	24
Figure 7. Regulation of mitochondrial respiration in tumours with <i>KRAS</i> +, <i>BRAF</i> + mutations, wild-type tumours, and control tissues. ....	25
Figure 8. Regulation of mitochondrial respiration in polyps with <i>KRAS</i> +, <i>BRAF</i> + mutations, wild-type polyps, and control tissues.....	26
Figure 9. The apparent Michaelis-Menten constant ( $K_m(\text{ADP})$ ) values for ADP in colorectal polyps, CRC and control tissues .....	27
Figure 10. Comparison of maximal respiration ( $V_{max}$ ) and apparent Michaelis–Menten constant ( $K_m(\text{ADP})$ ) values for ADP for both distal and proximal tumours. ....	28
Figure 11. Western blot analysis for the presence of total $\beta$ and $\beta$ II-tubulin in HL-1 cells. ....	30
Figure 12. Western blot analysis for tubulin isoforms in N2a cells.....	31
Figure 13. Confocal immunofluorescence imaging of the mitochondrial VDAC1 protein, $\beta$ II-tubulin, the nucleus and their overlapping presence in HL-1 tumour cells.....	31
Figure 14. Confocal immunofluorescence imaging of the mitochondrial VDAC1 protein, tubulin isoforms and the nucleus in N2a cells. ....	32
Figure 15. Confocal immunofluorescence imaging of VDAC1 and HK2. ....	34

## List of tables

Table 1. Apparent $K_m$ and maximum respiration rate ( $V_{max}$ ) values for CRC and the corresponding adjacent healthy tissues.. .....	22
Table 2. Modelled percentage of mitochondria with low oxidative capacity in tumours with <i>KRAS</i> , <i>BRAF</i> mutations, wild-type tumours.....	28
Table 3. The effect of taxol and colchicine treatment in uN2a, dN2a, and HL-1 cells. ...	33

## References

- Amamoto, R., T. Uchiumi, M. Yagi, K. Monji, Y. Song, Y. Oda, M. Shiota, A. Yokomizo, S. Naito and D. Kang (2016). "The Expression of Ubiquitous Mitochondrial Creatine Kinase Is Downregulated as Prostate Cancer Progression." J Cancer **7**(1): 50-59.
- Amoedo, N. D., M. F. Rodrigues and F. D. Rumjanek (2014). "MITOCHONDRIA: Are mitochondria accessory to metastasis?" The International Journal of Biochemistry & Cell Biology **51**: 53-57.
- Bellance, N., L. Pabst, G. Allen, R. Rossignol and D. Nagrath (2012). "Oncosecretomics coupled to bioenergetics identifies alpha-amino adipic acid, isoleucine and GABA as potential biomarkers of cancer: Differential expression of c-Myc, Oct1 and KLF4 coordinates metabolic changes." Biochim Biophys Acta **1817**(11): 2060-2071.
- Carre, M., N. Andre, G. Carles, H. Borghi, L. Bricchese, C. Briand and D. Braguer (2002). "Tubulin is an inherent component of mitochondrial membranes that interacts with the voltage-dependent anion channel." Journal of Biological Chemistry **277**(37): 33664-33669.
- Cesar Mde, C. and J. E. Wilson (1998). "Further studies on the coupling of mitochondrially bound hexokinase to intramitochondrially compartmented ATP, generated by oxidative phosphorylation." Arch Biochem Biophys **350**(1): 109-117.
- Chance, B. and G. R. Williams (1955). "Respiratory enzymes in oxidative phosphorylation. I. Kinetics of oxygen utilization." J Biol Chem **217**(1): 383-393.
- Chekulayev, V., K. Mado, I. Shevchuk, A. Koit, A. Kaldma, A. Klepinin, N. Timohhina, K. Tepp, M. Kandashvili, L. Ounpuu, K. Heck, L. Truu, A. Planken, V. Valvere and T. Kaambre (2015). "Metabolic remodeling in human colorectal cancer and surrounding tissues: alterations in regulation of mitochondrial respiration and metabolic fluxes." Biochem Biophys Rep **4**: 111-125.
- Chevrollier, A., D. Loiseau, P. Reynier and G. Stepien (2011). "Adenine nucleotide translocase 2 is a key mitochondrial protein in cancer metabolism." Biochimica et Biophysica Acta (BBA) - Bioenergetics **1807**(6): 562-567.
- Cicchillitti, L., R. Penci, M. Di Michele, F. Filippetti, D. Rotilio, M. B. Donati, G. Scambia and C. Ferlini (2008). "Proteomic characterization of cytoskeletal and mitochondrial class III beta-tubulin." Molecular Cancer Therapeutics **7**(7): 2070-2079.
- Cruz, M. D., S. Ledbetter, S. Chowdhury, A. K. Tiwari, N. Momi, R. K. Wali, C. Bliss, C. Huang, D. Lichtenstein, S. Bhattacharya, A. Varma-Wilson, V. Backman and H. K. Roy (2017). "Metabolic reprogramming of the premalignant colonic mucosa is an early event in carcinogenesis." Oncotarget **8**(13): 20543-20557.
- Database, T. H. S. a. H. R. (2020). PK10: Pahaloomuliste kasvajate esmasjuhud paikme, soo ja vanuserühma järgi. National Institute for Health Development.
- Development, N. I. f. H. (2020). SD21: Surmad põhjuse, soo ja vanuserühma järgi. The Health Statistics and Health Research Database.

- Diokmetzidou, A., E. Soumaka, I. Kloukina, M. Tsikitis, M. Makridakis, A. Varela, C. H. Davos, S. Georgopoulos, V. Anesti, A. Vlahou and Y. Capetanaki (2016). "Desmin and alphaB-crystallin interplay in maintenance of mitochondrial homeostasis and cardiomyocyte survival." J Cell Sci.
- Donohoe, D. R., N. Garge, X. Zhang, W. Sun, T. M. O'Connell, M. K. Bunger and S. J. Bultman (2011). "The microbiome and butyrate regulate energy metabolism and autophagy in the mammalian colon." Cell Metab **13**(5): 517-526.
- Drewes, J. L., F. Housseau and C. L. Sears (2016). "Sporadic colorectal cancer: microbial contributors to disease prevention, development and therapy." British Journal of Cancer **115**(3): 273-280.
- Dzeja, P. and A. Terzic (2009). "Adenylate kinase and AMP signaling networks: metabolic monitoring, signal communication and body energy sensing." Int J Mol Sci **10**(4): 1729-1772.
- Dzeja, P. P., R. J. Zeleznikar and N. D. Goldberg (1998). "Adenylate kinase: kinetic behavior in intact cells indicates it is integral to multiple cellular processes." Mol Cell Biochem **184**(1-2): 169-182.
- Dzeja, P. P. and A. Terzic (2003). "Phosphotransfer networks and cellular energetics." J Exp Biol **206**(Pt 12): 2039-2047.
- Fendt, S.-M., C. Frezza and A. Erez (2020). "Targeting Metabolic Plasticity and Flexibility Dynamics for Cancer Therapy." Cancer Discovery **10**(12): 1797-1807.
- Findeisen, P., S. Mühlhausen, S. Dempewolf, J. Hertzog, A. Zietlow, T. Carlomagno and M. Kollmar (2014). "Six subgroups and extensive recent duplications characterize the evolution of the eukaryotic tubulin protein family." Genome Biol Evol **6**(9): 2274-2288.
- Fujisawa, K., S. Terai, T. Takami, N. Yamamoto, T. Yamasaki, T. Matsumoto, K. Yamaguchi, Y. Owada, H. Nishina, T. Noma and I. Sakaida (2016). "Modulation of anti-cancer drug sensitivity through the regulation of mitochondrial activity by adenylate kinase 4." J Exp Clin Cancer Res **35**: 48.
- Globocan (2020). Cancer Fact Sheets, World Health Organization.
- Gogvadze, V., S. Orrenius and B. Zhivotovsky (2009). "Mitochondria as targets for cancer chemotherapy." Semin Cancer Biol **19**(1): 57-66.
- Gogvadze, V., S. Orrenius and B. Zhivotovsky (2009). "Mitochondria as targets for chemotherapy." Apoptosis **14**(4): 624-640.
- Goodpaster, B. H. and L. M. Sparks (2017). "Metabolic Flexibility in Health and Disease." Cell Metabolism **25**(5): 1027-1036.
- Guzun, R., T. Kaambre, R. Bagur, A. Grichine, Y. Usson, M. Varikmaa, T. Anmann, K. Tepp, N. Timohhina, I. Shevchuk, V. Chekulayev, F. Boucher, P. Dos Santos, U. Schlattner, T. Wallimann, A. V. Kuznetsov, P. Dzeja, M. Aliev and V. Saks (2015). "Modular organization of cardiac energy metabolism: energy conversion, transfer and feedback regulation." Acta Physiol (Oxf) **213**(1): 84-106.
- Han, C. Y., D. A. Patten, S. G. Lee, R. J. Parks, D. W. Chan, M. E. Harper and B. K. Tsang (2019). "p53 Promotes chemoresponsiveness by regulating hexokinase II gene transcription and metabolic reprogramming in epithelial ovarian cancer." Mol Carcinog **58**(11): 2161-2174.
- Hanahan, D. and R. A. Weinberg (2000). "The hallmarks of cancer." Cell **100**(1): 57-70.



- Hutton, J. E., X. Wang, L. J. Zimmerman, R. J. C. Slebos, I. A. Trenary, J. D. Young, M. Li and D. C. Liebler (2016). "Oncogenic KRAS and BRAF Drive Metabolic Reprogramming in Colorectal Cancer \*<sup><sup></sup></sup>." Molecular & Cellular Proteomics **15**(9): 2924-2938.
- Izuishi, K., Y. Yamamoto, T. Sano, R. Takebayashi, Y. Nishiyama, H. Mori, T. Masaki, A. Morishita and Y. Suzuki (2012). "Molecular mechanism underlying the detection of colorectal cancer by 18F-2-fluoro-2-deoxy-D-glucose positron emission tomography." J Gastrointest Surg **16**(2): 394-400.
- Iwamoto, M., K. Kawada, Y. Nakamoto, Y. Itatani, S. Inamoto, K. Toda, H. Kimura, T. Sasazuki, S. Shirasawa, H. Okuyama, M. Inoue, S. Hasegawa, K. Togashi and Y. Sakai (2014). "Regulation of <sup>18</sup>F-FDG Accumulation in Colorectal Cancer Cells with Mutated KRAS." Journal of Nuclear Medicine **55**(12): 2038-2044.
- Kaambre, T., V. Chekulayev, I. Shevchuk, M. Karu-Varikmaa, N. Timohhina, K. Tepp, J. Bogovskaja, R. Kutner, V. Valvere and V. Saks (2012). "Metabolic control analysis of cellular respiration in situ in intraoperational samples of human breast cancer." J Bioenerg Biomembr **44**(5): 539-558.
- Kaldma, A., A. Klepinin, V. Chekulayev, K. Mado, I. Shevchuk, N. Timohhina, K. Tepp, M. Kandashvili, M. Varikmaa, A. Koit, M. Planken, K. Heck, L. Truu, A. Planken, V. Valvere, E. Rebane and T. Kaambre (2014). "An in situ study of bioenergetic properties of human colorectal cancer: the regulation of mitochondrial respiration and distribution of flux control among the components of ATP synthasome." Int J Biochem Cell Biol **55**: 171-186.
- Kay, L., Z. Li, M. Mericskay, J. Olivares, L. Tranqui, E. Fontaine, T. Tiivel, P. Sikk, T. Kaambre, J. L. Samuel, L. Rappaport, Y. Usson, X. Leverve, D. Paulin and V. A. Saks (1997). "Study of regulation of mitochondrial respiration in vivo. An analysis of influence of ADP diffusion and possible role of cytoskeleton." Biochim Biophys Acta **1322**(1): 41-59.
- Klepinin, A., V. Chekulayev, N. Timohhina, I. Shevchuk, K. Tepp, A. Kaldma, A. Koit, V. Saks and T. Kaambre (2014). "Comparative analysis of some aspects of mitochondrial metabolism in differentiated and undifferentiated neuroblastoma cells." J Bioenerg Biomembr **46**(1): 17-31.
- Klepinin, A., L. Ounpuu, R. Guzun, V. Chekulayev, N. Timohhina, K. Tepp, I. Shevchuk, U. Schlattner and T. Kaambre (2016). "Simple oxygraphic analysis for the presence of adenylate kinase 1 and 2 in normal and tumor cells." J Bioenerg Biomembr **48**(5): 531-548.
- Klepinin, A., L. Ounpuu, K. Mado, L. Truu, V. Chekulayev, M. Puurand, I. Shevchuk, K. Tepp, A. Planken and T. Kaambre (2018). "The complexity of mitochondrial outer membrane permeability and VDAC regulation by associated proteins." J Bioenerg Biomembr **50**(5): 339-354.
- Klepinina, L., A. Klepinin, L. Truu, V. Chekulayev, H. Vija, K. Kuus, I. Teino, M. Pook, T. Maimets and T. Kaambre (2021). "Colon cancer cell differentiation by sodium butyrate modulates metabolic plasticity of Caco-2 cells via alteration of phosphotransfer network." PLoS One **16**(1): e0245348.

- Koita, A., I. Shevchuk, L. Ounpuu, A. Klepinin, V. Chekulayev, N. Timohhina, K. Tepp, M. Puurand, L. Truu, K. Heck, V. Valvere, R. Guzun and T. Kaambre (2017). "Mitochondrial Respiration in Human Colorectal and Breast Cancer Clinical Material Is Regulated Differently." *Oxid Med Cell Longev* **2017**: 1372640.
- Kuznetsov, A. V., D. Strobl, E. Ruttmann, A. Konigsrainer, R. Margreiter and E. Gnaiger (2002). "Evaluation of mitochondrial respiratory function in small biopsies of liver." *Anal Biochem* **305**(2): 186-194.
- Kuznetsov, A. V., T. Tiivel, P. Sikk, T. Kaambre, L. Kay, Z. Daneshrad, A. Rossi, L. Kadaja, N. Peet, E. Seppet and V. A. Saks (1996). "Striking differences between the kinetics of regulation of respiration by ADP in slow-twitch and fast-twitch muscles in vivo." *Eur J Biochem* **241**(3): 909-915.
- Kuznetsov, A. V., V. Veksler, F. N. Gellerich, V. Saks, R. Margreiter and W. S. Kunz (2008). "Analysis of mitochondrial function in situ in permeabilized muscle fibers, tissues and cells." *Nat Protoc* **3**(6): 965-976.
- Lamb, R., G. Bonuccelli, B. Ozsvari, M. Peiris-Pages, M. Fiorillo, D. L. Smith, G. Bevilacqua, C. M. Mazzanti, L. A. McDonnell, A. G. Naccarato, M. Chiu, L. Wynne, U. E. Martinez-Outschoorn, F. Sotgia and M. P. Lisanti (2015). "Mitochondrial mass, a new metabolic biomarker for stem-like cancer cells: Understanding WNT/FGF-driven anabolic signaling." *Oncotarget* **6**(31): 30453-30471.
- Leandro-Garcia, L. J., S. Leskela, I. Landa, C. Montero-Conde, E. Lopez-Jimenez, R. Leton, A. Cascon, M. Robledo and C. Rodriguez-Antona (2010). "Tumoral and tissue-specific expression of the major human beta-tubulin isoforms." *Cytoskeleton (Hoboken)* **67**(4): 214-223.
- Lemasters, J. J. and E. Holmuhamedov (2006). "Voltage-dependent anion channel (VDAC) as mitochondrial governor--thinking outside the box." *Biochim Biophys Acta* **1762**(2): 181-190.
- Ludueña, R. F., E. M. Shooter and L. Wilson (1977). "Structure of the tubulin dimer." *J Biol Chem* **252**(20): 7006-7014.
- Mahmod, A. I., S. K. Haif, A. Kamal, I. A. Al-ataby and W. H. Talib (2022). "Chemoprevention effect of the Mediterranean diet on colorectal cancer: Current studies and future prospects." *Frontiers in Nutrition* **9**.
- Majewski, N., V. Nogueira, P. Bhaskar, P. E. Coy, J. E. Skeen, K. Gottlob, N. S. Chandel, C. B. Thompson, R. B. Robey and N. Hay (2004). "Hexokinase-mitochondria interaction mediated by Akt is required to inhibit apoptosis in the presence or absence of Bax and Bak." *Mol Cell* **16**(5): 819-830.
- Maldonado, E. N. (2017). "VDAC-Tubulin, an Anti-Warburg Pro-Oxidant Switch." *Front Oncol* **7**: 4.
- Maldonado, E. N. and J. J. Lemasters (2012). "Warburg revisited: regulation of mitochondrial metabolism by voltage-dependent anion channels in cancer cells." *J Pharmacol Exp Ther* **342**(3): 637-641.
- Maldonado, E. N., J. Patnaik, M. R. Mullins and J. J. Lemasters (2010). "Free tubulin modulates mitochondrial membrane potential in cancer cells." *Cancer Res* **70**(24): 10192-10201.

- Maldonado, E. N., K. L. Sheldon, D. N. DeHart, J. Patnaik, Y. Manevich, D. M. Townsend, S. M. Bezrukov, T. K. Rostovtseva and J. J. Lemasters (2013). "Voltage-dependent anion channels modulate mitochondrial metabolism in cancer cells: regulation by free tubulin and erastin." J Biol Chem **288**(17): 11920-11929.
- Mathupala, S. P., Y. H. Ko and P. L. Pedersen (2006). "Hexokinase II: cancer's double-edged sword acting as both facilitator and gatekeeper of malignancy when bound to mitochondria." Oncogene **25**(34): 4777-4786.
- Mathupala, S. P., Y. H. Ko and P. L. Pedersen (2009). "Hexokinase-2 bound to mitochondria: cancer's stygian link to the "Warburg Effect" and a pivotal target for effective therapy." Semin Cancer Biol **19**(1): 17-24.
- Mattiuzzi, C., F. Sanchis-Gomar and G. Lippi (2019). "Concise update on colorectal cancer epidemiology." Ann Transl Med **7**(21): 609.
- McGuirk, S., Y. Audet-Delage and J. St-Pierre (2020). "Metabolic Fitness and Plasticity in Cancer Progression." Trends Cancer **6**(1): 49-61.
- Michaelis, L. and M. L. Menten (1913). "Die kinetik der invertinwirkung Biochem Z 49: 333-369." [Find this article online.](#)
- Missiaglia, E., B. Jacobs, G. D'Ario, A. F. Di Narzo, C. Sonesson, E. Budinska, V. Popovici, L. Vecchione, S. Gerster, P. Yan, A. D. Roth, D. Klingbiel, F. T. Bosman, M. Delorenzi and S. Tejpar (2014). "Distal and proximal colon cancers differ in terms of molecular, pathological, and clinical features." Annals of Oncology **25**(10): 1995-2001.
- Monge, C., N. Beraud, A. V. Kuznetsov, T. Rostovtseva, D. Sackett, U. Schlattner, M. Vendelin and V. A. Saks (2008). "Regulation of respiration in brain mitochondria and synaptosomes: restrictions of ADP diffusion in situ, roles of tubulin, and mitochondrial creatine kinase." Mol Cell Biochem **318**(1-2): 147-165.
- Moreno-Sanchez, R., A. Marin-Hernandez, E. Saavedra, J. P. Pardo, S. J. Ralph and S. Rodriguez-Enriquez (2014). "Who controls the ATP supply in cancer cells? Biochemistry lessons to understand cancer energy metabolism." Int J Biochem Cell Biol **50**: 10-23.
- Moreno-Sanchez, R., S. Rodriguez-Enriquez, A. Marin-Hernandez and E. Saavedra (2007). "Energy metabolism in tumor cells." FEBS J **274**(6): 1393-1418.
- Ounpuu, L., A. Klepinin, M. Pook, I. Teino, N. Peet, K. Paju, K. Tepp, V. Chekulayev, I. Shevchuk, S. Koks, T. Maimets and T. Kaambre (2017). "2102Ep embryonal carcinoma cells have compromised respiration and shifted bioenergetic profile distinct from H9 human embryonic stem cells." Biochim Biophys Acta Gen Subj **1861**(8): 2146-2154.
- Ounpuu, L., A. Klepinin, M. Pook, I. Teino, N. Peet, K. Paju, K. Tepp, V. Chekulayev, I. Shevchuk, S. Koks, T. Maimets and T. Kaambre (2017). "2102Ep embryonal carcinoma cells have compromised respiration and shifted bioenergetic profile distinct from H9 human embryonic stem cells." Biochim Biophys Acta **1861**(8): 2146-2154.
- Ounpuu, L., L. Truu, I. Shevchuk, V. Chekulayev, A. Klepinin, A. Koit, K. Tepp, M. Puurand, E. Rebane-Klemm and T. Kaambre (2018). "Comparative analysis of the bioenergetics of human adenocarcinoma Caco-2 cell line and postoperative tissue samples from colorectal cancer patients." Biochem Cell Biol: 1-10.

- Pavlova, Natalya N. and Craig B. Thompson (2016). "The Emerging Hallmarks of Cancer Metabolism." Cell Metabolism **23**(1): 27-47.
- Pedersen, P. L. (2007). "Warburg, me and Hexokinase 2: Multiple discoveries of key molecular events underlying one of cancers' most common phenotypes, the "Warburg Effect", i.e., elevated glycolysis in the presence of oxygen." J Bioenerg Biomembr **39**(3): 211-222.
- Phipps, A. I., D. D. Buchanan, K. W. Makar, A. K. Win, J. A. Baron, N. M. Lindor, J. D. Potter and P. A. Newcomb (2013). "KRAS-mutation status in relation to colorectal cancer survival: the joint impact of correlated tumour markers." British Journal of Cancer **108**(8): 1757-1764.
- Puurand, M., K. Tepp, A. Klepinin, L. Klepinina, I. Shevchuk and T. Kaambre (2018). "Intracellular Energy-Transfer Networks and High-Resolution Respirometry: A Convenient Approach for Studying Their Function." Int J Mol Sci **19**(10).
- Puurand, M., K. Tepp, N. Timohhina, J. Aid, I. Shevchuk, V. Chekulayev and T. Kaambre (2019). "Tubulin betaII and betaIII Isoforms as the Regulators of VDAC Channel Permeability in Health and Disease." Cells **8**(3).
- Rebane-Klemm, E., L. Truu, L. Reinsalu, M. Puurand, I. Shevchuk, V. Chekulayev, N. Timohhina, K. Tepp, J. Bogovskaja, V. Afanasjev, K. Suurmaa, V. Valvere and T. Kaambre (2020). "Mitochondrial Respiration in KRAS and BRAF Mutated Colorectal Tumors and Polyps." Cancers (Basel) **12**(4).
- Reinsalu, L., M. Puurand, V. Chekulayev, S. Miller, I. Shevchuk, K. Tepp, E. Rebane-Klemm, N. Timohhina, A. Terasmaa and T. Kaambre (2021). "Energy Metabolic Plasticity of Colorectal Cancer Cells as a Determinant of Tumor Growth and Metastasis." Front Oncol **11**: 698951.
- Rostovtseva, T. K., P. A. Gurnev, D. P. Hoogerheide, A. Rovini, M. Sirajuddin and S. M. Bezrukov (2018). "Sequence diversity of tubulin isoforms in regulation of the mitochondrial voltage-dependent anion channel." J Biol Chem **293**(28): 10949-10962.
- Rostovtseva, T. K., K. L. Sheldon, E. Hassanzadeh, C. Monge, V. Saks, S. M. Bezrukov and D. L. Sackett (2008). "Tubulin binding blocks mitochondrial voltage-dependent anion channel and regulates respiration." Proc Natl Acad Sci U S A **105**(48): 18746-18751.
- Saks, V., P. Dzeja, U. Schlattner, M. Vendelin, A. Terzic and T. Wallimann (2006). "Cardiac system bioenergetics: metabolic basis of the Frank-Starling law." J Physiol **571**(Pt 2): 253-273.
- Saks, V. A., Y. O. Belikova and A. V. Kuznetsov (1991). "In vivo regulation of mitochondrial respiration in cardiomyocytes: specific restrictions for intracellular diffusion of ADP." Biochim Biophys Acta **1074**(2): 302-311.
- Saks, V. A., A. V. Kuznetsov, Z. A. Khuchua, E. V. Vasilyeva, J. O. Belikova, T. Kesvatera and T. Tiivel (1995). "Control of cellular respiration in vivo by mitochondrial outer membrane and by creatine kinase. A new speculative hypothesis: possible involvement of mitochondrial-cytoskeleton interactions." J Mol Cell Cardiol **27**(1): 625-645.

- Saks, V. A., V. I. Veksler, A. V. Kuznetsov, L. Kay, P. Sikk, T. Tiivel, L. Tranqui, J. Olivares, K. Winkler, F. Wiedemann and W. S. Kunz (1998). "Permeabilized cell and skinned fiber techniques in studies of mitochondrial function in vivo." Mol Cell Biochem **184**(1-2): 81-100.
- Shaukat, A., C. J. Kahi, C. A. Burke, L. Rabeneck, B. G. Sauer and D. K. Rex (2021). "ACG Clinical Guidelines: Colorectal Cancer Screening 2021." Am J Gastroenterol **116**(3): 458-479.
- Shirasawa, S., M. Furuse, N. Yokoyama and T. Sasazuki (1993). "Altered growth of human colon cancer cell lines disrupted at activated Ki-ras." Science **260**(5104): 85-88.
- Shoshan-Barmatz, V., A. Israelson, D. Brdiczka and S. S. Sheu (2006). "The voltage-dependent anion channel (VDAC): function in intracellular signalling, cell life and cell death." Curr Pharm Des **12**(18): 2249-2270.
- Shoshan-Barmatz, V., Y. Krelin, A. Shteinfein-Kuzmine and T. Arif (2017). "Voltage-Dependent Anion Channel 1 As an Emerging Drug Target for Novel Anti-Cancer Therapeutics." Front Oncol **7**: 154.
- Shoshan-Barmatz, V., M. Zakar, K. Rosenthal and S. Abu-Hamad (2009). "Key regions of VDAC1 functioning in apoptosis induction and regulation by hexokinase." Biochim Biophys Acta **1787**(5): 421-430.
- Sninsky, J. A., B. M. Shore, G. V. Lupu and S. D. Crockett (2022). "Risk Factors for Colorectal Polyps and Cancer." Gastrointest Endosc Clin N Am **32**(2): 195-213.
- Society, A. C. (2008). Cancer facts & figures, The Society.
- Zhou, Y., F. Tozzi, J. Chen, F. Fan, L. Xia, J. Wang, G. Gao, A. Zhang, X. Xia, H. Brasher, W. Widger, L. M. Ellis and Z. Weihua (2012). "Intracellular ATP levels are a pivotal determinant of chemoresistance in colon cancer cells." Cancer Res **72**(1): 304-314.
- Tepp, K., K. Mado, M. Varikmaa, A. Klepinin, N. Timohhina, I. Shevchuk, V. Chekulayev, A. V. Kuznetsov, R. Guzun and T. Kaambre (2014). "The role of tubulin in the mitochondrial metabolism and arrangement in muscle cells." J Bioenerg Biomembr **46**(5): 421-434.
- Timohhina, N., R. Guzun, K. Tepp, C. Monge, M. Varikmaa, H. Vija, P. Sikk, T. Kaambre, D. Sackett and V. Saks (2009). "Direct measurement of energy fluxes from mitochondria into cytoplasm in permeabilized cardiac cells in situ: some evidence for Mitochondrial Interactosome." J Bioenerg Biomembr **41**(3): 259-275.
- Wallace, D. C. (1999). "Mitochondrial diseases in man and mouse." Science **283**(5407): 1482-1488.
- Vander Heiden, M. G., L. C. Cantley and C. B. Thompson (2009). "Understanding the Warburg effect: the metabolic requirements of cell proliferation." Science **324**(5930): 1029-1033.
- Wang, P., M. Song, Z.-l. Zeng, C.-f. Zhu, W.-h. Lu, J. Yang, M.-z. Ma, A.-m. Huang, Y. Hu and P. Huang (2015). "Identification of NDUFAF1 in mediating K-Ras induced mitochondrial dysfunction by a proteomic screening approach." Oncotarget **6**(6).

- Warburg, O. (1956). "On respiratory impairment in cancer cells." Science **124**(3215): 269-270.
- Warburg, O., F. Wind and E. Negelein (1927). "The Metabolism of Tumors in the Body." J Gen Physiol **8**(6): 519-530.
- Warburg, O. H. and F. Dickens (1930). The metabolism of tumours. London, Constable.
- Varikmaa, M., R. Bagur, T. Kaambre, A. Grichine, N. Timohhina, K. Tepp, I. Shevchuk, V. Chekulayev, M. Metsis, F. Boucher, V. Saks, A. V. Kuznetsov and R. Guzun (2014). "Role of mitochondria-cytoskeleton interactions in respiration regulation and mitochondrial organization in striated muscles." Biochim Biophys Acta **1837**(2): 232-245.
- Yeh, I. T. and R. F. Luduena (2004). "The betaII isotype of tubulin is present in the cell nuclei of a variety of cancers." Cell Motil Cytoskeleton **57**(2): 96-106.
- Yun, J., C. Rago, I. Cheong, R. Pagliarini, P. Angenendt, H. Rajagopalan, K. Schmidt, J. K. Willson, S. Markowitz, S. Zhou, L. A. Diaz, Jr., V. E. Velculescu, C. Lengauer, K. W. Kinzler, B. Vogelstein and N. Papadopoulos (2009). "Glucose deprivation contributes to the development of KRAS pathway mutations in tumor cells." Science **325**(5947): 1555-1559.

## Acknowledgements

I would like to extend my deepest gratitude to my supervisor Tuuli Käämbre, whose guidance and expertise were instrumental in shaping this research. Your unwavering support and invaluable insights have been a cornerstone of this journey. I would also like to express my heartfelt thanks to the people in the Laboratory of Chemical Biology, whose assistance and dedication played a crucial role in the successful completion of my experiments. I would like to specially bring out and thank Marju Puurand and Egle Rebane-Klemm, since your collaborative spirit and strive for excellence have been truly inspiring.

I am immensely grateful to the people involved from the Department of Chemistry and Biotechnology for their steadfast belief in my abilities and for never giving up on me, even during the most challenging times. Your encouragement and faith have been a source of strength and motivation, driving me to persevere and succeed.

I owe a special gratitude to my colleagues from SYNLAB for their support both in time and motivation. Especially, Andrio and Kaspar, your camaraderie, experience, and encouragement have been invaluable to my research and personal well-being. The environment of mutual support and dedication we have shared has been instrumental in overcoming challenges and maintaining focus.

To my mother Elle, words cannot express my appreciation for your unconditional love and support. You have been the backbone of my academic journey, enabling me to prioritize my studies. Your sacrifices and unwavering belief in me have been the driving force behind my achievements.

Lastly, I owe a special debt of gratitude to my partner Henrik, who has been my rock throughout this process already from the 10th grade. Your psychological support and understanding have been invaluable. Your encouragement and empathy have been a constant source of comfort and reassurance, helping me navigate the ups and downs of this academic endeavor.

To all of you, I am eternally grateful, thank you from the bottom of my heart.

## Abstract

### The permeability of mitochondrial outer membrane and metabolic plasticity in colorectal cancer

This doctoral thesis provides a detailed investigation into the metabolic reprogramming of colorectal cancer (CRC), emphasizing the crucial role of mitochondrial alterations in cancer progression and the potential for targeted therapies. The novelty of this work lies in its in-depth examination of mitochondrial function in CRC using clinical samples in addition to cell culture models. This approach offers a more accurate representation of the molecular metabolism of the disease, contributing to a better understanding of CRC.

Employing high-resolution respirometry, the study measured the maximal rate of ADP-activated respiration ( $V_{\max}$ ) and determined apparent  $K_m$  values for exogenously added ADP ( $K_m(\text{ADP})$ ) in permeabilized postoperative tissues, including CRC, colon polyps, and normal colon tissue. The methodologies encompassed a range of techniques such as mitochondrial respiration/oxygraphic measurements, immunofluorescence analysis, *KRAS*, and *BRAF* mutation analysis.

The research findings revealed that tumours with wild-type characteristics exhibited the highest  $V_{\max}$ , whereas *BRAF* or *KRAS* mutated tumours displayed significantly lower values, indicating a glycolytic shift in mitochondrial metabolism. This observation underscores the involvement of oncogenic *KRAS* and *BRAF* in steering CRC metabolism toward a more glycolytic profile. In addition, notable differences in  $V_{\max}$  values were observed between *BRAF* mutated and *KRAS* mutated tumours, with the  $V_{\max}$  of *BRAF* mutated tumours resembling that of control tissues. Whereas, the result that polyps with *KRAS* mutations exhibited indications of enhanced mitochondrial biogenesis was unexpected, suggesting a possible evolution towards aggressively metastatic malignant tumours. This suggests that alterations in mitochondrial biogenesis might be an initial event, already evident in the pre-malignant phase.

The study also found that an increase in  $V_{\max}$  during the initial stages of CRC showed significant differences in comparison to control samples, but this trend declined in advanced stages. This result challenges the reliability of the disease stage at the time of diagnosis as a dependable indicator of aggressiveness. The  $V_{\max}$  pattern in colorectal polyps closely mirrored that of the corresponding tumours, while polyps harbouring the *BRAF* mutation displayed a tendency toward lower OXPHOS rates compared to mutated *KRAS* and wild-type groups. This suggests a distinctive role of mutated *KRAS* and *BRAF* in influencing mitochondrial biogenesis and likely contributing to tissue differentiation.

Furthermore, the heterogeneity of colon tissue was explored, revealing a biphasic pattern in respiration regulation in healthy colon tissues. Higher  $V_{\max}$  values in CRC cells compared to normal colon tissue suggest robust metabolic activity and are correlated with mitochondrial density.

In the study, it was found that  $\beta$ II-tubulin does not influence the permeability of the mitochondrial outer membrane (MOM) for adenine nucleotides in N2a and HL-1 cell models. Consequently, it appears that  $\beta$ II-tubulin is not a competitor for HK in attaching to the VDAC binding sites in cancer cells. This is further supported by the observation of a close association between VDAC and HK2, suggesting a predisposition of these cells towards aerobic glycolysis. In conclusion, this thesis underscores the complexity and significance of metabolic reprogramming in CRC, particularly in the regulation of mitochondrial respiration.



The results provide valuable insights into the metabolic heterogeneity of CRC and highlight the importance of considering mitochondrial density and metabolic plasticity in understanding CRC progression. This research contributes significantly to the field by elucidating metabolic alterations at the mitochondrial level and their implications in cancer development and progression, paving the way for further studies to explore the potential of targeting mitochondrial metabolism in cancer therapy.

## Lühikokkuvõte

### Mitokondrite välismembraani läbitavus ja metaboolne plastilisus käärsoolevähis

See doktoritöö pakub põhjalikku uurimust käärsoolevähi (CRC) ainevahetuse ümberprogrammeerimisest, rõhutades mitokondriaalsete muutuste olulisust vähktõve arengus ja sihipäraste teraapiate potentsiaali. Selle töö uuenduslikkus seisneb CRC mitokondrite funktsiooni süvitsi uurimises, kasutades kliinilisi proove lisaks rakukultuuri mudelitele. Selline lähenemine pakub täpsemat ülevaadet haiguse molekulaarsest ainevahetusest, aidates paremini mõista käärsoolevähi teket ja arengut.

Kasutades kõrglahutusega respiromeetriaat, mõõdeti uurimuses ADP-aktiveeritud hingamise maksimaalset kiirust ( $V_{max}$ ) ja määrati Michaelis-Menteni konstant ADP suhtes ( $K_m(ADP)$ ) permeabiliseeritud postoperatiivsetes kudedes, sealhulgas käärsoole vähis, polüüpides ja normaalses soolekoes. Töös kasutati erinevaid meetodikaid nagu oksügraafilised mõõtmised, immunofluorestsentsanalüüs, *KRAS* ja *BRAF* mutatsioonide analüüs.

Uurimistulemused näitasid, et metsiktüüpi omadustega kasvajakasvajad ilmutasid kõrgeimat  $V_{max}$  väärtust, samas kui *KRAS* ja *BRAF* mutatsioonidega kasvajakasvajad näitasid selle oluliselt madalamaid väärtusi, viidates glükolüütilisele nihkele mitokondriaalses ainevahetuses. See leid rõhutab onkogeensete *KRAS* ja *BRAF* mutatsioonide osalust CRC ainevahetuse suunamisel glükolüütilise profiili suunas. Lisaks täheldati olulisi erinevusi  $V_{max}$  väärtustes *KRAS* ja *BRAF* mutatsioonidega kasvajate vahel, kusjuures *BRAF* mutatsioonidega kasvajate  $V_{max}$  oli võrreldav kontrollkoe omaga. Samas oli üllatav, et *KRAS* mutatsioonidega polüüpidel ilmnes stimuleeritud mitokondriaalsele biogeneesile vihjavaid parameetreid, mis viitab potentsiaalsele arengule agressiivsete metastaatiliste pahaloomuliste kasvajate suunas. See näitab omakorda, et muutused mitokondriaalses biogeneesis võivad ilmuda juba koe premaliigsetes faasides.

Töös leiti samuti, et  $V_{max}$  väärtuse suurenemine juba käärsoolevähi algfaasides näitas olulisi erinevusi võrreldes kontrollproovidega, kuid see trend vähenes haiguse hilises staadiumis. See avastus seab küsimärgi alla haiguse staadiumi kui diagnoosimise hetkel kasutatava agressiivsuse indikaatori usaldusväärsuse. CRC polüüpides täheldatud  $V_{max}$  väärtuste muster oli sarnane vastavate kasvajate omaga, samal ajal kui *BRAF* mutatsiooniga polüübid näitasid madalamat oksüdatiivse fosforüleerimise kiirust võrreldes *KRAS* mutatsioonidega ja metsiktüüpi grupiga. See viitab *KRAS* ja *BRAF* mutatsioonide erinevatele rollidele mitokondriaalse biogeneesi mõjutamisel ja tõenäoliselt koe diferentseerumisele.

Lisaks tehti käärsoolekoe heterogeensuse uuringuid, mille käigus ilmnes, et tervete käärsoolekoe rakkude hingamise regulatsioon varieerub sõltuvalt koe tüübist. Kõrgemad  $V_{max}$  väärtused käärsoolevähi rakkudes võrreldes normaalse käärsoolekoe rakkudega viitavad suurele metabolismi aktiivsusele ja on seotud mitokondrite arvukuse tõusuga.

Töös leiti ka, et  $\beta$ II-tubuliin ei mõjuta mitokondriaalse välismembraani (MOM) läbilaskvust ADP-le N2a ja HL-1 rakumudelites. Seetõttu näib, et  $\beta$ II-tubuliin ei konkureeri heksokinaasiga (HK) pingest-sõltuva anioonkanali (VDAC) sidumiskohtadele kasvajakarakkudes.

Kokkuvõttes rõhutab see doktoritöö käärsoolevähi energiametabolismi ümberprogrammeerimise keerukust ja olulisust, eriti ATP sünteesi regulatsiooni osas. Tulemused pakuvad väärtuslikke teadmisi CRC ainevahetuslikust heterogeensusest ja

rõhutavad mitokondrite tiheduse ja metaboolse plastilisuse tähtsust kasvaja arengu mõistmisel. Uurimus annab olulise panuse onkoloogia ja molekulaarbioloogia valdkonda, selgitades ainevahetuslikke muutusi mitokondrites ja nende mõju vähi arengule ja progresseerumisele, sillutades teed edasistele uuringutele, et uurida mitokondriaalse ainevahetuse potentsiaali suunatud vähiravis ja diagnostikas.

# Appendix 1

## **Publication I**

Koit, A., I. Shevchuk, L. Ounpuu, A. Klepinin, V. Chekulayev, N. Timohhina, K. Tepp, M. Puurand, L. Truu, K. Heck, V. Valvere, R. Guzun and T. Kaambre (2017). "Mitochondrial Respiration in Human Colorectal and Breast Cancer Clinical Material Is Regulated Differently." *Oxid Med Cell Longev* 2017: 1372640.



## Research Article

# Mitochondrial Respiration in Human Colorectal and Breast Cancer Clinical Material Is Regulated Differently

Andre Koit,<sup>1</sup> Igor Shevchuk,<sup>1</sup> Lyudmila Ounpuu,<sup>1</sup> Aleksandr Klepinin,<sup>1</sup> Vladimir Chekulayev,<sup>1</sup> Natalja Timohhina,<sup>1</sup> Kersti Tepp,<sup>1</sup> Marju Puurand,<sup>1</sup> Laura Truu,<sup>1</sup> Karoliina Heck,<sup>2</sup> Vahur Valvere,<sup>2</sup> Rita Guzun,<sup>3</sup> and Tuuli Kaambre<sup>1,4</sup>

<sup>1</sup>Laboratory of Bioenergetics, National Institute of Chemical Physics and Biophysics, Tallinn, Estonia

<sup>2</sup>Oncology and Haematology Clinic at the North Estonia Medical Centre, Tallinn, Estonia

<sup>3</sup>Laboratory of Fundamental and Applied Bioenergetics, INSERM, University Grenoble Alpes, U1055 Grenoble, France

<sup>4</sup>School of Natural Sciences and Health, Tallinn University, Tallinn, Estonia

Correspondence should be addressed to Tuuli Kaambre; [tuuli.kaambre@kbfi.ee](mailto:tuuli.kaambre@kbfi.ee)

Received 27 January 2017; Revised 10 April 2017; Accepted 19 April 2017; Published 11 July 2017

Academic Editor: Moh H. Malek

Copyright © 2017 Andre Koit et al. This is an open access article distributed under the Creative Commons Attribution License, which permits unrestricted use, distribution, and reproduction in any medium, provided the original work is properly cited.

We conducted quantitative cellular respiration analysis on samples taken from human breast cancer (HBC) and human colorectal cancer (HCC) patients. Respiratory capacity is not lost as a result of tumor formation and even though, functionally, complex I in HCC was found to be suppressed, it was not evident on the protein level. Additionally, metabolic control analysis was used to quantify the role of components of mitochondrial interactosome. The main rate-controlling steps in HBC are complex IV and adenine nucleotide transporter, but in HCC, complexes I and III. Our kinetic measurements confirmed previous studies that respiratory chain complexes I and III in HBC and HCC can be assembled into supercomplexes with a possible partial addition from the complex IV pool. Therefore, the kinetic method can be a useful addition in studying supercomplexes in cell lines or human samples. In addition, when results from culture cells were compared to those from clinical samples, clear differences were present, but we also detected two different types of mitochondria within clinical HBC samples, possibly linked to two-compartment metabolism. Taken together, our data show that mitochondrial respiration and regulation of mitochondrial membrane permeability have substantial differences between these two cancer types when compared to each other to their adjacent healthy tissue or to respective cell cultures.

## 1. Introduction

The field of cellular bioenergetics is gaining increased attention and studies performed during the last years have shown that targeting cancer cell energy metabolism may be a new and promising area for selective tumor treatment [1]. The literature describing changes in energy metabolism and mitochondrial function during carcinogenesis is, unfortunately, full of contradictions. Majority of previous studies about the bioenergetics of malignant tumors were performed in vitro on different cell models with the conclusion that cancer cells have increased glucose uptake and, due to mitochondrial damage, it is not metabolized via oxidative phosphorylation (OXPHOS) [2–4]. It is clear that for many

tumors, glycolysis is the main energy provider, but in others, OXPHOS is still crucial for survival and progression and produces necessary ATP [1, 5, 6]. Recently, a new concept for tumor metabolism was proposed—metabolic coupling between mitochondria in cancer cells and catabolism in stromal cells—which promotes tumor growth and development of metastases. In other words, tumor cells induce reprogramming in surrounding nontumor cells so that the latter acquire the Warburg phenotype [7] and start producing and exporting the necessary fuels for the anabolic cancer cells (“reverse Warburg”). The cancer cells will then metabolize these fuels via their tricarboxylic acid cycle and OXPHOS [8–10]. Complex interplay between developing cancer cells and host physiology, possibly mediated by “waves” of gene expression

in the tumor [11, 12], can only develop *in vivo* and therefore *in vitro* studies cannot give conclusive information about the functional activity and capacity of OXPHOS in human samples. *In vitro* models ignore many factors arising from the tumor microenvironment (TME), which can and will exert significant effects *in vivo*. TME consists of nonmalignant cells, soluble growth factors, signaling molecules, and extracellular matrix that support tumor progression [13], but high heterogeneity within cancers cell population on top of it contributes to even further complexity in clinical samples [14]. At the same time, the metabolic profiles of tumor cells that are grown in culture have significant variations primarily due to the culture conditions, such as concentrations of glucose, glutamine, and/or fetal serum. Cells grown in glucose-free medium display relatively high rates of oxygen consumption, but cultivation in high-glucose medium increases their glycolytic capacity together with reduced respiratory flux [15–19].

In addition to intercellular differences, there are also intracellular rearrangements resulting from tumor formation. The functional units within cells are often macromolecular complexes rather than single species [20]. In case of OXPHOS, it has been shown that complexes of the respiratory chain can form assemblies—supercomplexes—that lead to kinetic and possibly homeostatic advantages [21]. Therefore, pure genome or transcriptome data are not sufficient for describing the final *in situ* modifications and the final outcomes of a pathway or cellular processes are defined by actual activities of their separate proteins—or their assemblies—together with the respective regulatory mechanisms. More specifically, previous studies have shown that in cardiac and yeast cells, a large protein supercomplex is centrally positioned in regulation of mitochondrial respiration and mitochondrial energy fluxes. The supercomplex consists of ATP synthasome, mitochondrial creatine kinase (MtCK) or hexokinase (HK), voltage-dependent anion channel (VDAC), and some regulatory proteins expectedly coordinate the selective permeability of it. This complex is known as mitochondrial interactosome (MI) [22], and it is located in the contact sites of outer and inner mitochondrial membranes. This unit also includes supercomplexes formed by the respiratory chain [23, 24]. Changes in the content of ATP synthasome and respiratory chain supercomplexes in pathological conditions are still poorly studied. Inhibiting key respiratory enzymes or avoiding restructuring of mitochondrial supercomplexes in tumors has potential to disrupt disease progression without affecting normal cells, thus, providing a powerful new approach for developing novel therapeutic targets. Specifically, Rohlenova et al. recently demonstrated that breast cancer cells expressing HER2 oncogene develop specific RC supercomplexes which make complex I in these susceptible to treatment with chemically altered tamoxifen called MitoTam [25]. MitoTam is taken to a phase I clinical study [25], and there are other clinical studies undergoing that target OXPHOS in different cancer types (e.g., trial numbers NCT01957735 and NCT02650804). Therefore, despite the assumed glycolytic nature of human tumors, inhibition of oxidative respiration is proving to be a viable therapeutic strategy and further studies are needed to define differences

between cancer types but also individual patients in regard to such treatment.

We have previously shown on clinical samples that both human breast cancer (HBC) and human colorectal cancer (HCC) are not purely glycolytic, but these tumors have sustained OXPHOS as a substantial provider of ATP [26–28]. Here, we extend our studies by comparing bioenergetics of HBC and HCC using kinetic methods.

## 2. Materials and Methods

**2.1. Chemicals.** All chemicals were purchased from Sigma-Aldrich (USA) and were of the highest purity available (>98%).

**2.2. Clinical Materials.** The tissue samples were provided by the Oncology and Haematology Clinic at the North Estonia Medical Centre (Tallinn). All the samples were analyzed immediately after surgery. Only primary tumors were examined and information from respective pathology reports was provided by the North Estonia Medical Centre for all the analyzed samples. Informed consent was obtained from all the patients and coded identity protection was applied. All investigations were approved by the Tallinn Medical Research Ethics Committee and were in accordance with the Helsinki Declaration and Convention of the Council of Europe on Human Rights and Biomedicine. The entire group consisted of 34 patients with breast cancer and 55 with colorectal cancer.

**2.3. Cell Cultures.** MDA-MB-231 and MCF-7 cells were grown as adherent monolayers in low glucose (1.0 g/L) Dulbecco's modified Eagle's medium (DMEM) with stable L-glutamine and sodium pyruvate (from Capricorn Scientific GmbH) supplemented with 10% heat-inactivated fetal bovine serum, 10  $\mu\text{g}/\text{mL}$  human recombinant Zn insulin, and antibiotics: penicillin (100 U/mL), streptomycin (100  $\mu\text{g}/\text{mL}$ ), and gentamicin at a final concentration of 50  $\mu\text{g}/\text{mL}$ . Cells were grown at 37°C in a humidified incubator containing 5% CO<sub>2</sub> in air and were subcultured at 2–3-day intervals.

**2.4. Mitochondrial Respiration in Saponin-Permeabilized Tissue Samples.** Numerous studies have demonstrated that isolated mitochondria behave differently from mitochondria *in situ* [29–32]. We therefore have investigated respiratory activity of tumor and control tissues *in situ* using the skinned sample technique [26, 28, 29, 33]. This method allows analysis of the function of mitochondria in cells in their natural environment and leaves links between cytoskeletal structures and mitochondrial outer membranes intact [34–37]. Cytochrome c test was used to confirm integrity of the mitochondrial outer membrane (MOM) [22, 26, 28, 33]; mitochondrial inner membrane quality was checked using a carboxyatractylolide (CAT) test as the last procedure in every experiment [22, 26, 28, 33]. Rates of O<sub>2</sub> consumption were assayed at 25°C using Oxygraph-2k high-resolution respirometer (Oroboros Instruments, Innsbruck, Austria) loaded with pre-equilibrated respiration buffer medium B [26]. Activity of the respiratory chain was measured by substrate-inhibitor

titration as described earlier [26, 38]. The solubility of oxygen at 25°C was taken as 240 nM/mL [39]. The solubility of oxygen is much lower at 37 than at 25°C, but also, the skinned samples from malignant clinical material are more stable at 25°C. All rates of respiration ( $V$ ) are expressed in nM O<sub>2</sub>/min per mg dry tissue weight for solid tumors and in nM O<sub>2</sub>/min per million cells for cell cultures.

**2.5. Metabolic Control Analysis.** Metabolic control analysis (MCA) is a method for studying regulatory mechanisms in complex metabolic systems [40–42]. Flux control coefficient (FCC) is defined as the ratio of fractional change in a system variable to fractional change in a biochemical activity that caused the change in the given system [42]. FCC or  $C_{vi}^J$  is the extent to which an enzyme in a pathway controls the flux ( $J$ ); it corresponds to the percentage decrease in flux caused by a 1% decrease in the activity ( $v_i$ ) of that enzyme [41, 43]:

$$C_{vi}^J = \frac{(dJ/dv_i)}{(J/v_i)} = \frac{d \ln J}{d \ln v_i}. \quad (1)$$

This method shows how the control is shared between the enzymes and the transporters of the pathway and enables to identify the steps that could be modified to achieve successful alteration of the flux or metabolite concentration in the pathway. But it also permits the identification of system components that are crucial in the regulation of energy transfer and regulatory networks [40–42, 44–46].

MCA has previously been applied in our lab to human breast and colorectal cancer skinned samples to determine the FCCs for respiratory chain complexes. The flux was measured as the rate of O<sub>2</sub> consumption in permeabilized tissues derived from HCC patients when all components of the OXPHOS system were titrated with specific irreversible or pseudoirreversible inhibitors to stepwise decrease selected respiratory chain complex activities according to a previously published method [26, 27, 47, 48].

**2.6. Western Blot Analysis of the Level of Mitochondrial RC Complexes Expression.** Postoperative human tissue samples (70–100 mg) were crushed in liquid nitrogen and homogenized in 20 volumes of RIPA lysis buffer (50 mM Tris-HCl pH 8.0, 150 mM NaCl, 2 mM EDTA, 0.5% sodium deoxycholate, 0.1% SDS, 0.1% Triton X-100, and complete protease inhibitor cocktail (Roche)) by Retsch Mixer Mill at 25 Hz for 2 min. After homogenization, samples were incubated for 30 min on ice and centrifuged at 12,000 rpm for 20 min at 4°C. The proteins in the supernatants were precipitated using acetone/TCA to remove nonprotein contaminants. Briefly, supernatants were mixed with 8 volumes of ice-cold acetone and 1 volume of 100% TCA, kept at –20°C for 1 h and then pelleted at 11500 rpm for 15 min at 4°C. The pellets were washed twice with acetone and resuspended in 1x Laemmli sample buffer.

Proteins were separated by polyacrylamide gel electrophoresis, transferred to a polyvinylidene difluoride (PVDF) membrane, and subjected to immunoblotting with the total OXPHOS antibody cocktail (ab110411). Then, the membranes were incubated with corresponding horseradish

peroxidase-conjugated secondary antibody and visualized using an enhanced chemiluminescence system (ECL; Pierce, Thermo Fisher Scientific). After chemiluminescence reaction, the PVDF membranes were stained with Coomassie brilliant blue R250 to measure the total protein amount. The complexes I–V signal intensities were calculated by ImageJ software and normalized to total protein intensities.

Expression levels of complex I in HCC and normal tissues were additionally estimated using anti-NDUFA9 antibody that corresponds to NADH dehydrogenase 1 $\alpha$  sub-complex 9 (SAB1100073). The samples were incubated and visualized as described above. Levels of NDUFA9 encoding protein were normalized to total protein content.

**2.7. Citrate Synthase Activity.** Activity of citrate synthase in tissue homogenates was measured as described by Srere [49]. Reactions were performed in 96-well plates containing 100 mM Tris-HCl pH 8.1, 0.3 mM AcCoA, 0.5 mM oxaloacetate, and 0.1 mM DTNB using FLUOstar Omega plate reader spectrophotometer (BMG Labtech).

**2.8. Data Analysis.** Data in the text, tables, and figures are presented as mean  $\pm$  standard error (SEM). Results were analyzed by the Student  $t$ -test;  $p$  values <0.05 were considered statistically significant.

### 3. Results and Discussion

**3.1. Respiratory Chain Analysis and Presence of Supercomplexes.** Suppression of mitochondrial electron transport chain function is widespread in cancer, and this is closely connected to apoptosis resistance [50–54]. However, studies are often conducted on cell cultures and therefore little is known about respiratory chain (RC) function in clinical human breast and colorectal carcinomas in situ. To reveal possible disturbances, we conducted comparative quantitative analysis on the respiration rates for different RC complexes in permeabilized HBC and HCC and their adjacent normal tissue samples. Data for healthy breast tissue has been left out from most of the following calculations due to very low ADP-dependent oxygen consumption in this tissue type as it is not sufficient to assess inhibitory effects of antimycin A or rotenone or compare these results to other studied samples.

Multiple substrate-inhibitor titration protocol was used for measuring respiratory capacities of different respiratory chain segments (Table 1) [30, 55]. All respiration rates corresponding to the activities of different RC complexes are increased in both investigated human cancers when compared to their adjacent normal tissue. The mean value of basal respiration (state 2,  $V_o$ ) in skinned HCC samples is higher than that in normal tissue and depends on the used respiratory substrates. Specifically, in the presence of glutamate and malate, HCC and its control tissue fibers exhibit lower state 2 respiration rates than in the presence of glutamate, malate, and succinate; similar dependence was observed for the breast cancer samples (Figure 1). One possible reason for this difference can be succinate-dependent proton leak in tumor tissue [56–58]. Addition of 2 mM



MgADP for studying complex I-based state 3 (in the presence of glutamate and malate without succinate) increased mitochondrial respiration rates in all tissue samples and following addition of complex I-specific inhibitor (rotenone) inhibited the respiration back to the initial state 2 levels (Table 1). Similarly, the function of complex II was quantified upon ADP-stimulated respiration in the presence of rotenone and succinate; at these conditions, the complex I activity is inhibited and apparent respiration rate originates from complex II. Complex III in both HBC and HCC was confirmed to be fully functional as an addition of antimycin A inhibited the electron flow from complex III to mitochondrial complex IV (COX) (Table 1). The activation of mitochondrial complex IV (addition of 5 mM ascorbate and 1 mM tetramethyl-p-phenylenediamine) resulted in a remarkable increase in the rate of  $O_2$  consumption in all examined samples, both cancerous and normal, but the increase was nearly two times higher in cancer tissue.

Complex I deficiency is the hallmark of multiple mitochondrial diseases and is generally considered to be an intrinsic property of some cancers [58–63]. Indeed, our experiments confirm that development of HCC results in reduced  $V_{\text{Glut}}/V_{\text{Succ}}$  ratio which indicates relative suppression of the complex I-dependent respiration [58]. Similar results have previously been described for gastric and ovarian cancer tissues but also in some cancer cell cultures [58, 63–66]. Deficiency of complex I in some tumors might be an early event causing an increase in mitochondrial biogenesis in an attempt to compensate for the reduction in OXPHOS function [63]. Computer modeling predicts that the mechanisms of this compensation can use multiple pathways like  $\beta$ -oxidation of fatty acids, mitochondrial folate metabolism, and others [67]. Our results showed that this suppression is pronounced on the functional level in HCC (Figure 2(a)), but to identify the changes on the protein expression level, we analyzed the RC complexes with total OXPHOS antibody cocktail (Figure 3). Based on this type of approach, the suppression of RC complex I was found to be absent if the results were normalized to total protein. The suppression of complex I in HCC was additionally studied by Western blot analysis with antibodies against only one complex I subunit—NDUFA9 (see Supplementary Fig 1 available online at <https://doi.org/10.1155/2017/1372640>). This result, however, confirmed the suppression of complex I. As seen from those experiments, analysis of RC, using the semi-quantitative WB method, can be strongly dependent on experimental conditions: against what complex I subunit the antibodies were used and which normalization conditions are applied. Additionally, complex II in colon samples did not indicate possible suppression in that alternative pathway as differences in  $V_{\text{Succ}}/V_{\text{COX}}$  ratios were not significant (Figure 2(b)) [68].

In contrast to HCC, mitochondrial respiration in HBC samples is not accompanied with suppression of complex I-dependent respiration (Figures 2(a) and 2(b)). Altogether, the relative complex I deficiency on the functional level in our oxygen consumption measurements is characteristic for HCC but not for HBC tissue.

TABLE 1: Characterization of respiratory parameters of permeabilized tissue samples derived from patients with breast or colorectal cancer.

Parameters	HBC patients, $n = 7$ [26]		HCC patients, $n = 7$ [28]	
	Tumor	Control	Tumor	Control
$V_o$	$0.294 \pm 0.024$	$0.004 \pm 0.007$	$1.06 \pm 0.14$	$0.82 \pm 0.15$
$V_{\text{ADP}}$	$0.71 \pm 0.06$	$0.055 \pm 0.004$	$2.02 \pm 0.21$	$1.39 \pm 0.21$
$V_{\text{rot}}$	$0.34 \pm 0.04$	$0.070 \pm 0.015$	$0.91 \pm 0.11$	$0.85 \pm 0.14$
$V_{\text{Succ}}$	$0.74 \pm 0.10$	$0.076 \pm 0.008$	$2.22 \pm 0.26$	$1.33 \pm 0.18$
VANM	$0.38 \pm 0.04$	$0.071 \pm 0.018$	$1.04 \pm 0.09$	$0.69 \pm 0.07$
$V_{\text{COX}}$	$2.36 \pm 0.33$	$1.23 \pm 0.18$	$6.59 \pm 0.71$	$3.84 \pm 0.58$

Note: here, each data point is the mean  $\pm$  SEM of respiratory values.  $V_o$ : basal respiration without ADP or ATP;  $V_{\text{ADP}}$ : ADP-stimulated respiration (final concentration 2 mM) in the presence of 5 mM glutamate and 2 mM malate (indicating the function of the respiratory chain complex I);  $V_{\text{rot}}$ : rates of respiration after addition of 50  $\mu\text{M}$  rotenone (an inhibitor of complex I);  $V_{\text{Succ}}$ : ADP-stimulated respiration in the presence of rotenone and 10 mM succinate (to estimate the function of complex II); VANM: rates of respiration after addition 10  $\mu\text{M}$  antimycin-A (an inhibitor of complex III);  $V_{\text{COX}}$ : rates of  $O_2$  consumption in the presence of complex IV substrates (5 mM ascorbate jointly with 1 mM tetramethyl-p-phenylenediamine).

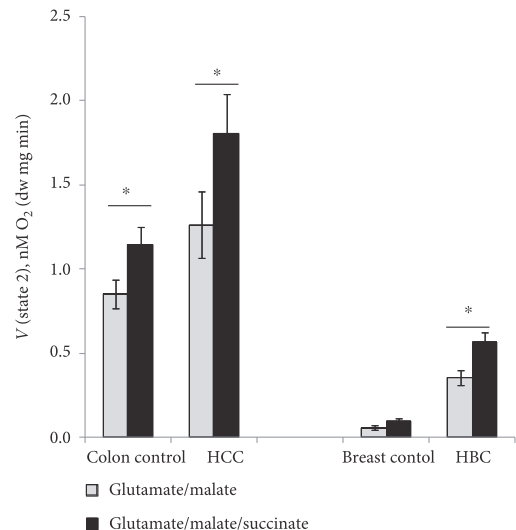


FIGURE 1: Assessment of state 2 respiration rates of the permeabilized HCC, HBC, and normal adjacent tissue samples in the presence of different combinations of respiratory substrates (5 mM glutamate, 2 mM malate, and 10 mM succinate). Bars are SEM,  $n = 8$  for colon samples, and  $n = 12$  for breast tissue samples,  $*p < 0.05$ .

Remarkable numbers of studies have shown that RC complexes can form protein assemblies (supercomplexes). These supramolecular structures provide kinetic advantage such as substrate channeling, increased efficiency in electron transport, prevention of destabilization, and degradation of respiratory enzyme complexes [21] and means to regulate

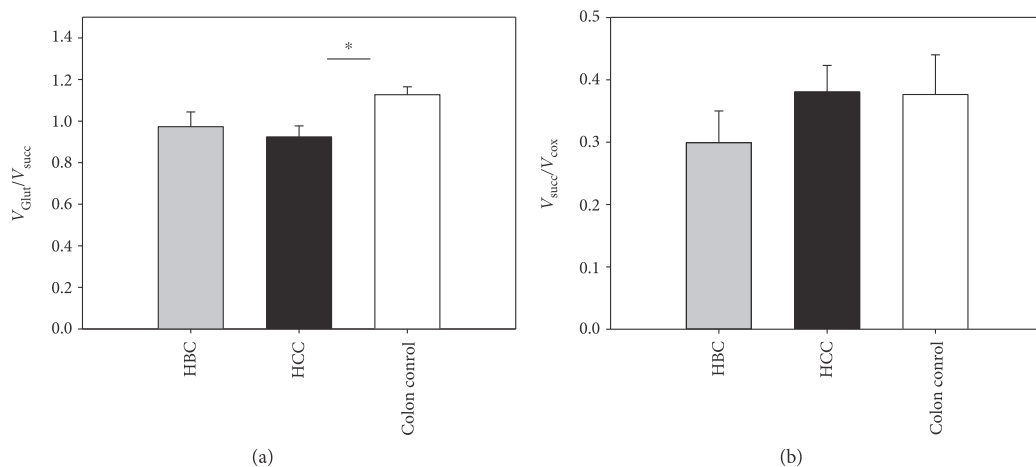


FIGURE 2: (a) Oxygraphic analysis of the functioning of complex I in skinned tissues from patients with HBC or HCC; here,  $V_{\text{Glut}}/V_{\text{Succ}}$  is the ratio of ADP-stimulated respiration rate in the presence of 5 mM glutamate and 2 mM malate (activity of complex I) to ADP-stimulated respiration rate in the presence of 50  $\mu\text{M}$  rotenone and 10 mM succinate (activity of complex II). (b)  $V_{\text{Succ}}/V_{\text{COX}}$  is the ratio of complex II respiration rate to complex IV respiration rate. Data shown as mean  $\pm$  SEM;  $n = 7$  for colon [28] and breast tissue samples [26], \* $p < 0.05$ .

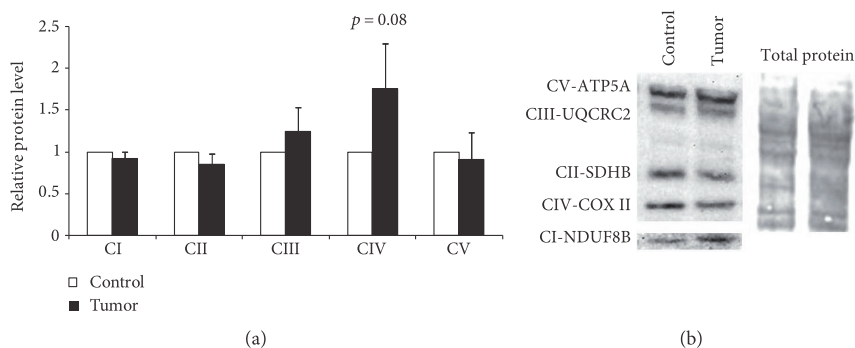


FIGURE 3: Quantitative analysis of the expression levels of the respiratory chain complexes in HCC and normal tissue samples (a) along with a representative Western blot image (b). Protein levels were normalized to total protein staining by Coomassie blue; data shown as mean  $\pm$  SEM of 5 independent experiments.

ROS levels in the cell (most of the mitochondrial ROS originates from complexes I and III) [69] and hence, homeostasis. The RC complex I is considered to be the most important component in these assemblies, and it is a member of almost all known respirasomes [70–74]. In previous studies, complexes I, III, and IV were found to be assembled into super-complexes in different configurations, but complex II was not confirmed to be a component of these RC super-complexes and was assumed to move freely in the mitochondrial inner membrane [70, 75, 76]. Relative deficiency of the RC complex I on the functional level (as shown above) may be a result of changes in supercomplex composition as a part of malignant transformation.

In addition to RC super-complexes, along with respirasomes, one more molecular transmembrane protein supercomplex (which is known as ATP synthasome; [77])

was identified as the component of the OXPHOS system. The ATP synthasome complex consists of ATP synthase, inorganic phosphate carrier, and adenine nucleotide translocator (ANT) [48]. The current model of mitochondrial inter-actosome (MI) considers the ATP synthasome and RC complexes together with voltage-dependent anion channel (VDAC) and mitochondrial creatine kinase (MtCK) as components of intracellular energetic units [22]. Even though MI is proven in striated muscles, the functional role of it, together with MtCK, in malignant samples remains controversial [78], but it indicates that both ATP synthasome and RC complexes can form even more complex functional structures.

In addition to steady-state proteome studies, kinetic testing of metabolic fluxes using MCA can provide preliminary information about supramolecular organization in the

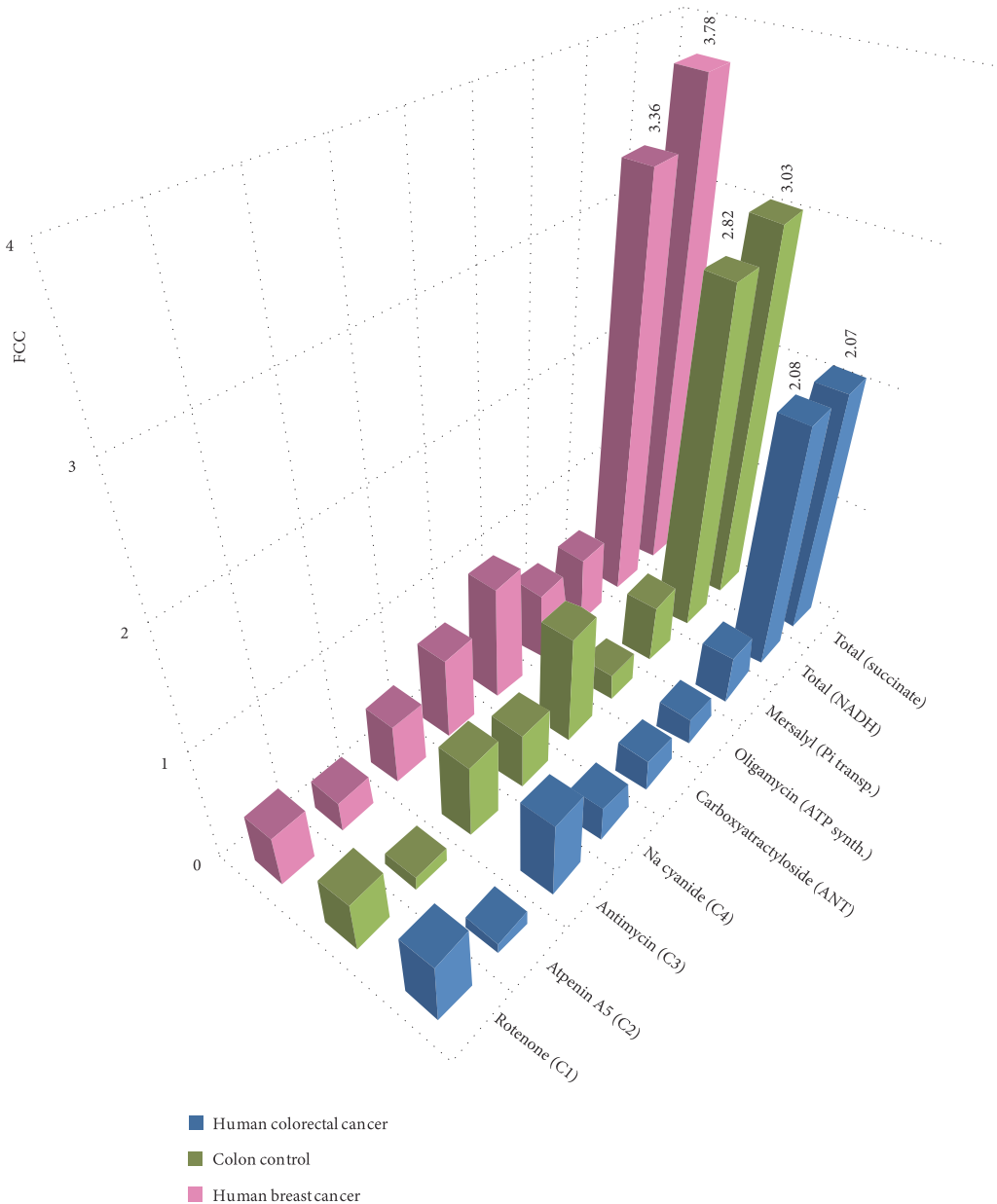


FIGURE 4: FCCs for ATP synthasome and RC complexes as determined by MCA. Two ways of electron transfer were examined: NADH-dependent and succinate-dependent electron transfers, and respective sums of FCCs are calculated as the last bars. Data for HBC is published before in [26], except for complex II with atpenin A5. Isolated mucosal tissue was used for colon control.

energy transfer system and enables to quantify the flux exerted by the different RC and the ATP synthasome complexes [27, 28, 79]. MCA can discriminate between two prevailing models: the former model, based on the assumption that each enzyme can be rate controlling to a different extent,

and a subsequent model, where whole metabolic pathway can behave as a single channel and inhibition of any of its components would give the same flux control [80]. Bianchi et al. proposed that both complexes I and III are highly rate controlling in NADH oxidation, suggesting the existence of

TABLE 2: FCCs for different components in mitochondrial Interactosome and ranges of the concentrations of inhibitors.

MI component	Inhibitor	Range of inhibitor concentration	FCC		
			HCC	Control colon tissue (mucosa)	HBC
Complex I	Rotenone	1–100 nM	0.56	0.45	0.46*
Complex II	Atpenin A5	0.1–6 $\mu$ M	0.12	0.13	0.28
Complex III	Antimycin	1–200 nM	0.68	0.66	0.54*
Complex IV	Na cyanide	0.1–40 $\mu$ M	0.31	0.50	0.74*
ANT	Carboxyatractyloside	1–200 nM	0.28	0.97	1.02*
ATP synthase	Oligomycin	1–600 nM	0.25	0.24	0.61*
Pi transporter	Mersalyl	1–200 $\mu$ M	0.43	0.53	0.60*
<b>Sum 1, 3–7</b>	<b>Total (NADH)</b>		<b>2.08</b>	<b>2.82</b>	<b>3.36</b>
<b>Sum 2–7</b>	<b>Total (succinate)</b>		<b>2.07</b>	<b>3.03</b>	<b>3.78</b>

Note: \* from [26].

functional association between these two complexes [80]. To confirm the formation of supercomplexes in HCC- and HBC-skinned samples using MCA, we investigated the flux control coefficients (FCCs) for the complexes involved in aerobic NADH oxidation (I, III, and IV), in succinate oxidation (II, III, and IV), and for components of the ATP synthasome. For this purpose, cancerous and normal tissue samples were titrated with increasing concentrations of specific inhibitors against all of the ATP synthasome and RC complexes. Figure 4 summarizes the data analyzed in three different ways: by a graphical model [40, 41, 81], according to Small [82], and the Gellerich model [44]. The obtained FCC values did not depend on which exact method was used for calculations. The main problem in these calculations is high heterogeneity of the clinical material, which from the one hand originates from cancer molecular subtypes (e.g., Luminal A/B, HER2 or triple negative in HBC; unknown subtypes in HCC) but on the other hand originates from heterogeneity of tumor cells within each tumor [14] or irregular stromal burden. Therefore, the obtained coefficient values do not only depend on which patients were included to the study, but the results may also depend on which particular tumor region was used from each patient sample. This can be considered as an inevitable part in analyzing clinical samples.

Previous work has shown that the main respiratory rate-controlling steps in HBC cells are complex IV (FCC = 0.74) and adenine nucleotide transporter (ANT, FCC = 1.02) [26]. Similar control distribution was not observed within HCC ATP synthasome complex as FCCs for ANT were found to be significantly lower when HCC was compared to the results of healthy colon mucosa (FCC = 0.284 for HCC and FCC = 0.970 for healthy colon). These results show that ANT exerts high flux control in healthy colon tissue (and in HBC), but ANT seems to lose its limiting role in HCC. Ramsay et al. believe that hexokinase-voltage-dependent anion channel-ANT complex, which spans across the outer and inner mitochondrial membranes, is critical in cancer cells as this complex is the link between glycolysis, oxidative phosphorylation, and mitochondrial-mediated apoptosis [83]. Therefore, the difference between HBC and HCC, in regard to ANT-exerted flux control, indicates to distinct difference in energy metabolism between these two tumor types

(Table 2; Figure 4). In addition, HBC is showing equal FCCs for ATP synthase and inorganic phosphate transporter (Pi) in ATP synthasome, but this phenomenon is not characteristic neither for healthy colon mucosa nor for colorectal cancer. These alterations could be related to mitochondrial permeability transition pore (mtPTP) and apoptosis. Bernardi et al. studied the key regulatory features of the mtPTP [84–87], and the same group of authors has pointed to the fact that ANT can modulate the mtPTP, possibly through its effects on the surface potential, but it is not a mandatory component of this channel.

FCCs within the RC system in HBC do not differ significantly and the flux control is distributed almost uniformly throughout the different complexes (Table 2, Figure 4). Such condition is an indication of possible presence of protein supercomplexes (approximately equal values of FCCs for RC complexes I and III—0.46 versus 0.54, resp.). On the other hand, the flux distribution for normal colon tissue, when compared to HCC, showed slight difference for that for complex IV (FCC 0.50 versus 0.31), but flux control coefficients with close values were calculated for complex I (FCC 0.45 versus 0.56) and complex III (FCC 0.66 versus 0.68). Similarity in FCCs for complex I and complex III for both HCC and healthy colon tissue enables to propose that in healthy conditions, complex III is attached to complex I (possibly together with multiple copies of complex IV), but during carcinogenesis, the supercomplex assembly changes and even though complex I and complex III seem to stay linked, the participation of complex IV in this assembly becomes uncertain. Functional assembly of complexes I and III together with their rate-limiting roles will lead to sum of FCCs being greater than 1 [73] (see below).

Role of complex IV is multifaceted as three populations of it have previously been suggested: population assembled with complex I and complex III, population assembled with complex III alone and a non-interacting population [74]. Several data show that the absence of functional supercomplex assembly factor I (SCAF1) may be involved in distribution of complex IV [74, 75, 88]. As outlined in the review article by Enriquez, total cell respiration (glucose, pyruvate, and glutamine as substrates) was significantly higher in cells lacking functional SCAF1

[74]. High total cell respiration was registered also for both cancer types described in this paper, but presence or absence of functional SCAF1 was not investigated.

The sums of the determined FCCs within cancerous and healthy sample groups were calculated to be in the range from 2.07 to 3.78. In theory, sum of FCCs in a linear system is 1 [5, 40, 42–44, 89, 90], but the value of it can increase if the system includes enzyme–enzyme interactions, direct channeling, and/or recycling within multienzyme complexes (i.e., system becomes nonlinear) [79, 80, 91, 92]. The higher sum of FCCs from our tests is not a result of diffusion restrictions because the concentration ranges for all of the inhibitors in various samples were similar and did not depend on the nature of the samples [26, 28, 47, 48].

The organization of RC complexes in the mitochondrial inner membrane has been an object of intense debate and it is not studied systematically in human normal or cancerous tissues. Given the known theoretical framework, our results confirm the plasticity model and agree with the data from Bianchi et al. [80], but the distribution of complex IV remains unclear—both random distribution and association into I-III-IV supercomplex can be possible. Large FCC for complex II is not characteristic neither for HBC, for HCC, nor for healthy colon tissue, and therefore, our kinetic studies confirmed previous findings that this complex is not a part of RC supercomplexes.

The question about the changes in the composition and stoichiometry of protein supercomplexes, which result from carcinogenesis, needs further studies, and in addition, as mitochondria have other additional roles in cellular metabolism, it can be presumed that changes in RC are also affecting cataplerotic processes sprouting from the mitochondria, but such link has not yet been studied yet.

**3.2. ADP-Regulated Mitochondrial Respiration in HBC and HCC Fibers.** Table 3 summarizes ADP-regulated mitochondrial respiration parameters determined for skinned tissue samples taken from both patient groups. Differences in the rates of maximal ADP-activated respiration ( $V_{\max}$ ) in colon tissue samples are corresponding to the differences in the content of mitochondria in these cells (the amount of mitochondria in HCC is 50% higher than that in healthy control tissue [28] (supplementary Table 1)). Our previous experiments have shown that HBC tissue, too, contains an increased number of mitochondria in comparison to its adjacent normal tissue [27, 93] (supplementary Table 1). As indicated above, ADP-dependent respiration in healthy human breast tissue is absent. Breast samples contain lot of fat tissue, but low  $V_{\max}$  values were evident even if clearly lobular/ductal structures were separated and tested. Low respiratory capacity can also be indicating to lowered metabolic activity in normal ductal/lobular tissue in older women (average age of HBC patients in this study was 63.4 years). In contrast to normal breast tissue, the colon control tissue samples have significantly higher respiration rates (Table 3). Specifically, respiratory capacity is higher in apparent mucosal/submucosal section of the normal colon tissue samples compared to that of the underlying smooth muscle part as we manually

TABLE 3: Apparent  $K_m$  ( $^{app}K_m$ ) and maximal rate of respiration ( $V_{\max}$ ) values for ADP-dependent respiration calculated for HBC, HCC and their adjacent healthy tissue samples.

Tissues	$^{app}K_m, \mu M \pm SEM$	$V_{\max} \pm SEM$
Human breast cancer tissue	114.8 ± 13.6*	1.09 ± 0.04*
Healthy adjacent breast control tissue	—	0.02 ± 0.01*
Human colorectal cancer tissue	93.6 ± 7.7**	2.41 ± 0.32
Healthy adjacent colon control tissue	256** ± 34	0.71 ± 0.23

Note: \* from [26] and \*\* [38];  $V_{\max}$  values are presented as nM  $O_2$ /min/mg dry tissue weight without proton leak rates. These  $K_m$  and  $V_{\max}$  values for ADP were determined from corresponding titration curves by fitting experimental data to non-linear regression equation according to a Michaelis–Menten model. 35 patients used for analysis of HBC and 35 for HCC.

separated and tested these two layers in a selection of colon tissue samples (Figure 5(b)).

HBC arises from tissue with almost absent ADP-related respiration, but once formed, the mechanism of energy conversion seems to acquire a more complicated form and it can be associated with both increased mitochondrial biogenesis and interplay between cancer and stromal cells [26]. HBC can be classified into four clinically distinct and significant molecular subtypes: luminal-A, luminal-B, HER2 expressing, and triple negative. Clinically, luminal-A is considered the least and triple negative as the most aggressive subtype. Therefore, we expected to see clear differences when respiratory parameters of those two extreme subtypes were measured. Initially, respiration rates were analyzed in Luminal-A type MCF7 and triple negative MDA-MB-231 cell lines. When compared, respiration rates in presence of glutamate or pyruvate clearly showed that oxygen consumption in luminal-A subtype cells is remarkably higher (Figure 5(b)). But in contrast, the exact opposite was registered for the same parameters in clinical samples (Figure 5(a)) as the highest respiratory rates were registered for the most aggressive triple negative subtype. From the one hand, this contradicting result shows that cell cultures are not directly comparable to respective clinical counterparts and can lead to misleading expectations. On the other hand, it proves that the role of OXPHOS becomes increasingly important in clinical samples as aggressiveness of the tumor increases, but it is not evident in the respective culture cells. In the present case, it is not a result of increased glucose availability in the growth medium, which could lead the cells to acquire glycolytic phenotype and explain the difference with clinical samples, because low-glucose media was used.

For HCC, which is without distinct clinical subtypes, we compared disease stage to average  $V_{\max}$  value for that stage (Figure 6(a)). Even though increase in  $V_{\max}$  in initial stages can be calculated in comparison to control sample, the decrease in  $V_{\max}$  for stages IIIC and IVB does not fit this increase in dependence. The disease stage at diagnosis itself is not a valid marker of aggressiveness and therefore such plotting can be debated. Therefore, we gathered initial longitudinal data on patient progression in our HCC cohort and confirmed that 7 out of 32 eligible patients had died (median

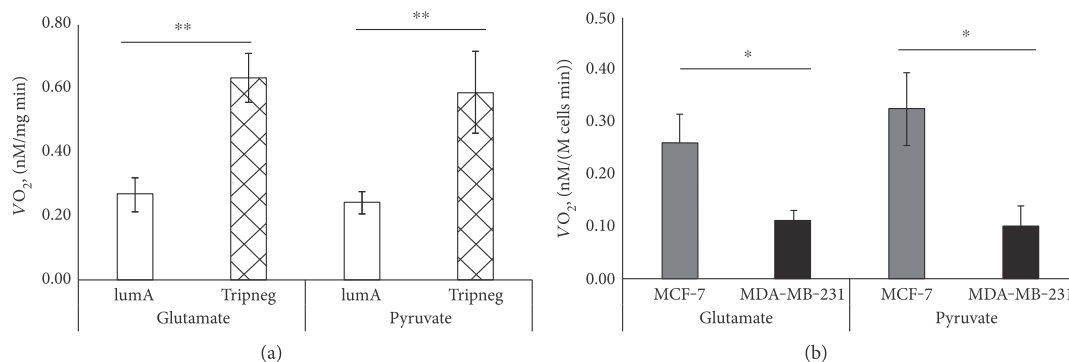


FIGURE 5: (a) Respiration rates for clinical samples of luminal-A and triple negative HBC subtypes in the presence of 5 mM glutamate or 5 mM pyruvate;  $n = 13/12$  for luminal-A and  $n = 7/8$  for triple negative subtypes, respectively. (b) Respiratory rates for luminal-A type MCF-7 and triple negative MDA-MB-231 cells in the presence of 5 mM glutamate or 5 mM pyruvate;  $n = 3$  for each measurement; \* $p < 0.05$ , \*\* $p < 0.005$ .

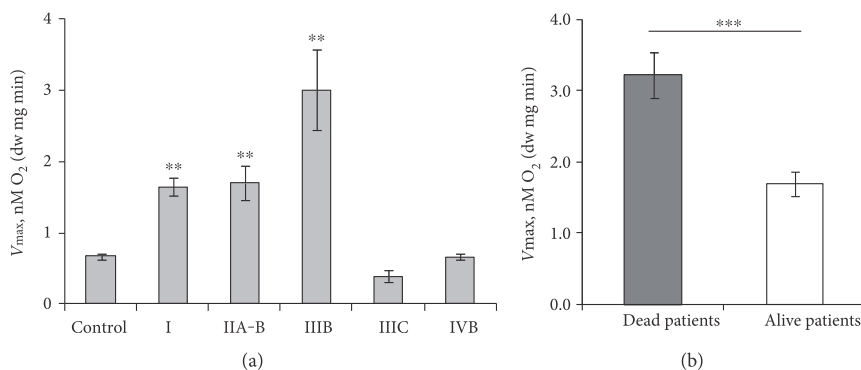


FIGURE 6: (a) Dependence of maximal rate of mitochondrial respiration ( $V_{max}$ ) compared with the HCC at different stages. Stage I was calculated as the mean of 13 patients, IIA, IIB - 13 patients, IIIB-4 patients, IIIC-3 patients and IVB-1 patient. Control colon tissue was obtained from 34 patients. Maximal respiration rate  $V_{max}$  is compared with that in control tissue. Bars are SEM; \*\* $p < 0.005$ . (b)  $V_{max}$  in HCC patients based on disease state in follow-up setting. Seven patients out of 32 are confirmed to have succumbed to HCC ( $V_{max} = 3.19 \pm 0.34$ ); 25 patients out of 32 stay in remission ( $V_{max} = 1.70 \pm 0.17$ ), \*\*\* $p < 0.001$ .

follow-up time  $47.3 \pm 4.9$  months).  $V_{max}$  values in patients that succumbed to the disease were significantly higher than that in the currently not progressed group (Figure 6(b)). As was shown for HBC above, higher respiratory capacity was registered for the most aggressive triple negative subgroup. Therefore, it can be argued based on similarity that higher tumor respiratory parameters in the dead HCC patients were indicating to more aggressive disease. In addition, lower than expected respiratory rate in some triple negative tumors can therefore indicate that given patient, when compared to the average in the triple negative subgroup, has less aggressive disease than could be expected. To confirm this in larger cohorts and relate aggressiveness in HCC and HBC to  $V_{max}$  value, additional longitudinal studies are necessary.

We next measured apparent Michaelis–Menten constants ( $K_m$ ) for ADP to characterize the affinity of mitochondria for exogenous ADP (i.e., permeability of mitochondrial outer membrane). Corresponding  $K_m$  values for permeabilized tumor and nontumorous tissues were determined from titration experiments using exogenously added ADP. The obtained data were plotted as rates of  $O_2$  consumption versus ADP concentration and apparent  $K_m$  values were calculated from these plots by nonlinear regression equation. Healthy colon tissue displayed low affinity for ADP ( $K_m = 256 \pm 3 \mu M$ ), whereas that in HCC is significantly higher ( $K_m = 93.6 \pm 7.7 \mu M$ ) [38]. The  $K_m$  (ADP) value for HBC tissue samples ( $K_m = 114.8 \pm 13.6 \mu M$ ) was similar to that for HCC [26].

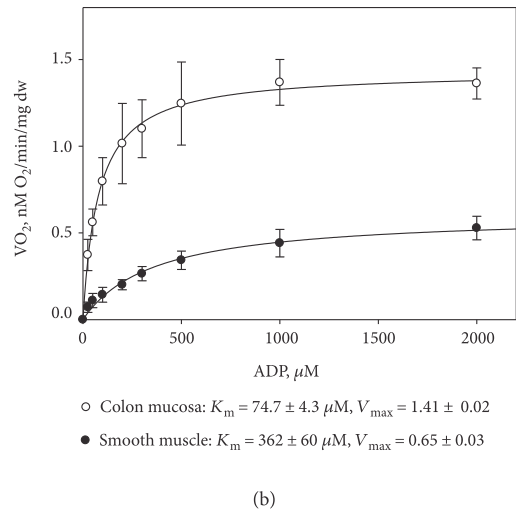
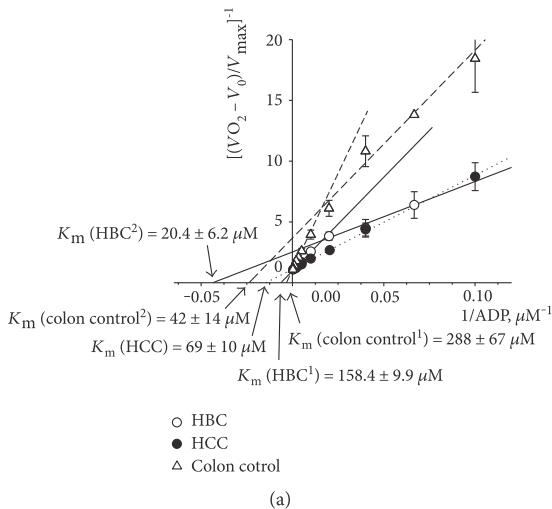


FIGURE 7: (a) Dependences of normalized respiration rate values for HCC (dotted line), HBC (solid line), and healthy colon tissue samples (dashed line); double reciprocal Lineweaver-Burk plots. Samples from 32 patients with breast cancer and 10 patients with colorectal cancer were examined. (b) ADP-dependent respiration in healthy colon mucosa and smooth muscle tissue samples (Michaelis-Menten curve,  $n = 8$ ). Here,  $V_0$  and  $V_{\max}$  are rates of basal and maximal ADP-activated respiration, respectively.

According to the classical studies by Chance and Williams [94, 95] and the data of many other investigators [29, 30, 37], the apparent  $K_m$  value for ADP for isolated mitochondria is low, about  $15 \mu\text{M}$ , but the observed apparent  $K_m$  values in our study for permeabilized clinical HBC and HCC samples were 6–8 times higher than this value (Table 3). Our previous studies have shown that sensitivity of the mitochondrial respiration for exogenous ADP for permeabilized NB HL-1 cells is also high as the apparent  $K_m$  equaled to  $25 \pm 4 \mu\text{M}$  and was similar to that of isolated heart mitochondria [34, 96]. The similar low apparent  $K_m$  values were also registered for undifferentiated and differentiated neuroblastoma culture cells, where the corresponding  $K_m$  for ADP were measured as  $20.3 \pm 1.4 \mu\text{M}$  and  $19.4 \pm 3.2 \mu\text{M}$ , respectively [97]. The registered difference between culture cells and clinical samples, despite the used preparation method, again indicates to differences present in these two sample groups.

We treated permeabilized samples with incremental concentrations of ADP and the measured  $\text{O}_2$  consumption rates (normalized to  $V_{\max}$ ) were analyzed against respective ADP concentration values as double reciprocal Lineweaver-Burk plots (Figures 7(a) and 7(b)) [29]. Figure 7(a) shows the results of the Lineweaver-Burk treatment of the experimental data linked with ADP-regulated mitochondrial respiration in skinned fibers of HCC, healthy colon, and HBC. Corresponding  $V_{\max}$  and  $K_m$  values were calculated from the linearization approach. Saks and colleagues have previously shown that the presence of biphasic respiration regulation on the graph curve indicates the existence of two populations of mitochondria with different affinities for ADP [29]. Our results indicated such differences in colon

control and HBC samples. Specifically, monophasic regulation of mitochondrial respiration is apparent in HCC tissue, but in healthy colon tissue, two populations of mitochondria with very different properties were found (Figure 7(a)). One population of mitochondria is characterized with lower  $K_m$  ( $42 \pm 14 \mu\text{M}$ ), whereas the apparent  $K_m$  (ADP) value for the second mitochondrial population is nearly seven times higher ( $288 \pm 67 \mu\text{M}$ ). We thereafter again separated mucosal and smooth muscle parts from the colon samples before additional  $K_m$  measurements to characterize their isolated contributions. Apparent  $K_m$  value for mucosal part was measured to be  $74.7 \pm 4.3 \mu\text{M}$  and the same value for colon smooth muscle tissues was found to be  $362 \pm 60 \mu\text{M}$  (Figure 7(b)). Therefore, results after separation explain the results from the initial experiment where the entire colon wall was analyzed and two separate groups of mitochondria were discovered. Additionally, we could also distinguish two differently regulated types of mitochondria in HBC samples: one with apparent  $K_m$  value for MgADP of  $20.4 \pm 6.2 \mu\text{M}$ , but the same for the second mitochondrial population was nearly ten times higher,  $158.5 \pm 9.9 \mu\text{M}$  (Figure 4(a)). The phenomenon shown in Figure 7(a) can be associated, on the one hand, simply with elevated stromal content (in such case, similar results should have been also registered for HCC), but on the other hand, with possible two-compartment tumor metabolism in HBC, what states that tumor cells function as metabolic parasites and extract energy from supporting host cells such as fibroblasts [98–103]. In such case, the stromal part of the HBC samples can be characterized with glycolytic metabolism representing the low  $K_m$  value due to high levels of autophagy, mitophagy, glycolysis, and lipolysis, while cancer cells

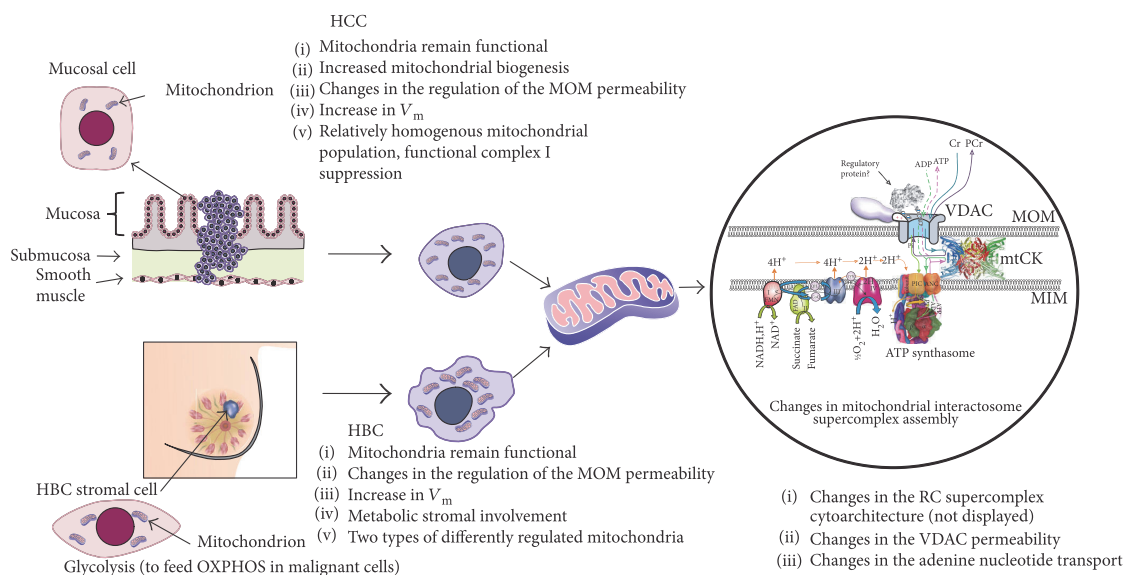


FIGURE 8: Mitochondrial alterations in HCC and HBC tissue cells. Mitochondrial interactosome is a large supercomplex consisting of ATP synthasome, VDAC, mitochondrial kinases like adenylate kinase, hexokinase or mitochondrial creatine kinase (MtCK), and respiratory chain (super)complexes. Here, the octameric MtCK characteristic is shown for the striated muscles and also as the possible component of the MI in the healthy colon [108–110]. The complex of VDAC together with other proteins controls the exchange of adenine nucleotides and regulates energy fluxes between mitochondrial and cytosolic compartments. Changes in the structure and function of MI are the important parts of cancer mitochondrial metabolism.

have high mitochondrial mass, OXPHOS, and  $\beta$ -oxidation activity, which is represented by the mitochondrial population with the high  $K_m$  (ADP) values. From the given comparison between HBC and HCC, the two subpopulations of mitochondria are specific only to HBC samples (confirmed in 32 cases out of the total 34) but not to HCC samples, and it indicates that tumor formation leads to distinct changes, which is related to the tissue type the tumor originates from.

Altogether, these results indicate the remarkable differences in the regulation of mitochondrial outer membrane (MOM) permeability between cultured tumor cells and clinical material (including between different tumor types and even between patients). Even further, the results can be contradictory as registered for respiration parameters. It can be estimated, based on the results from our lab, that low  $K_m$  value for ADP can be a common characteristic for cancer cells grown in culture, but in vivo tumor samples, the regulation of MOM permeability is more complicated and probably related to interplay between energy transfer pathways and changes in the phosphorylation state of VDAC channels [32, 104–107] and also with modulation of cytoskeleton or membrane potential as a result of tumor formation.

#### 4. Concluding Remarks

To understand the energy metabolism of tumors, it is necessary to detect bioenergetic fingerprints of each individual

tumor type. Our results confirmed that respiratory capacity is preserved in both HBC and HCC as these both demonstrated substantial rates of oxidative phosphorylation, which contradicts with earlier widespread understanding that the metabolism of human breast and colorectal carcinomas is prevalently glycolytic. Studies on cell lines up to now have led to many lifesaving technologies and treatments in humans, but the scientific level might be nearing the end of readily transferrable results between the cell model and human physiology. Our results indicated that apparent glycolytic nature of some breast cancer types could be expected based on cell cultures, but this presumption was in sharp conflict when culture cell results were compared with these from respective clinical samples. In addition, when compared to their healthy adjacent tissue, both clinical cancer types showed increased respiratory capacity. Despite the increased respiratory capacity in HCC, relative deficiency of complex I was registered for it on the functional level Western blot analysis was not sufficient to confirm this deficiency on the protein level as two different antibody approaches gave conflicting results, but this result proves the necessity to measure pathways also on the functional level whenever possible to compare the function to steady-state markers like presence or abundance of certain enzymes. Our experiments indicate that the respiratory chain and ATP synthasome can form macromolecular assemblies (supercomplexes) with reorganized composition and/or stoichiometry while the changes are specific for different tumor types. This is in good agreement with recent studies from other laboratories [25] and



the current work shows that equal results can be obtained using kinetic methods, but additional studies are warranted to include results from protein level studies using the blue native gel electrophoresis (BNGE) technique. Our  $K_m$  measurements confirmed that two populations of mitochondria registered in healthy colon tissue can be categorized as different layers of the colon wall, but in HBC, the subgroups can be linked to two-compartment metabolism where tumor acts as a metabolic parasite on normal stromal cells. Mitochondria of HCC are homogenous in terms of regulation of the mitochondrial outer membrane permeability and MCA (Figure 8).

Mitochondria are not only the centers of cellular energy conversion but are also the important part in biosynthetic metabolism and apoptosis. Therefore, direct detection of profound changes in the ATP synthasome components and in the architecture of the respiratory chain complexes, as shown in the current work, can support development of new predictive models or therapies.

## Abbreviations

ANT:	Adenine nucleotide translocator
CAT:	Carboxyatractyloside
COX:	Cytochrome c oxidase
FCC:	Flux control coefficient
HBC:	Human breast cancer
HCC:	Human colorectal cancer
HK:	Hexokinase
MCA:	Metabolic control analysis
MI:	Mitochondrial interactosome
MOM:	Mitochondrial outer membrane
MtCK:	Mitochondrial creatine kinase
mtPTP:	Mitochondrial permeability transition pore
OXPHOS:	Oxidative phosphorylation
RC:	Respiratory chain
SCAF1:	Supercomplex assembly factor I
TME:	Tumor microenvironment
VDAC:	Voltage-dependent anion channel.

## Additional Points

**Highlights.** (1) Relative complex I functional deficiency is characteristic for HCC but not for HBC. (2) HBC respiratory capacity severely higher than in adjacent normal breast tissue. (3) Complexes I and III expectedly assembled in both tumorous and normal tissues. (4)  $K_m$  for ADP shows distinct differences between cell cultures and clinical samples. (5) Two distinct mitochondrial populations present in HBC but not in HCC.

## Conflicts of Interest

The authors declare that they have no conflicts of interest.

## Acknowledgments

This work was supported by the institutional research funding IUT23-1 of the Estonian Ministry of Education.

## References

- [1] S. Rodríguez-Enríquez, L. Hernández-Esquivel, A. Marín-Hernández et al., "Mitochondrial free fatty acid beta-oxidation supports oxidative phosphorylation and proliferation in cancer cells," *The International Journal of Biochemistry & Cell Biology*, vol. 65, pp. 209–221, 2015.
- [2] L. S. Gomez, P. Zancan, M. C. Marcondes et al., "Resveratrol decreases breast cancer cell viability and glucose metabolism by inhibiting 6-phosphofructo-1-kinase," *Biochimie*, vol. 95, no. 6, pp. 1336–1343, 2013.
- [3] Y. Ma, R. K. Bai, R. Trieu, and L. J. Wong, "Mitochondrial dysfunction in human breast cancer cells and their trans-mitochondrial cybrids," *Biochimica et Biophysica Acta (BBA) - Bioenergetics*, vol. 1797, no. 1, pp. 29–37, 2010.
- [4] R. C. Sun, M. Fadia, J. E. Dahlstrom, C. R. Parish, P. G. Board, and A. C. Blackburn, "Reversal of the glycolytic phenotype by dichloroacetate inhibits metastatic breast cancer cell growth in vitro and in vivo," *Breast Cancer Research and Treatment*, vol. 120, no. 1, pp. 253–260, 2010.
- [5] R. Moreno-Sanchez, A. Marín-Hernández, E. Saavedra, J. P. Pardo, S. J. Ralph, and S. Rodríguez-Enríquez, "Who controls the ATP supply in cancer cells? Biochemistry lessons to understand cancer energy metabolism," *The International Journal of Biochemistry & Cell Biology*, vol. 50, pp. 10–23, 2014.
- [6] S. Rodríguez-Enríquez, J. C. Gallardo-Pérez, A. Marín-Hernández et al., "Oxidative phosphorylation as a target to arrest malignant neoplasias," *Current Medicinal Chemistry*, vol. 18, no. 21, pp. 3156–3167, 2011.
- [7] O. Warburg, "On respiratory impairment in cancer cells," *Science*, vol. 124, no. 3215, pp. 269–270, 1956.
- [8] M. P. Lisanti, U. E. Martinez-Outschoorn, and F. Sotgia, "Oncogenes induce the cancer-associated fibroblast phenotype: metabolic symbiosis and "fibroblast addiction" are new therapeutic targets for drug discovery," *Cell Cycle*, vol. 12, no. 17, pp. 2740–2749, 2013.
- [9] F. Sotgia, D. Whitaker-Menezes, U. E. Martinez-Outschoorn et al., "Mitochondrial metabolism in cancer metastasis: visualizing tumor cell mitochondria and the "reverse Warburg effect" in positive lymph node tissue," *Cell Cycle*, vol. 11, no. 7, pp. 1445–1454, 2012.
- [10] A. K. Witkiewicz, D. Whitaker-Menezes, A. Dasgupta et al., "Using the "reverse Warburg effect" to identify high-risk breast cancer patients: stromal MCT4 predicts poor clinical outcome in triple-negative breast cancers," *Cell Cycle*, vol. 11, no. 6, pp. 1108–1117, 2012.
- [11] K. Smolkova, L. Plecítá-Hlavatá, N. Bellance, G. Benard, R. Rossignol, and P. Ježek, "Waves of gene regulation suppress and then restore oxidative phosphorylation in cancer cells," *The International Journal of Biochemistry & Cell Biology*, vol. 43, no. 7, pp. 950–968, 2011.
- [12] V. L. Payen, P. E. Porporato, B. Baselet, and P. Sonveaux, "Metabolic changes associated with tumor metastasis, part 1: tumor pH, glycolysis and the pentose phosphate pathway," *Cellular and Molecular Life Sciences*, vol. 73, no. 7, pp. 1333–1348, 2016.
- [13] M. A. Swartz, N. Iida, E. W. Roberts et al., "Tumor microenvironment complexity: emerging roles in cancer therapy," *Cancer Research*, vol. 72, no. 10, pp. 2473–2480, 2012.
- [14] N. McGranahan and C. Swanton, "Biological and therapeutic impact of intratumor heterogeneity in cancer evolution," *Cancer Cell*, vol. 27, no. 1, pp. 15–26, 2015.

- [15] R. H. Swerdlow, E. Lezi, D. Aires, and J. Lu, "Glycolysis-respiration relationships in a neuroblastoma cell line," *Biochimica et Biophysica Acta (BBA) - General Subjects*, vol. 1830, no. 4, pp. 2891–2898, 2013.
- [16] C. Jose and R. Rossignol, "Rationale for mitochondria-targeting strategies in cancer bioenergetic therapies," *The International Journal of Biochemistry & Cell Biology*, vol. 45, no. 1, pp. 123–129, 2013.
- [17] E. Gnaiger and R. B. Kemp, "Anaerobic metabolism in aerobic mammalian cells: information from the ratio of calorimetric heat flux and respirometric oxygen flux," *Biochimica et Biophysica Acta (BBA) - Bioenergetics*, vol. 1016, no. 3, pp. 328–332, 1990.
- [18] G. Gstraunthaler, T. Seppi, and W. Pfaller, "Impact of culture conditions, culture media volumes, and glucose content on metabolic properties of renal epithelial cell cultures. Are renal cells in tissue culture hypoxic?" *Cellular Physiology and Biochemistry*, vol. 9, no. 3, pp. 150–172, 1999.
- [19] C. J. Sherr and R. A. DePinho, "Cellular senescence: mitotic clock or culture shock?" *Cell*, vol. 102, no. 4, pp. 407–410, 2000.
- [20] R. Moreno-Sanchez, E. Saavedra, J. C. Gallardo-Pérez, F. D. Rumjanek, and S. Rodríguez-Enríquez, "Understanding the cancer cell phenotype beyond the limitations of current omics analyses," *The FEBS Journal*, vol. 283, no. 1, pp. 54–73, 2016.
- [21] G. Lenaz and M. L. Genova, "Kinetics of integrated electron transfer in the mitochondrial respiratory chain: random collisions vs. solid state electron channeling," *American Journal of Physiology. Cell Physiology*, vol. 292, no. 4, pp. C1221–C1239, 2007.
- [22] N. Timohhina, R. Guzun, K. Tepp et al., "Direct measurement of energy fluxes from mitochondria into cytoplasm in permeabilized cardiac cells in situ: some evidence for mitochondrial interactosome," *Journal of Bioenergetics and Biomembranes*, vol. 41, no. 3, pp. 259–275, 2009.
- [23] G. Lenaz and M. L. Genova, "Structural and functional organization of the mitochondrial respiratory chain: a dynamic super-assembly," *The International Journal of Biochemistry & Cell Biology*, vol. 41, no. 10, pp. 1750–1772, 2009.
- [24] J. Vonck and E. Schafer, "Supramolecular organization of protein complexes in the mitochondrial inner membrane," *Biochimica et Biophysica Acta (BBA) - Molecular Cell Research*, vol. 1793, no. 1, pp. 117–124, 2009.
- [25] K. Rohlenova, K. Sachaphibulkij, J. Stursa et al., "Selective disruption of respiratory supercomplexes as a new strategy to suppress Her2high breast cancer," *Antioxidants & Redox Signaling*, vol. 26, no. 2, pp. 84–103, 2017.
- [26] T. Kaambre, V. Chekulayev, I. Shevchuk et al., "Metabolic control analysis of cellular respiration in situ in intraoperative samples of human breast cancer," *Journal of Bioenergetics and Biomembranes*, vol. 44, no. 5, pp. 539–558, 2012.
- [27] T. Kaambre, V. Chekulayev, I. Shevchuk et al., "Metabolic control analysis of respiration in human cancer tissue," *Frontiers in Physiology*, vol. 4, article 151, pp. 1–6, 2013.
- [28] A. Kaldma, A. Klepinin, V. Chekulayev et al., "An in situ study of bioenergetic properties of human colorectal cancer: the regulation of mitochondrial respiration and distribution of flux control among the components of ATP synthasome," *The International Journal of Biochemistry & Cell Biology*, vol. 55, pp. 171–186, 2014.
- [29] V. A. Saks, V. I. Veksler, A. V. Kuznetsov et al., "Permeabilized cell and skinned fiber techniques in studies of mitochondrial function in vivo," *Molecular and Cellular Biochemistry*, vol. 184, no. 1–2, pp. 81–100, 1998.
- [30] A. V. Kuznetsov, D. Strobl, E. Ruttmann, A. Königsrainer, R. Margreiter, and E. Gnaiger, "Evaluation of mitochondrial respiratory function in small biopsies of liver," *Analytical Biochemistry*, vol. 305, no. 2, pp. 186–194, 2002.
- [31] A. V. Kuznetsov, "Structural organization and dynamics of mitochondria in the cells in vivo," in *Molecular System Bioenergetics: Energy for Life*, V. Saks, Ed., pp. 137–162, Wiley-VCH Verlag GmbH & Co KGaA, Weinheim, Germany, 2007.
- [32] M. Varikmaa, R. Bagur, T. Kaambre et al., "Role of mitochondria-cytoskeleton interactions in respiration regulation and mitochondrial organization in striated muscles," *Biochimica et Biophysica Acta (BBA) - Bioenergetics*, vol. 1837, no. 2, pp. 232–245, 2014.
- [33] A. V. Kuznetsov, V. Veksler, F. N. Gellerich, V. Saks, R. Margreiter, and W. S. Kunz, "Analysis of mitochondrial function in situ in permeabilized muscle fibers, tissues and cells," *Nature Protocols*, vol. 3, no. 6, pp. 965–976, 2008.
- [34] C. Monge, N. Beraud, K. Tepp et al., "Comparative analysis of the bioenergetics of adult cardiomyocytes and nonbeating HL-1 cells: respiratory chain activities, glycolytic enzyme profiles, and metabolic fluxes," *Canadian Journal of Physiology and Pharmacology*, vol. 87, no. 4, pp. 318–326, 2009.
- [35] F. Appaix, A. V. Kuznetsov, Y. Usson et al., "Possible role of cytoskeleton in intracellular arrangement and regulation of mitochondria," *Experimental Physiology*, vol. 88, no. 1, pp. 175–190, 2003.
- [36] A. V. Kuznetsov, T. Tiivel, P. Sikk et al., "Striking differences between the kinetics of regulation of respiration by ADP in slow-twitch and fast-twitch muscles in vivo," *European Journal of Biochemistry*, vol. 241, no. 3, pp. 909–915, 1996.
- [37] V. A. Saks, A. V. Kuznetsov, Z. A. Khuchua et al., "Control of cellular respiration in vivo by mitochondrial outer membrane and by creatine kinase. A new speculative hypothesis: possible involvement of mitochondrial-cytoskeleton interactions," *Journal of Molecular and Cellular Cardiology*, vol. 27, no. 1, pp. 625–645, 1995.
- [38] V. Chekulayev, K. Mado, I. Shevchuk et al., "Metabolic remodeling in human colorectal cancer and surrounding tissues: alterations in regulation of mitochondrial respiration and metabolic fluxes," *Biochemistry and Biophysics Reports*, vol. 4, pp. 111–125, 2015.
- [39] E. Gnaiger, "Oxygen solubility in experimental media," *OROBOROS Bioenerg. News*, vol. 6, no. 3, pp. 1–6, 2001.
- [40] H. Kacser and J. A. Burns, "The control of flux," *Symposia of the Society for Experimental Biology*, vol. 27, pp. 65–104, 1973.
- [41] D. Fell, "Understanding the control of metabolism," in *Frontiers in Metabolism 2*, K. Snell, Ed., vol. xiip. 301, Portland Press, London, Miami, 1997.
- [42] D. Fell, "Metabolic control analysis," in *Systems Biology*, L. Alberghina and H. V. Westerhoff, Eds., pp. 69–80, Springer: Verlag, Berlin, 2005.
- [43] R. Moreno-Sanchez, E. Saavedra, S. Rodríguez-Enríquez, and V. Olin-Sandoval, "Metabolic control analysis: a tool for designing strategies to manipulate metabolic pathways," *Journal of Biomedicine & Biotechnology*, vol. 2008, Article ID 597913, 30 pages, 2008.
- [44] F. N. Gellerich, W. S. Kunz, and R. Bohnsack, "Estimation of flux control coefficients from inhibitor titrations by non-

- linear regression," *FEBS Letters*, vol. 274, no. 1-2, pp. 167–170, 1990.
- [45] A. V. Kuznetsov, J. F. Clark, K. Winkler, and W. S. Kunz, "Increase of flux control of cytochrome c oxidase in copper-deficient mottled brindled mice," *The Journal of Biological Chemistry*, vol. 271, no. 1, pp. 283–288, 1996.
- [46] A. V. Kuznetsov, K. Winkler, E. Kirches, H. Lins, H. Feistner, and W. S. Kunz, "Application of inhibitor titrations for the detection of oxidative phosphorylation defects in saponin-skinned muscle fibers of patients with mitochondrial diseases," *Biochimica et Biophysica Acta (BBA) - Molecular Basis of Disease*, vol. 1360, no. 2, pp. 142–150, 1997.
- [47] K. Tepp, I. Shevchuk, V. Chekulayev et al., "High efficiency of energy flux controls within mitochondrial interactosome in cardiac intracellular energetic units," *Biochimica et Biophysica Acta (BBA) - Bioenergetics*, vol. 1807, no. 12, pp. 1549–1561, 2011.
- [48] K. Tepp, N. Timohhina, V. Chekulayev, I. Shevchuk, T. Kaambre, and V. Saks, "Metabolic control analysis of integrated energy metabolism in permeabilized cardiomyocytes - experimental study," *Acta Biochimica Polonica*, vol. 57, no. 4, pp. 421–430, 2010.
- [49] P. A. Srere, "[1] Citrate synthase," *Methods in Enzymology*, vol. 13, pp. 3–11, 1969.
- [50] M. Davoudi, H. Kotarsky, E. Hansson, and V. Fellman, "Complex I function and supercomplex formation are preserved in liver mitochondria despite progressive complex III deficiency," *PLoS One*, vol. 9, no. 1, article e86767, 2014.
- [51] M. Castro-Gago, M. O. Blanco-Barca, C. Gómez-Lado, J. Eiris-Puñal, Y. Campos-González, and J. Arenas-Barbero, "Respiratory chain complex I deficiency in an infant with Ohtahara syndrome," *Brain dev*, vol. 31, no. 4, pp. 322–325, 2009.
- [52] J. Finsterer, G. G. Kovacs, H. Rauschka, and U. Ahting, "Adult, isolated respiratory chain complex IV deficiency with minimal manifestations," *Folia Neuropathologica*, vol. 53, no. 2, pp. 153–157, 2015.
- [53] D. Mowat, D. M. Kirby, K. R. Kamath, A. Kan, D. R. Thorburn, and J. Christodoulou, "Respiratory chain complex III [correction of complex] in deficiency with pruritus: a novel vitamin responsive clinical feature," *The Journal of Pediatrics*, vol. 134, no. 3, pp. 352–354, 1999.
- [54] A. Lemarie and S. Grimm, "Mitochondrial respiratory chain complexes: apoptosis sensors mutated in cancer?" *Oncogene*, vol. 30, no. 38, pp. 3985–4003, 2011.
- [55] M. Eimre, K. Paju, S. Pelloux et al., "Distinct organization of energy metabolism in HL-1 cardiac cell line and cardiomyocytes," *Biochimica et Biophysica Acta (BBA) - Bioenergetics*, vol. 1777, no. 6, pp. 514–524, 2008.
- [56] E. Seppet, M. Eimre, N. Peet et al., "Compartmentation of energy metabolism in atrial myocardium of patients undergoing cardiac surgery," *Molecular and Cellular Biochemistry*, vol. 270, no. 1-2, pp. 49–61, 2005.
- [57] N. Parker, A. Vidal-Puig, and M. D. Brand, "Stimulation of mitochondrial proton conductance by hydroxyphenol requires a high membrane potential," *Bioscience Reports*, vol. 28, no. 2, pp. 83–88, 2008.
- [58] M. Puurand, N. Peet, A. Piirsoo et al., "Deficiency of the complex I of the mitochondrial respiratory chain but improved adenylate control over succinate-dependent respiration are human gastric cancer-specific phenomena," *Molecular and Cellular Biochemistry*, vol. 370, no. 1-2, pp. 69–78, 2012.
- [59] R. H. Triepels, L. P. Van Den Heuvel, J. M. Trijbels, and J. A. Smeitink, "Respiratory chain complex I deficiency," *American Journal of Medical Genetics*, vol. 106, no. 1, pp. 37–45, 2001.
- [60] H. Swalwell, D. M. Kirby, E. L. Blakely et al., "Respiratory chain complex I deficiency caused by mitochondrial DNA mutations," *European Journal of Human Genetics*, vol. 19, no. 7, pp. 769–775, 2011.
- [61] E. Ostergaard, R. J. Rodenburg, M. van den Brand et al., "Respiratory chain complex I deficiency due to NDUFA12 mutations as a new cause of Leigh syndrome," *Journal of Medical Genetics*, vol. 48, no. 11, pp. 737–740, 2011.
- [62] D. M. Kirby, M. Crawford, M. A. Cleary, H. H. Dahl, X. Dennett, and D. R. Thorburn, "Respiratory chain complex I deficiency: an underdiagnosed energy generation disorder," *Neurology*, vol. 52, no. 6, pp. 1255–1264, 1999.
- [63] H. Simonnet, J. Demont, K. Pfeiffer et al., "Mitochondrial complex I is deficient in renal oncocytomas," *Carcinogenesis*, vol. 24, no. 9, pp. 1461–1466, 2003.
- [64] M. Gruno, N. Peet, A. Tein et al., "Atrophic gastritis: deficient complex I of the respiratory chain in the mitochondria of corpus mucosal cells," *Journal of Gastroenterology*, vol. 43, no. 10, pp. 780–788, 2008.
- [65] H. Y. Lim, Q. S. Ho, J. Low, M. Choolani, and K. P. Wong, "Respiratory competent mitochondria in human ovarian and peritoneal cancer," *Mitochondrion*, vol. 11, no. 3, pp. 437–443, 2011.
- [66] E. Bonora, A. M. Porcelli, G. Gasparre et al., "Defective oxidative phosphorylation in thyroid oncocyctic carcinoma is associated with pathogenic mitochondrial DNA mutations affecting complexes I and III," *Cancer Research*, vol. 66, no. 12, pp. 6087–6096, 2006.
- [67] Ł. P. Zieliński, A. C. Smith, A. G. Smith, and A. J. Robinson, "Metabolic flexibility of mitochondrial respiratory chain disorders predicted by computer modelling," *Mitochondrion*, vol. 31, pp. 45–55, 2016.
- [68] S. Demine, N. Reddy, P. Renard, M. Raes, and T. Arnould, "Unraveling biochemical pathways affected by mitochondrial dysfunctions using metabolomic approaches," *Metabolites*, vol. 4, no. 3, pp. 831–878, 2014.
- [69] M. L. Genova and G. Lenaz, "The interplay between respiratory supercomplexes and ROS in aging," *Antioxidants & Redox Signaling*, vol. 23, no. 3, pp. 208–238, 2015.
- [70] R. Acin-Perez and J. A. Enriquez, "The function of the respiratory supercomplexes: the plasticity model," *Biochimica et Biophysica Acta (BBA) - Bioenergetics*, vol. 1837, no. 4, pp. 444–450, 2014.
- [71] N. V. Dudkina, M. Kudryashev, H. Stahlberg, and E. J. Boekema, "Interaction of complexes I, III, and IV within the bovine respirasome by single particle cryoelectron tomography," *Proceedings of the National Academy of Sciences of the United States of America*, vol. 108, no. 37, pp. 15196–15200, 2011.
- [72] D. Moreno-Lastres, F. Fontanesi, I. García-Consuegra et al., "Mitochondrial complex I plays an essential role in human respirasome assembly," *Cell Metabolism*, vol. 15, no. 3, pp. 324–335, 2012.
- [73] G. Lenaz, G. Tioli, A. I. Falasca, and M. L. Genova, "Complex I function in mitochondrial supercomplexes," *Biochimica et*

- Biophysica Acta (BBA) - Bioenergetics*, vol. 1857, no. 7, pp. 991–1000, 2016.
- [74] J. A. Enriquez, “Supramolecular organization of respiratory complexes,” *Annual Review of Physiology*, vol. 78, pp. 533–561, 2016.
- [75] E. Lapuente-Brun, R. Moreno-Loshuertos, R. Acín-Pérez et al., “Supercomplex assembly determines electron flux in the mitochondrial electron transport chain,” *Science*, vol. 340, no. 6140, pp. 1567–1570, 2013.
- [76] R. Acín-Pérez, P. Fernández-Silva, M. L. Peleato, A. Pérez-Martos, and J. A. Enriquez, “Respiratory active mitochondrial supercomplexes,” *Molecular Cell*, vol. 32, no. 4, pp. 529–539, 2008.
- [77] P. L. Pedersen, “Voltage dependent anion channels (VDACs): a brief introduction with a focus on the outer mitochondrial compartment’s roles together with hexokinase-2 in the “Warburg effect” in cancer,” *Journal of Bioenergetics and Biomembranes*, vol. 40, no. 3, pp. 123–126, 2008.
- [78] X. L. Qian, Y. Q. Li, F. Gu et al., “Overexpression of ubiquitous mitochondrial creatine kinase (uMtCK) accelerates tumor growth by inhibiting apoptosis of breast cancer cells and is associated with a poor prognosis in breast cancer patients,” *Biochemical and Biophysical Research Communications*, vol. 427, no. 1, pp. 60–66, 2012.
- [79] G. Lenaz and M. L. Genova, “Supramolecular organisation of the mitochondrial respiratory chain: a new challenge for the mechanism and control of oxidative phosphorylation,” *Advances in Experimental Medicine and Biology*, vol. 748, pp. 107–144, 2012.
- [80] C. Bianchi, M. L. Genova, G. P. Castelli, and G. Lenaz, “The mitochondrial respiratory chain is partially organized in a supercomplex assembly: kinetic evidence using flux control analysis,” *The Journal of Biological Chemistry*, vol. 279, no. 35, pp. 36562–36569, 2004.
- [81] A. K. Groen, R. J. Wanders, H. V. Westerhoff, R. Van der Meer, and J. M. Tager, “Quantification of the contribution of various steps to the control of mitochondrial respiration,” *The Journal of Biological Chemistry*, vol. 257, no. 6, pp. 2754–2757, 1982.
- [82] J. R. Small, “Flux control coefficients determined by inhibitor titration: the design and analysis of experiments to minimize errors,” *The Biochemical Journal*, vol. 296, Part 2, pp. 423–433, 1993.
- [83] E. E. Ramsay, P. J. Hogg, and P. J. Dilda, “Mitochondrial metabolism inhibitors for cancer therapy,” *Pharmaceutical Research*, vol. 28, no. 11, pp. 2731–2744, 2011.
- [84] P. Bernardi, “The mitochondrial permeability transition pore: a mystery solved?” *Frontiers in Physiology*, vol. 4, article 95, pp. 1–12, 2013.
- [85] F. Di Lisa, F. Fogolari, and G. Lippe, “From ATP to PTP and back: a dual function for the mitochondrial ATP synthase,” *Circulation Research*, vol. 116, no. 11, pp. 1850–1862, 2015.
- [86] P. Bernardi, A. Rasola, M. Forte, and G. Lippe, “The mitochondrial permeability transition pore: channel formation by F-ATP synthase, integration in signal transduction, and role in pathophysiology,” *Physiological Reviews*, vol. 95, no. 4, pp. 1111–1155, 2015.
- [87] A. Rasola and P. Bernardi, “The mitochondrial permeability transition pore and its adaptive responses in tumor cells,” *Cell Calcium*, vol. 56, no. 6, pp. 437–445, 2014.
- [88] T. Althoff, D. J. Mills, J. L. Popot, and W. Kühlbrandt, “Arrangement of electron transport chain components in bovine mitochondrial supercomplex IIIIII2IV1,” *The EMBO Journal*, vol. 30, no. 22, pp. 4652–4664, 2011.
- [89] A. Marín-Hernández, S. Y. López-Ramírez, J. C. Gallardo-Pérez, S. Rodríguez-Enriquez, R. Moreno-Sánchez, and E. Saavedra, “Systems biology approaches to cancer energy metabolism,” in *Systems Biology of Metabolic and Signaling Networks*, M. A. Aon, V. Saks and U. Schlattner, Eds., pp. 213–239, Springer, Berlin Heidelberg, 2014.
- [90] B. N. Kholodenko and H. V. Westerhoff, “Metabolic channelling and control of the flux,” *FEBS Letters*, vol. 320, no. 1, pp. 71–74, 1993.
- [91] B. N. Kholodenko, J. M. Rohwer, M. Cascante, and H. V. Westerhoff, “Subtleties in control by metabolic channelling and enzyme organization,” *Molecular and Cellular Biochemistry*, vol. 184, no. 1-2, pp. 311–320, 1998.
- [92] B. N. Kholodenko, O. V. Demin, and H. V. Westerhoff, “‘Channelled’ pathways can be more sensitive to specific regulatory signals,” *FEBS Letters*, vol. 320, no. 1, pp. 75–78, 1993.
- [93] A. Cormio, F. Guerra, G. Cormio et al., “Mitochondrial DNA content and mass increase in progression from normal to hyperplastic to cancer endometrium,” *BMC Research Notes*, vol. 5, no. 1, p. 279, 2012.
- [94] B. Chance and G. R. Williams, “Respiratory enzymes in oxidative phosphorylation. I. Kinetics of oxygen utilization,” *The Journal of Biological Chemistry*, vol. 217, no. 1, pp. 383–393, 1955.
- [95] B. Chance and G. R. Williams, “Respiratory enzymes in oxidative phosphorylation. VI. The effects of adenosine diphosphate on azide-treated mitochondria,” *The Journal of Biological Chemistry*, vol. 221, no. 1, pp. 477–489, 1956.
- [96] T. Anmann, R. Guzun, N. Beraud et al., “Different kinetics of the regulation of respiration in permeabilized cardiomyocytes and in HL-1 cardiac cells. Importance of cell structure/organization for respiration regulation,” *Biochimica et Biophysica Acta (BBA) - Bioenergetics*, vol. 1757, no. 12, pp. 1597–1606, 2006.
- [97] A. Klepinin, V. Chekulayev, N. Timohhina et al., “Comparative analysis of some aspects of mitochondrial metabolism in differentiated and undifferentiated neuroblastoma cells,” *Journal of Bioenergetics and Biomembranes*, vol. 46, no. 1, pp. 17–31, 2014.
- [98] A. F. Salem, D. Whitaker-Menezes, Z. Lin et al., “Two-compartment tumor metabolism: autophagy in the tumor microenvironment and oxidative mitochondrial metabolism (OXPHOS) in cancer cells,” *Cell Cycle*, vol. 11, no. 13, pp. 2545–2556, 2012.
- [99] U. E. Martinez-Outschoorn, M. P. Lisanti, and F. Sotgia, “Catabolic cancer-associated fibroblasts transfer energy and biomass to anabolic cancer cells, fueling tumor growth,” *Seminars in Cancer Biology*, vol. 25, pp. 47–60, 2014.
- [100] U. Martinez-Outschoorn, F. Sotgia, and M. P. Lisanti, “Tumor microenvironment and metabolic synergy in breast cancers: critical importance of mitochondrial fuels and function,” *Seminars in Oncology*, vol. 41, no. 2, pp. 195–216, 2014.
- [101] F. Sotgia, D. Whitaker-Menezes, U. E. Martinez-Outschoorn et al., “Mitochondria “fuel” breast cancer metabolism: fifteen markers of mitochondrial biogenesis label epithelial cancer cells, but are excluded from adjacent stromal cells,” *Cell Cycle*, vol. 11, no. 23, pp. 4390–4401, 2012.

- [102] M. P. Lisanti, F. Sotgia, R. G. Pestell, A. Howell, and U. E. Martinez-Outschoorn, "Stromal glycolysis and MCT4 are hallmarks of DCIS progression to invasive breast cancer," *Cell Cycle*, vol. 12, no. 18, pp. 2935-2936, 2013.
- [103] F. Sotgia, U. E. Martinez-Outschoorn, S. Pavlides, A. Howell, R. G. Pestell, and M. P. Lisanti, "Understanding the Warburg effect and the prognostic value of stromal caveolin-1 as a marker of a lethal tumor microenvironment," *Breast Cancer Research*, vol. 13, no. 4, p. 213, 2011.
- [104] K. Tepp, K. Mado, M. Varikmaa et al., "The role of tubulin in the mitochondrial metabolism and arrangement in muscle cells," *Journal of Bioenergetics and Biomembranes*, vol. 46, no. 5, pp. 421-434, 2014.
- [105] M. Varikmaa, N. Timohhina, K. Tepp et al., "Formation of highly organized intracellular structure and energy metabolism in cardiac muscle cells during postnatal development of rat heart," *Biochimica et Biophysica Acta (BBA) - Bioenergetics*, vol. 1837, no. 8, pp. 1350-1361, 2014.
- [106] K. L. Sheldon, E. N. Maldonado, J. J. Lemasters, T. K. Rostovtseva, and S. M. Bezrukov, "Phosphorylation of voltage-dependent anion channel by serine/threonine kinases governs its interaction with tubulin," *PLoS One*, vol. 6, no. 10, article e25539, 2011.
- [107] T. K. Rostovtseva and S. M. Bezrukov, "VDAC inhibition by tubulin and its physiological implications," *Biochimica et Biophysica Acta (BBA) - Biomembranes*, vol. 1818, no. 6, pp. 1526-1535, 2012.
- [108] M. Gruno, N. Peet, E. Seppet et al., "Oxidative phosphorylation and its coupling to mitochondrial creatine and adenylate kinases in human gastric mucosa," *American Journal of Physiology. Regulatory, Integrative and Comparative Physiology*, vol. 291, no. 4, pp. R936-R946, 2006.
- [109] Y. Ishida, M. Wyss, W. Hemmer, and T. Wallimann, "Identification of creatine kinase isoenzymes in the guinea-pig. Presence of mitochondrial creatine kinase in smooth muscle," *FEBS Letters*, vol. 283, no. 1, pp. 37-43, 1991.
- [110] M. J. Kushmerick, "Energetics studies of muscles of different types," *Basic Research in Cardiology*, vol. 82, Supplement 2, pp. 17-30, 1987.

## Appendix 2

### **Publication II**

Klepinin, A., L. Ounpuu, K. Mado, L. Truu, V. Chekulayev, M. Puurand, I. Shevchuk, K. Tepp, A. Planken and T. Kaambre (2018). "The complexity of mitochondrial outer membrane permeability and VDAC regulation by associated proteins." *J Bioenerg Biomembr* 50(5): 339-354.





# The complexity of mitochondrial outer membrane permeability and VDAC regulation by associated proteins

Aleksandr Klepinin<sup>1</sup> · Lyudmila Ounpuu<sup>1</sup> · Kati Mado<sup>1</sup> · Laura Truu<sup>1</sup> · Vladimir Chekulayev<sup>1</sup> · Marju Puurand<sup>1</sup> · Igor Shevchuk<sup>1</sup> · Kersti Tepp<sup>1</sup> · Anu Planken<sup>2</sup> · Tuuli Kaambre<sup>1</sup>

Received: 15 January 2018 / Accepted: 5 July 2018 / Published online: 12 July 2018  
© The Author(s) 2018

## Abstract

Previous studies have shown that class II  $\beta$ -tubulin plays a key role in the regulation of oxidative phosphorylation (OXPHOS) in some highly differentiated cells, but its role in malignant cells has remained unclear. To clarify these aspects, we compared the bioenergetic properties of HL-1 murine sarcoma cells, murine neuroblastoma cells (uN2a) and retinoic acid - differentiated N2a cells (dN2a). We examined the expression and possible co-localization of mitochondrial voltage dependent anion channel (VDAC) with hexokinase-2 (HK-2) and  $\beta$ II-tubulin, the role of depolymerized  $\beta$ II-tubuline and the effect of both proteins in the regulation of mitochondrial outer membrane (MOM) permeability. Our data demonstrate that neuroblastoma and sarcoma cells are prone to aerobic glycolysis, which is partially mediated by the presence of VDAC bound HK-2. Microtubule destabilizing (colchicine) and stabilizing (taxol) agents do not affect the MOM permeability for ADP in N2a and HL-1 cells. The obtained results show that  $\beta$ II-tubulin does not regulate the MOM permeability for adenine nucleotides in these cells. HL-1 and NB cells display comparable rates of ADP-activated respiration. It was also found that differentiation enhances the involvement of OXPHOS in N2a cells due to the rise in their mitochondrial reserve capacity. Our data support the view that the alteration of mitochondrial affinity for ADNs is one of the characteristic features of cancer cells. It can be concluded that the binding sites for tubulin and hexokinase within the large intermembrane protein supercomplex Mitochondrial Interactosome, could be different between muscle and cancer cells.

**Keywords** Mitochondria · Adenylate kinase · Glycolysis · OXPHOS · Tubulin · Warburg effect

## Abbreviations

ADNs	Adenine nucleotides
AK	Adenylate kinase
BSA	Bovine serum albumin
CM	Cardiomyocyte
CAT	Carboxyatractyloside
CK	Creatine kinase

FCCP	Carbonyl cyanide p-(trifluoro-methoxy)phenyl-hydrazone
HK	Hexokinase
Km	MICHAELIS-Menten constant
NB	Neuroblastoma
N2a	NEURO-2a
uN2a	Undifferentiated N2a cells
dN2a	Differentiated N2a cells
MtCK	Mitochondrial creatine kinase
OXPHOS	Oxidative phosphorylation
MI	Mitochondrial Interactosome
MOM	Mitochondrial outer membrane
PBS	Phosphate buffered saline
PCr	Phosphocreatine
PEP	Phosphoenolpyruvate
PK	Pyruvate kinase
RA	All-trans-retinoic acid
SNS	Sympathetic nerve system
VDAC	Voltage dependent anion channel
Vo	Rate of basal respiration
Vm	Maximal respiration rate

Aleksandr Klepinin and Lyudmila Ounpuu contributed equally to this work.

**Electronic supplementary material** The online version of this article (<https://doi.org/10.1007/s10863-018-9765-9>) contains supplementary material, which is available to authorized users.

✉ Tuuli Kaambre  
tuuli.kaambre@kbfi.ee

<sup>1</sup> Laboratory of Bioenergetics, National Institute of Chemical Physics and Biophysics, Akadeemia tee 23, 12618 Tallinn, Estonia

<sup>2</sup> Oncology and Hematology Clinic at the North Estonia Medical Centre, Tallinn, Estonia



## Introduction

Malignant transformation of cells leads to reprogramming in numerous signaling and metabolic pathways, especially in regard to energy metabolism. Targeting of tumor-initiating and cancer cell energy metabolism has been proposed to be a novel and highly effective strategy for the selective ablation of malignant tumors (Aminzadeh et al. 2015; Gogvadze et al. 2009; Lamb et al. 2015; Moreno-Sanchez et al. 2007).

Recently, it was demonstrated that the mitochondrial outer membrane (MOM) voltage-dependent anion channel (VDAC) is the main switch between mitochondrial oxidative phosphorylation (OXPHOS) and glycolysis in malignant cells and it could be a good target for a new generation of cancer therapy (Carre et al. 2002; Maldonado 2017). Mitochondrial VDAC plays a key role in maintaining high rates of OXPHOS as well as in the realization of apoptotic programs (Shoshan-Barmatz et al. 2006, 2009, 2017). It was reported that in brain and tumor cells, some hexokinase isoforms can bind to the VDAC in the MOM thereby suppressing cytochrome c release and apoptotic cell death (Arzoine et al. 2009). This channel is involved in the transport of respiratory substrates,  $\text{Ca}^{2+}$ , ATP, ADP and inorganic phosphate across the external mitochondrial membranes supporting the high efficiency of OXPHOS and the Krebs cycle (Noskov et al. 2013; Rostovtseva and Colombini 1997; Shoshan-Barmatz et al. 2018).

Studies performed during the past decade have shown that in mammalian cells the permeability of mitochondrial VDAC towards adenine nucleotides (AND(s)) and respiratory substrates is a precisely controlled process (Rostovtseva and Bezrukov 2012). But, the precise regulatory factors mediating this VDAC permeability, especially, in cancer cells, are studied insufficiently. The regulation of MOM permeability has been quite thoroughly studied on heart and skeletal muscles. These *in situ* studies have shown that in slow-twitch skeletal and heart muscles the value of apparent Michaelis-Menten constant  $K_m$  for ADP is high (there exist diffusion obstacles for adenine nucleotides (ADNs), but for fast-twitch skeletal muscles the permeability of MOM for ADNs is normally high and the value of the Michaelis-Menten constant is 20 times lower than is oxidative muscles (Kuznetsov et al. 1996; Saks et al. 1995; Saks and Aliev 1996; Saks et al. 1994, 1998). Ultrastructural studies have revealed multiple connections between cytoskeletal elements and mitochondria in different types of cells. Several candidate proteins that can regulate the MOM permeability for AND(s) have been proposed like the  $\alpha$ - $\beta$  tubulin heterodimer (Guzun et al. 2015; Maldonado and Lemasters 2014; Maldonado et al. 2013; Rostovtseva and Bezrukov 2012; Saks et al. 2010), desmin (Appaix et al. 2003; Capetanaki et al. 2007; Guzun et al. 2012; Saetersdal et al. 1990; Winter et al. 2015), plectin (Reipert et al. 1999; Winter et al. 2008, 2015),  $\alpha$ -synuclein (Hoogerheide et al. 2017; Rostovtseva et al. 2015; Shen et al. 2014; Zhang et al.

2016),  $\alpha$ - $\beta$ -crystallin (Diokmetzidou et al. 2016), microtubule-associated proteins (Guzun et al. 2012), and some hexokinase (HK) isoforms (Beutner et al. 1996; Bryan and Raisch 2015; Lemeshko 2014; Lu et al. 2015; Mathupala et al. 2009; Nederlof et al. 2014).

In cells with a high energy demand the OXPHOS system is organized into large protein complexes, one of them is the protein supercomplex Mitochondrial Interactosome (MI) (Guzun et al. 2012; Saks et al. 2010; Tepp et al. 2011; Timohhina et al. 2009). MI is a large transmembrane complex consisting of ATP-synthase, mitochondrial creatine kinase (MtCK) or other representatives of mitochondrial kinases, VDAC, and some protein factors, which regulate the MOM permeability for adenine nucleotides. It has been demonstrated that in rat heart cardiomyocytes (CMs)  $\beta$ II-tubulin binds to VDAC regulating the permeability of this mitochondrial channel for adenine nucleotides and promoting thereby the generation of phosphocreatine (PCr) via MtCK (Guzun et al. 2015; Timohhina et al. 2009). It was found, that during carcinogenesis the composition and structure of MI may be radically reorganized due to profound alterations in the expression of its components (Chevrollier et al. 2011; Koit et al. 2017).

Two mechanisms by which the MOM permeability is regulated in cancer cells have been proposed. First, according to the model proposed by Pedersen and co-workers, the interaction of VDAC with HK-2 is one of the main pathways mediating the “Warburg effect” or aerobic glycolysis in cancer cells (Mathupala et al. 2009; Pedersen 2007b). It has been shown that HK-2 binding on VDAC channel keeps it in an open state (Majewski et al. 2004) and allows the HK-2 to use intra-mitochondrially generated ATP to phosphorylate glucose (Cesar Mde and Wilson 1998). The second mechanism proposed by Maldonado and co-workers, demonstrates that in hepatocarcinoma cells VDAC is blocked by free tubulin which induces malignant cells to switch to aerobic glycolysis (Maldonado et al. 2010). They have demonstrated that if the level of non-polymerized  $\alpha$ - $\beta$  heterodimer tubulin increases in liver cancer cells, it leads to rising of mitochondrial membrane potential, which induces closing of VDAC. Recently, our study on rat muscle tissues, suggested that only non-polymerized  $\beta$ II-tubulin in heart and soleus muscles plays an important role in the regulation of MOM permeability for ADP (Varikmaa et al. 2014). In both studies the free dimeric tubulin has been shown to affect VDAC permeability, but its effect depends on polymerized/dimeric tubulin ratio.

In the current study we therefore hypothesized that in cancer cells the free  $\beta$ II-tubulin can compete with HK-1 or HK-2 for the binding sites on VDAC(s) consequently, in order to regulate the aerobic glycolysis in tumor cells. The aim of the present study was to clarify the role of free/polymerized  $\beta$ II-tubulin and HK-2 in regulation of energy transfer in malignant

cells of different histological origin. For this purpose, experiments were performed on Warburg phenotype cell lines, such as undifferentiated murine neuroblastoma cells (N2a) and retinoic acid (RA)-differentiated NB cells, as well as on HL-1 cardiac sarcoma cells, where free/polymerized level was regulated by the tubulin depolymerizing agent colchicine and tubulin polymerizing agent taxol (See Graphical Abstract in [Supplementary material](#)).

## Materials and methods

### Chemicals

Dulbecco's Modified Eagle Medium (DMEM) and phosphate buffered saline (PBS, Ca/Mg free) were obtained from Corning, Inc. (USA) whereas heat-inactivated fetal bovine serum (FBS), accutase, penicillin-streptomycin solution (100×), gentamicin and 0.05% Trypsin-EDTA were purchased from Gibco Life Technologies (Grand Island, NY, USA). Primary and secondary antibodies were obtained from Santa Cruz Biotechnology Inc. (USA) or Abcam PLC (UK), rabbit polyclonal antibodies against VDAC1 kindly donated by Dr. Catherine Brenner from Paris-Sud University, France. Unless otherwise stated, all other chemicals were purchased from Sigma-Aldrich Company (St. Louis, USA).

### Cultivation of murine neuroblastoma (Neuro-2a) cells and their differentiation

The stock culture of N2a cells was obtained from the American Type Culture Collection (ATCC, Cat. No. CCL-131). These NB cells were grown in T75 flasks (Greiner bio-one) as a loosely adhering monolayer at 37 °C in 5% CO<sub>2</sub> in a high glucose (4.5 g/l) DMEM supplemented with L-glutamine, 10% FBS, 100 U/ml penicillin, 100 µg/ml streptomycin, and 50 µg/ml gentamicin. The neural differentiation of N2a cells to cholinergic neurons was induced by their cultivation with 10 µM all-trans-retinoic acid (RA) in a complete growth medium, but at a decreased (1%) concentration of FBS for seven days (Blanco et al. 2001; Klepinin et al. 2014).

### Cultivation of HL-1 tumor cells

The non-beating HL-1 cell line derived from tumoral atrial cardiac myocytes of mice (Claycomb et al. 1998; Pelloux et al. 2006) was used. These tumor cells were kindly provided by Dr. Andrey V. Kuznetsov (Innsbruck Medical University, Austria). HL-1 cells were grown in fibronectin gelatin coated (5 µg/ml and 0.2%, respectively) T75 flasks containing Claycomb medium (Sigma-Aldrich) supplemented with 10% FBS, 100 U/ml penicillin, 100 µg/ml streptomycin, 50 µg/ml

gentamicin, 2 mM L-glutamine, 0.1 mM norepinephrine, and 0.3 mM ascorbic acid.

### Cell viability and proliferation assays

The number of viable cells was estimated by trypan blue exclusion assay, while the rate of cell proliferation by MTT assay as described in our prior work (Klepinin et al. 2014).

### Cell permeabilization and measurements of OXPHOS function in cells

To examine the functional capacity of mitochondria in N2a and HL-1 tumor cells, we applied the permeabilized cell technique developed by Kuznetsov and colleagues (Kuznetsov et al. 2008). This method allows to studying the function of mitochondria in situ in tissues and cells without isolation of these organelles. The permeabilization procedure leaves intact intracellular interactions of mitochondria with cytoskeleton and other organelles.

Plasma membranes were permeabilized with saponin at 40 µg/ml (N2a cells) or digitonin at 25 µg/ml treatments (for HL-1 cells). The rate of O<sub>2</sub> consumption in permeabilized N2a or HL-1 cells was measured at 25 °C with an Oxygraph-2 K respirometer (Oroboros Instruments, Austria) in respiration medium-B (Kuznetsov et al. 2008) supplemented with 5 mM glutamate, 2 mM malate and 10 mM succinate as respiratory substrates; the solubility of oxygen was taken as 240 nmol/ml (Gnaiger 2001). For determination of the reserve respiratory capacity of mitochondria, the rate of cellular O<sub>2</sub> consumption was measured before and after a stepwise addition of the mitochondrial uncoupler – carbonyl cyanide p-(trifluoro-methoxy)phenyl-hydrazone (FCCP). The rates of O<sub>2</sub> consumption were normalized per mg cellular protein. The protein concentration in cell lysates was determined using the Pierce BCA Protein Kit.

### Determination of apparent Michaelis-Menten constant values for exogenously added ADP

The apparent K<sub>m</sub> and V<sub>m</sub> values for exogenously added ADP (<sup>ADP</sup>K<sub>m</sub>) were calculated from ADP titration experiments using the corresponding non-linear regression equation.

### Analysis of OXPHOS coupling with hexokinase (HK)-mediated processes

The coupling between mitochondrially bound HK(s) and the OXPHOS system in permeabilized cells was assayed by oxygraphy, through stimulation of mitochondrial respiration by locally generated ADP as described earlier (Eimre et al. 2008; Kaldma et al. 2014). The effect of glucose on mitochondrial respiration was expressed by the glucose index (I<sub>GLU</sub>) that

was calculated according to the equation  $I_{GLU} (\%) = [(V_{GLU} - V_{ATP}) / (V_{ADP} - V_{ATP})] * 100$ , where  $V_{ADP}$  is the rate of  $O_2$  consumption in the presence of 2 mM ADP,  $V_{GLU}$  is the respiration rate with 10 mM glucose and  $V_{ATP}$  is respiration rate with 0.1 mM ATP; i.e. this index reflects the degree of glucose-mediated stimulation of mitochondrial respiration as compared with the maximal ADP-activated rate of  $O_2$  consumption.

### Immunofluorescence analysis

Immunocytochemistry along with confocal microscopy imaging were applied to visualize the expression and possible colocalization of VDAC, with HK-2, and  $\beta$ II-tubulin in HL-1 and N2a cells. For immunofluorescence studies the following primary antibodies were used: rabbit polyclonal antibodies vs. VDAC1 (kindly provided by Dr. Catherine Brenner; Paris-Sud University, Paris, France), goat polyclonal antibodies vs. HK-2 (sc-6521; Santa Cruz Biotechnology, Inc., USA), and mouse monoclonal antibody to TUBB2A (ab92857; Abcam®, UK). After overnight incubation (at 4 °C) with the indicated primary antibodies, HL-1 cells were washed with a 2% BSA solution and co-incubated with the following secondary fluorescent antibodies: a) anti-rabbit IgG labeled with DyLight-488 (ab96895) giving green fluorescence, to visualize VDAC; b) anti-goat Cy-3 labeled IgG that gives red fluorescence, to stain HK-2; and c) donkey anti-mouse IgG-CFL: 647 sc-362,288 (violet color) or goat anti-mouse DyLight-550 labeled IgG (ab96880) yielding red, to stain  $\beta$ II-tubulin. ProLong Gold antifade reagent supplemented with 4',6-diamidino-2-phenylindole dihydrochloride (DAPI, Molecular Probes™) used for visualizing the cell nucleus. The cells were then imaged by an Olympus FluoView FV10i-W inverted laser scanning confocal microscope. For immunofluorescent studies, N2a cells were seeded in 12-well plates (at a density of  $1 \times 10^4$  cells/well) over glass coverslips, treated or not with 10  $\mu$ M RA, and then immunostained mostly as described above for HL-1 cells. The presence of mitochondria in N2a cells was also estimated through the selective labeling of the VDAC1 (sc-8828, Santa Cruz Biotechnology, Inc., USA). The visualization of VDAC1 protein expression was carried out using fluorescent secondary donkey anti-goat Cy-3 (ab97115) antibodies (red fluorescence) and to visualize  $\beta$ II-tubulin donkey anti-rabbit IgG (Alexa Fluor® 488, ab150073, green fluorescence).

### SDS-PAGE and western blot analysis of the levels of beta-tubulin isotypes in N2a and HL-1 cells

The cells were washed twice with Ca/Mg-free PBS and then treated with a microtubule lysing buffer consisting of 100 mM PIPES, 5 mM  $MgCl_2$ , 1 mM EGTA, 30% glycerol, 0.1% IGEPAL, 0.1% Tween-20, 0.1% Triton X-100, 0.1% beta-mercaptoethanol, 1 mM ATP, 0.1 mM GTP and a complete

protease inhibitor cocktail (Roche); the recipe is according to Cytoskeleton, Inc. (USA). The lysate was homogenized by Retsch Mixer Mill at 25 Hz for 2 min, and incubated for 30 min at 35 °C. The obtained cell lysates were clarified by centrifugation at 21000  $\times g$  for 40 min at 35 °C. The protein concentration in lysates was determined using the Pierce BCA Protein Kit. Proteins were separated by 12% SDS-PAGE and transferred onto the PVDF membrane by Trans-Blot Semi-Dry Transfer system (Bio-Rad, Inc., USA).

To determine the presence of beta-tubulin isotypes Abcam mono- and polyclonal antibodies (anti-beta I Tubulin (ab11312), anti-Tubb2A (ab170931) and anti-beta III Tubulin (ab52901) were used. After the chemiluminescence reaction, the PVDF membranes were stained with Coomassie brilliant blue R250 to measure the total protein amount. The tubulin signal intensity was normalized against total protein intensities obtained from Coomassie staining. Quantification was performed by ImageJ software.

### Evaluation of soluble and polymerized beta-tubulins

The content of free and polymerized tubulin in HL-1 and N2a cells was assessed using a “Microtubules/Tubulin in vivo Assay” kit (Cytoskeleton Inc.) in accordance with the manufacturer’s manual. Cells were homogenized in cell lysis and microtubule stabilization buffer (100 mM PIPES pH 6.9, 5 mM  $MgCl_2$ , 1 mM EGTA, 30% (v/v) glycerol, 0.1% Nonidet P40, 0.1% Triton X-100, 0.1%  $\beta$ -mercaptoethanol, 0.001% antifoam) supplemented with 0.1 mM GTP, 1 mM ATP and protease inhibitor cocktail. In addition, cell fractions containing 10  $\mu$ M taxol and 2 mM  $CaCl_2$  were used as the positive and negative controls. Lysates were centrifuged at 2000  $\times g$  for 5 min at 37 °C to remove intact cells. Supernatants were centrifuged at 100000  $\times g$  for 30 min at 37 °C to separate microtubules from soluble (free) tubulin. The pellets containing polymerized tubulin were suspended in ice-cold 2 mM  $CaCl_2$ .

Free tubulin and polymerized tubulin fractions were loaded on 10% polyacrylamide gels. Proteins were transferred using the Trans-Blot SD Semi-Dry Transfer Cell (BioRad). Blots were blocked in 5% nonfat milk and probed with anti Tubb2A (ab170931) antibody for 2 h at room temperature. Immunoblots were incubated with secondary antibodies (anti-mouse IgG, HRP, Abcam) for 1 h at room temperature. Detection was conducted using a chemiluminescence kit (Pierce ECL Western Blotting Substrate).

### Assessment of basic OXPHOS parameters in HL-1 and N2a cells pretreated with colchicine and taxol

Unless otherwise specified, these tumor cells were treated with colchicine (10  $\mu$ M), taxol (10  $\mu$ M) or DMSO (control) for 24 h at 37 °C. In some experiments, the influence of

colchicine and taxol on the affinity of mitochondria to exogenously added ADP as well as their respiratory reserve capacity was also examined after a short-term (for 20 min) exposure of tumor cells to these microtubular toxins. (Maldonado et al. 2010). The following OXPHOS parameters were then assessed: basal respiration, ATP-linked respiration, proton leak, maximal respiration and mitochondrial reserve capacity (Supplementary Fig. 3; Fig. 5). Basal respiration was measured in medium-B supplemented with 5 mM glutamate, 2 mM malate and 10 mM succinate. Then, oligomycin (2.5  $\mu$ M) was added to inhibit proton flow through ATP synthase blocking ATP-linked oxygen consumption. Maximal respiration was measured by exposing cells to carbonyl cyanide-p-trifluoromethoxyphenyl-hydrazone (FCCP), which uncoupled respiration from ATP production. In the presence of FCCP, respiration increased beyond the basal respiration by reserve capacity of mitochondria. Finally, the electron transport was inhibited by 10  $\mu$ M antimycin, a complex III inhibitor, indicating the non-mitochondrial oxygen consumption. Proton leak was calculated by subtracting the rate of non-mitochondrial respiration from respiration that remained after ATP-synthase inhibition. The maximal respiration capacity was calculated by subtracting non-mitochondrial respiration rates from the FCCP induced maximal respiration. Changes in the ATP-linked respiration, proton leak, maximal respiration and reserve capacity were expressed as a percentage of basal respiration.

### Statistical analysis

All data points are presented as means  $\pm$  standard error (SEM) from at least five separate experiments performed in duplicate. The statistical differences between the groups were calculated by the two-tailed Student's t-test. Differences were considered to be statistically significant when  $p < 0.05$ .

## Results

### The effect of saponin/digitonin treatment on the intactness of mitochondrial membranes in N2a and HL-1 cells

The mitochondrial respiration in all studied permeabilized cell types was activated with 2 mM ADP and the rate of  $O_2$  consumption was increased by about 3–4 times (Supplementary Fig. 1). The subsequent addition of cytochrome c (Cyt c) to permeabilized cells did not cause an increase of more than 10% in the rate of oxygen consumption, which indicated the intactness of the outer mitochondrial membrane. After that, addition of carboxyatractyloside (CAT), an inhibitor of the adenine nucleotide translocator, decreased the respiration rate back to the basal level ( $V_0$ ), showing the intactness of the

mitochondrial inner membrane. Experiments showed that all used cell cultures had similar rates of basal and State III respiration. Respiratory control index (RCI) values for uN2a, dN2a and HL-1 cells were calculated as  $4.51 \pm 0.63$ ,  $4.43 \pm 0.22$  and  $5.11 \pm 0.59$ , respectively.

We also showed that the permeabilization method does not affect the tubulin content in cell cultures (Supplementary Fig. 2).

### The intracellular content and distribution of tubulin in HL-1 and N2a cells

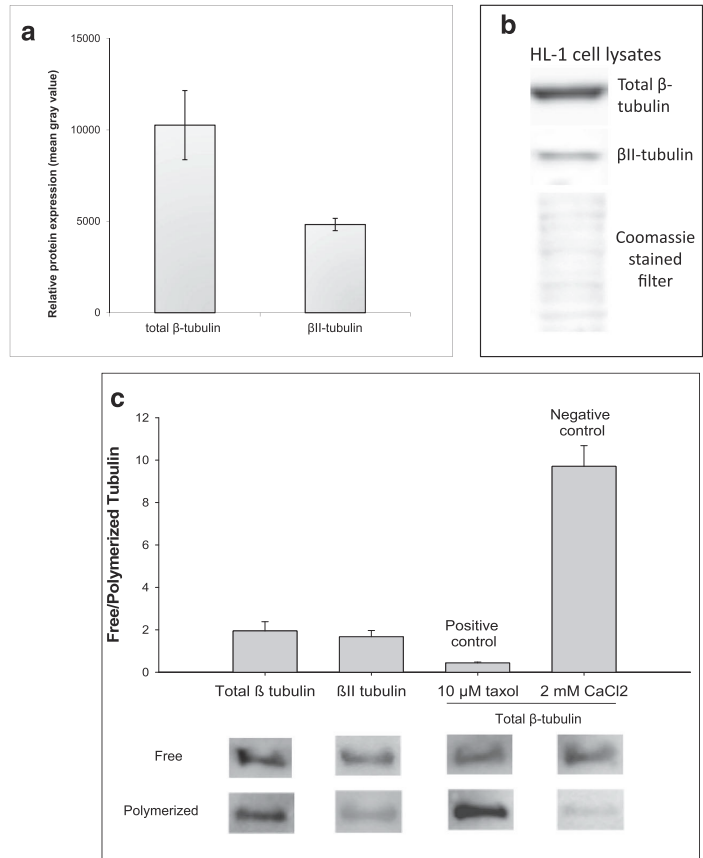
We checked total  $\beta$  and  $\beta$ -II tubulin expression in HL-1 cells. Our results showed that  $\beta$ -II tubulin constitutes about 50% of the total  $\beta$ -tubulin in those cells (Fig. 1a, b). Nevertheless, the amount of free/polymerized  $\beta$ -II tubulin and total  $\beta$ -tubulin was equal (Fig. 1c). Confocal microscopy showed, that a part of the mitochondria in HL-1 cells is distributed randomly, whereas other mitochondria are attached to  $\beta$ II-tubulin containing microfilaments, and concentrated around the cell nucleus - an area with an increased energy demand (Fig. 2).

As  $\beta$ II-tubulin has been shown to regulate MOM permeability in brain synaptosomes, we next characterized the profile of  $\beta$ -tubulin isoforms in cancer cells with neurological origin. N2a cells were maintained in differentiated and non-differentiated states to estimate the alteration of  $\beta$ -tubulin amount and distribution during differentiation. Our results demonstrated that significant changes occurred in the intracellular content of  $\beta$ I- and  $\beta$ III-tubulin, while  $\beta$ II-tubulin remained at the same level (Fig. 3). Immunofluorescence studies showed that differentiation of N2a was accompanied by remarkable shifts in the intracellular distribution of main  $\beta$ -tubulin isotypes. In uN2a cells,  $\beta$ I-,  $\beta$ II- and  $\beta$ III-tubulins were localized predominantly around the cell nucleus, whereas in RA-treated cells a part of  $\beta$ -tubulin isotypes were assembled in filamentous structures that crossed the entire cell and neurites (Fig. 4a–c).

### Mitochondrial reserve respiratory capacity in HL-1 sarcoma cells, undifferentiated and differentiated N2a cells

Several works have demonstrated that VDAC gating is regulated by several molecules including glutamate (Gincel et al. 2000), NADH (Zizi et al. 1994) and tubulin (Timohhina et al. 2009). Therefore in the current study we further explored how the availability of main respiratory substrates influences mitochondrial respiration and respiratory reserve capacity. The maximal mitochondrial respiration in the uncoupled state of the respiratory chain was measured by titration of intact HL-1 cells with the mitochondrial uncoupler FCCP in cells growth medium and in medium-B (see Materials and methods). FCCP is

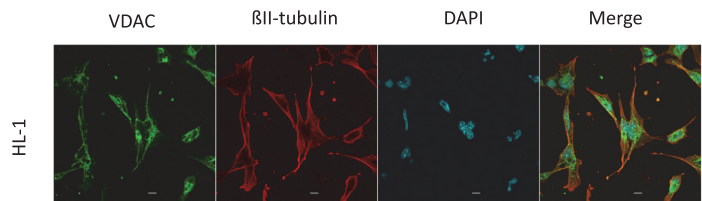
**Fig. 1** Western blot analysis for the presence of total  $\beta$  and  $\beta$ II-tubulin in HL-1 cells (a, b) as well as the levels of free and polymerized total  $\beta$ - and  $\beta$ II-tubulin in these tumor cell line (c); here, lower panel shows the representative immunoblot test for free and polymerized total  $\beta$  and  $\beta$ II tubulin in HL-1 cell. Upper panel shows a densitometric quantification of the total  $\beta$  and  $\beta$ II tubulin in the soluble and insoluble fractions of HL-1 cells. Error bars are the mean  $\pm$  SE from 3 separate experiments; \* $p < 0.05$  when compared to total  $\beta$  tubulin in HL-1 cells; \*\* $p < 0.005$  when compared to  $\beta$ II-tubulin in HL-1 cells



a protonophore that uncouples electron transport and mitochondrial respiration from ATP synthesis by dissipating the proton gradient. We found that high levels of FCCP inhibited mitochondrial respiration in these cells. The FCCP concentration for cells growth medium was 4  $\mu$ M and for medium-B 2  $\mu$ M. The mitochondrial reserve capacity was calculated from the  $V_F/V_o$  ratio (Table 1). In HL-1 cells no difference in respiration rate and mitochondrial reserve capacity was seen between growth medium and medium-B. To compare differentiated and undifferentiated N2a cells, both cell cultures were titrated with FCCP in the medium-B. The optimal concentration of

FCCP for both cell types was 2  $\mu$ M. Our results showed that the RA-mediated differentiation of N2a cells increased their mitochondrial capacity in the presence of complex I and II respiration substrates (Table 2). The contribution of complexes I and II to the total mitochondrial reserve capacity was also examined. The complex II activated respiration was measured in the presence of rotenone, an inhibitor of complex I. The addition of rotenone (1  $\mu$ M) resulted in a 20–30% decrease in the rate of  $V_o$  in both uN2a and RA-treated cells (Table 2). Experiments with FCCP suggested that the mitochondrial capacity increased not only through the activation of

**Fig. 2** Confocal immunofluorescence imaging of the mitochondrial VDAC1 protein (green),  $\beta$ II-tubulin (red), nucleus (blue) and their colocalization in HL-1 tumor cells; bars are 10  $\mu$ m



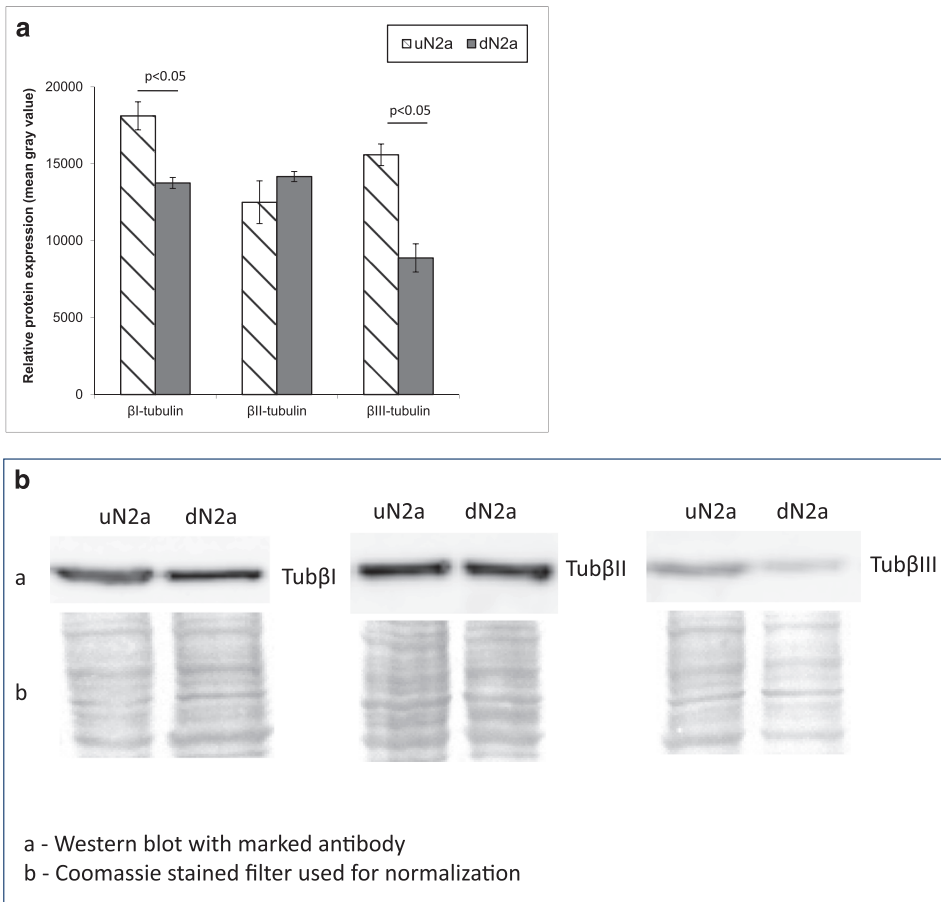


**Fig. 3** Western blot (WB) analysis of the expression levels of  $\beta$ I-,  $\beta$ II- and  $\beta$ III-tubulin in undifferentiated and RA-differentiated N2a cells (**a**) as well as the representative WB images (**b**). Error bars are the mean  $\pm$  SE from 5 independent experiments

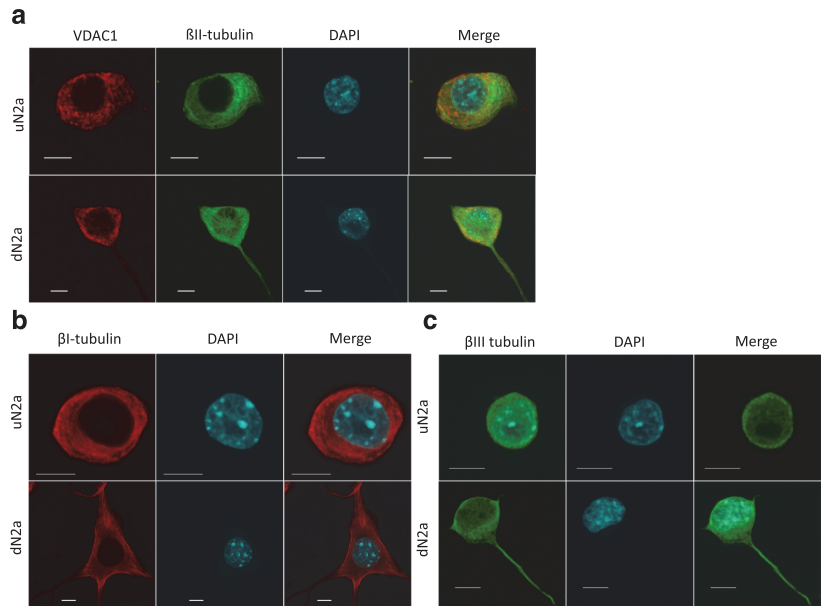
complex I, but also complex II during the differentiation of N2a cells.

### Mitochondrial contribution to the energy metabolism in HL-1 cells with polymerized and unpolymerized tubulin

For understanding the influence of polymerized and unpolymerized tubulin on the mitochondrial contribution of energy metabolism, we analyzed the oxygen consumption rate of the HL-1 cells in the presence of respiratory chain inhibitors (oligomycin, antimycin) and uncoupler of OXPHOS (FCCP) (Fig. 5 a, b). After measurement of basal respiration, the inhibitor of ATP synthase oligomycin was added to uncouple the ATP-linked respiration from the proton leak. The addition of FCCP resulted in an increase of oxygen consumption levels in all samples, but compared

to the control, the taxol treatment showed higher response than observed in colchicine treated cells (Fig. 5a). Finally, mitochondrial respiration was inhibited by antimycin. Similar inhibition effects were noticed in drug treated (colchicine, taxol) and untreated HL-1 cells (Fig. 5a). Next, the ATP link, proton leak, maximal respiration capacity and reserve capacity were calculated according to the mitochondrial stress protocol (Supplementary Fig. 3; 4). The mitochondrial stress protocol revealed that both colchicine and taxol treatment increased ATP-linked respiration at the same time decreased proton leak compared to control HL-1 cells (Fig. 5b). However, taxol and colchicine influenced the mitochondrial maximal respiration capacity as well as reserve capacity in different way. On the one hand, taxol increased both mitochondrial capacity parameters, but on the other hand, colchicine decreased them compared to control HL-1 cells (Fig. 5b).

**Fig. 4** Confocal immunofluorescence imaging of the mitochondrial VDAC1 protein (red),  $\beta$ II-tubulin (green) and their colocalization in undifferentiated (uN2a) and RA-differentiated (dN2a) cells (a) distribution of  $\beta$ I- (red) (b) and  $\beta$ III-tubulin isoforms (green) (c) in uN2a and dN2a cells. The cell nuclei were stained with DAPI (blue); bars are 10  $\mu$ m



### Mitochondrial contribution to the energy metabolism in HL-1 cells with polymerized and unpolymerized tubulin

In neuroblastoma cells colchicine and taxol had no effect on their bioenergetics parameters (Supplementary Fig. 4).

### Analysis of OXPHOS coupling with hexokinase-2

On the basis of the Pedersen model (Pedersen 2007b), the mechanisms of aerobic glycolysis were examined for HL-

**Table 1** The effects of FCCP on the respiratory activity of non-permeabilized HL-1 cells

Respiratory medium	Rates of O <sub>2</sub> consumption, nmol/min per mg protein, mean $\pm$ SE, <i>n</i> = 6
Claycomb medium <sup>(a)</sup>	<sup>(b)</sup> V <sub>0</sub> = 4.9 $\pm$ 0.27 <sup>(c)</sup> V <sub>F</sub> = 11.34 $\pm$ 0.45 V <sub>F</sub> /V <sub>0</sub> = 2.33 $\pm$ 0.16
Succ + Mal + Glut <sup>(d)</sup>	V <sub>0</sub> = 4.81 $\pm$ 0.17 V <sub>F</sub> = 12.10 $\pm$ 0.03 V <sub>F</sub> /V <sub>0</sub> = 2.52 $\pm$ 0.09

<sup>a</sup> full Claycomb medium supplemented with 10% FBS and antibiotics

<sup>b</sup> V<sub>0</sub> is the initial rate of O<sub>2</sub> consumption

<sup>c</sup> V<sub>F</sub> is the maximal rate of mitochondrial respiration in the presence of 4  $\mu$ M FCCP

<sup>d</sup> in medium-B

**Table 2** The effects of FCCP on the respiratory activity of non-permeabilized N2a cells (both undifferentiated and RA-treated) in medium-B with/without the presence of rotenone - an inhibitor of complex-I of the mitochondrial respiratory chain

Respiratory substrates <sup>(a)</sup>	Rates of O <sub>2</sub> consumption, nmol/min per mg protein, mean $\pm$ SE, <i>n</i> = 5	
	Undifferentiated N2a cells	Differentiated N2a cells
Mal + Glut	<sup>(b)</sup> V <sub>0</sub> = 1.86 $\pm$ 0.04 V <sub>F</sub> = 3.03 $\pm$ 0.14 V <sub>F</sub> /V <sub>0</sub> = 1.65 $\pm$ 0.08	V <sub>0</sub> = 1.92 $\pm$ 0.1 V <sub>F</sub> = 4.21 $\pm$ 0.28 V <sub>F</sub> /V <sub>0</sub> = 2.16 $\pm$ 0.07; p = 0.005)
Suc + Mal + Glut	V <sub>0</sub> = 2.55 $\pm$ 0.07 V <sub>F</sub> = 4.65 $\pm$ 0.03 V <sub>F</sub> /V <sub>0</sub> = 1.84 $\pm$ 0.06	V <sub>0</sub> = 2.55 $\pm$ 0.12 V <sub>F</sub> = 5.81 $\pm$ 0.2 V <sub>F</sub> /V <sub>0</sub> = 2.33 $\pm$ 0.13; p = 0.01
Suc + Mal + Glut in the presence of Rot	V <sub>0</sub> = 2.75 $\pm$ 0.25 V <sub>R</sub> = 1.84 $\pm$ 0.12 (67%*) V <sub>F</sub> = 3.0 $\pm$ 0.2 <sup>(c)</sup> V <sub>F</sub> /V <sub>R</sub> = 1.65 $\pm$ 0.04	V <sub>0</sub> = 2.8 $\pm$ 0.2 V <sub>R</sub> = 2.27 $\pm$ 0.17 (81.1%*) V <sub>F</sub> = 4.56 $\pm$ 0.32 V <sub>F</sub> /V <sub>R</sub> = 2.06 $\pm$ 0.09; p = 0.005

<sup>a</sup> Succinate (Suc, at 10 mM), malate (Mal, at 2 mM), and glutamate (Glut, at 5 mM) served as respiratory substrates

<sup>b</sup> V<sub>0</sub> is the initial rate of O<sub>2</sub> consumption

<sup>c</sup> V<sub>F</sub> and V<sub>R</sub> are the rates of O<sub>2</sub> consumption in the presence of 2  $\mu$ M FCCP and 1  $\mu$ M rotenone, respectively (rotenone was added 5 min before titrations with FCCP); \* % from V<sub>0</sub> value

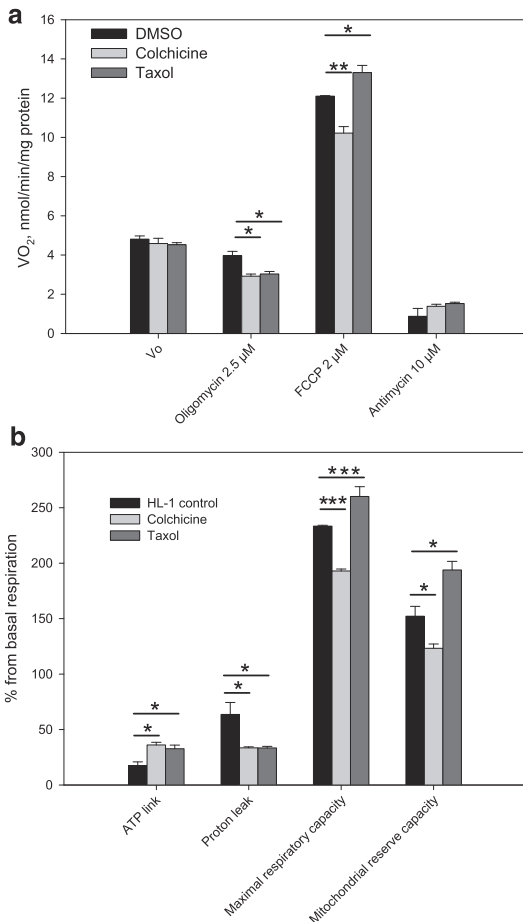


**Fig. 5** The effects of taxol and colchicine on mitochondrial bioenergetics in HL-1 cardiac tumor cells. **a** Basal respiration – V<sub>o</sub>, responses to treatment with 2.5 μM oligomycin, FCCP and antimycin A. **b** Effects of taxol and colchicine on proton leak, ATP linked respiration, maximal respiratory capacity and mitochondrial respiratory reserve capacity in HL-1 cells compared to control (DMSO treated) cells. Data are shown as mean ± SEM (n = 4). Significance stars depict changes in mitochondrial respiration compared to DMSO treated control cells: \* p < 0.05, \*\* p < 0.01, \*\*\* p < 0.001

1 and both N2a cell types. Immunostaining of HL-cells showed clearly the possibility of interactions between VDAC and HK-2 (Pearson’s coefficient = 0.96 ± 0.02; Fig. 6a). The addition of glucose (10 mM) in the presence of ATP resulted in an increase in the rate of O<sub>2</sub> consumption by these cells, demonstrating thereby the coupling between HK-2 catalyzed reactions and the OXPHOS system, where the strength of functional coupling was quantified by the glucose index (Fig. 7). The same mechanism of aerobic glycolysis was examined for undifferentiated and RA-treated N2a cells. There were no significant differences between respiratory

states in these cell cultures. The confocal microscopy of immunostained preparations of undifferentiated and dN2a cells revealed a similar degree for the HK-2-VDAC colocalization (corresponding Pearson’s coefficients were measured as 0.83 ± 0.07 and 0.84 ± 0.07, respectively; Fig. 6b). These data, along with the oxygraphic analysis of the functional coupling between HK-2 and OXPHOS (Fig. 7), indicated that differentiation of NB cells had no effect on the binding of HK-2 to VDAC. It is important to emphasize that differentiation of N2a cells has also no effect on the expression of βII-tubulin, a potential competitor for HK-2 for binding sites on the mitochondrial VDAC, in these NB cells (Fig. 3a).

**Rates of maximal respiration and the permeability of mitochondrial outer membrane for ADP in HL-1 and N2a cells**

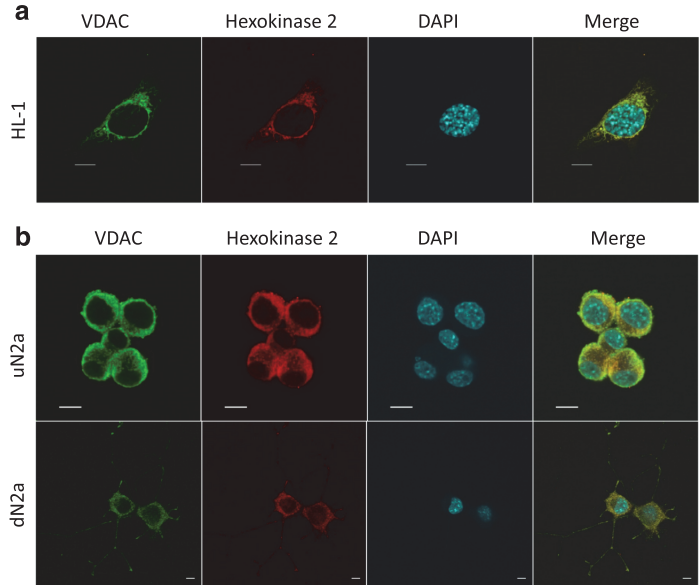
The current study showed the interaction of VDAC with HK-2 in both cardiac sarcoma and N2a cells (Fig. 6). Furthermore, we demonstrated that a big part of total β-tubulin and also βII-tubulin existed as non-polymerized forms (Fig. 1c). Study on N2a cells confirmed that during differentiation towards neuronal cells, the βII-tubulin expression remained at the same level (Fig. 3a). Several studies have indicated that β-tubulin (Maldonado et al. 2010) blocks and HK-2 (Majewski et al. 2004) oppositely keeps VDAC in its open state. Therefore, to clarify the possible role of βII-tubulin and HK-2 in the regulation of VDAC permeability for ADP, tumor cells were titrated with ADP (Fig. 8). Titration experiments showed that the rates of maximal ADP-activated respiration (V<sub>m</sub>) were lower in HL-1 cells compared to NB, as well as the V<sub>m</sub> did not change during N2a cell differentiation. The affinity of mitochondria for ADP was similarly high in all cells, which indicated that VDAC in tumor cells was in an open state. In addition, treatment of cells with the microtubule destabilizer colchicine, and stabilizer taxol, did not reveal any changes in VDAC permeability for ADP (Table 4).

**Discussion**

Recent discoveries in tumor biology propose that targeting of cancer cell energy metabolism can be a novel and effective strategy for suppression of tumor growth and metastasis (Amoedo et al. 2014; Lamb et al. 2014, 2015; Lu et al. 2015). For a long time aerobic glycolysis (Warburg effect) has been considered to be one of the characteristic features of most human cancers (Aminzadeh et al. 2015; Palorini et al. 2014; Pedersen 2007a, b). Several studies have shown that during cancer formation MOM permeability for ADP is altered (Eimre et al. 2008; Kaambre et al. 2012; Kaldma et al. 2014; Klepinin et al. 2014; Maldonado 2017; Maldonado et al. 2010). There are possibly two mechanisms how the MOM



**Fig. 6** Confocal microscopy imaging of VDAC1 and hexokinase-2 (HK-2) along with their colocalization in HL-1 cells (a); and colocalization of VDAC1 with HK-2 in undifferentiated N2a (uN2a) and RA-treated N2a cells (dN2a) (b) the cell nucleus (blue, DAPI), HK-2 (red), VDAC1 (green); bars are 10  $\mu$ M



permeability for nucleotides is regulated in cancer cells. According to the Warburg-Pedersen model, in cancer cells the HK-2 interacts with VDAC and this interaction results with opened mitochondrial porin channel (Pedersen 2007b). Another mechanism, proposed by Maldonado and co-workers, states that free tubulin and protein kinases dynamically regulate mitochondrial function in cancer cells, but not in untransformed primary cells (Maldonado et al. 2010). Therefore, in the current

study we hypothesized that HK-2 and  $\beta$ II-tubulin compete with each other for the VDAC binding site.

Previous studies have shown that the MOM permeability for adenine nucleotides in CM(s) can be regulated through a direct interaction of VDAC with cytoskeletal protein  $\beta$ II-tubulin (Guzun et al. 2012; Varikmaa et al. 2014). Cardiac muscle cells exhibit high apparent  $K_m$  values ( $360 \pm 51 \mu$ M) (Table 3) for exogenously added ADP and this apparent mitochondrial affinity for ADP is not induced by intrinsic  $Mg^{2+}$ -ATPase activity (Appaix et al. 2003), but controlled by cytoplasmic proteins (Kuznetsov et al. 1996). In the current study, we found that in HL-1 cardiac sarcoma cells most of the cytoskeletal protein tubulin  $\beta$ II was present in the non-polymerized form and some parts of this protein could be associated with MOM (Fig. 1c). Despite this, the permeability of VDAC for ADP in these cells was high and was close to values of those for isolated mitochondria, as well as rat fast-twitch *gastrocnemius* muscle cells, where free  $\beta$ II-tubulin was absent (Varikmaa et al. 2014).

Taxol give a long-term stability to assembled microtubules, and decrease the free tubulin content inversely to the colchicine, which inhibits microtubule polymerization and increases free tubulin content in cells (Maldonado et al. 2010). As mentioned above, in neuroblastoma cell culture colchicine and taxol had no effect on their bioenergetics parameters (Supplementary Fig. 4, Table 4). From this, it can be concluded that the role of  $\beta$ II tubulin in mitochondrial energy metabolism of N2a cell culture is small or absent at all. In HL-1 cells colchicine lowered and taxol oppositely raised mitochondrial respiration reserve capacity (Fig. 5b). Our results showed that the mitochondrial respiratory

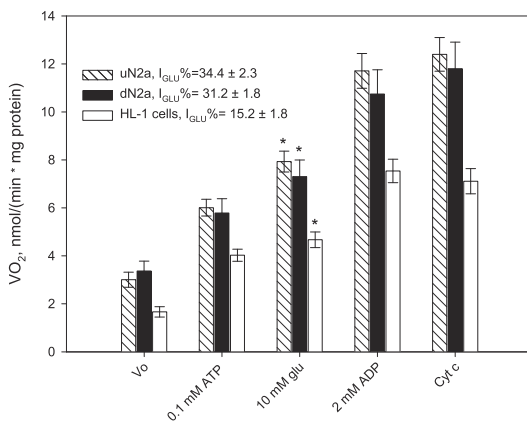


**Fig. 7** Analysis of the coupling of hexokinase (HK) catalyzed processes with OXPHOS in permeabilized HL-1 cells as well as in undifferentiated (uN2a) and RA-treated N2a cells (dN2a). The efficiency of the coupling between HK and OXPHOS was expressed by the glucose index ( $I_{GLU}$ ). Here: Vo – basal respiration; glu – glucose; and Cyt c – cytochrome c. All data points are the mean from 5 independent experiments; error bars are SEM. \* - significant difference,  $p < 0.05$

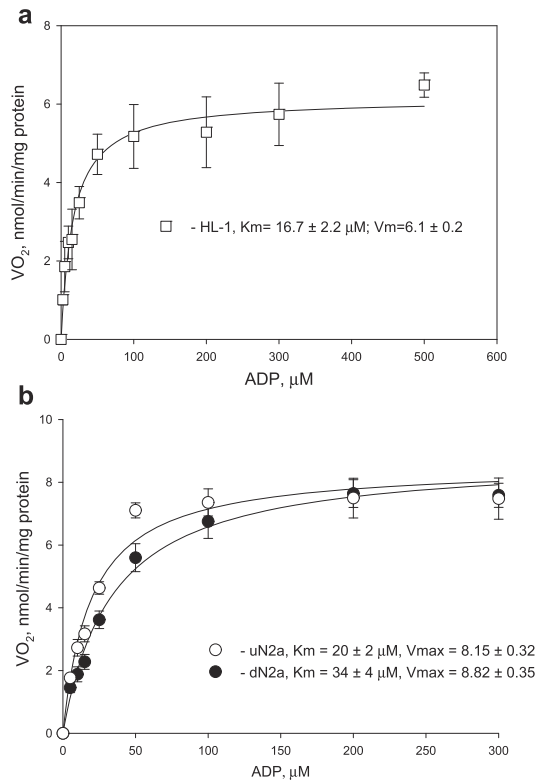


**Fig. 8** Apparent  $K_m$  values and rates of maximal ( $V_m$ ) ADP-activated respiration for HL-1 cells (a) as well as for undifferentiated (uN2a) and RA-treated N2a cells (dN2a) (b); bars are SEM,  $n = 7$

reserve capacity is dependent on the aggregation state of tubulin only in HL-1 cells. The stabilization of microtubules by taxol resulted in increased reserve capacity due to increased maximal respiration. Depolymerization of tubulin, on contrary, decreased respiratory reserve capacity by reducing maximal respiration. Recently, other groups have got similar results on a study on liver cancer cell line HepG2 (Maldonado et al. 2010). They demonstrated that taxol and colchicine not only influenced the cellular free/polymerized tubulin distribution, but also mitochondrial membrane potential. In addition, they found that the increase of free  $\beta$ -tubulin in cancer cells blocked VDAC permeability for nucleotides, and this was the reason why liver cancer tends to aerobic glycolysis. In addition, a study on HepG2 (Maldonado et al. 2010) cells demonstrated that in liver cancer cells the increase of free  $\beta$ -tubulin blocked VDAC permeability for ADP. Nonetheless, in the current study on NB cells and HL-1 cells, such a role of  $\beta$ -tubulin in the regulation of MOM permeability was not observed (Table 4).

A possible reason why in HL-1 cells VDACs still remains in an open state, is the interaction with HK-2. Indeed, previously Majewski and co-workers demonstrated that in cancer cells HK interaction with VDAC lead it open for adenine nucleotides (Majewski et al. 2004). Based on the Warburg-Pedersen model we have hereby shown, that in HL-1 cells there exists a tight coupling between HK-2 and OXPHOS (Fig. 6b).

Similar results have been published by another group, where they confirmed, that HK control energy metabolism in these cells (Eimre et al. 2008). The other consequence of the HK–VDAC interaction can result in the prevention of binding of the pro-apoptotic proteins to VDAC, mediating the increased resistance of malignant cells to apoptosis (Pastorino and Hoek 2008).

**Table 3** The rates of basal ( $V_o$ ), maximal ( $V_m$ ) ADP activated respiration, as well as apparent  $K_m$  values for ADP for permeabilized adult rat cardiomyocytes (CMs), N2a, and HL-1 tumor cells; these measurements were performed in medium-B with 2 mM malate, 5 mM glutamate and 10 mM succinate, as respiratory substrates

Cells and tissues	$V_o$	$V_m$ (ADP)	$K_m^{app}_{ADP}$ $\mu\text{M}$
Rat CM(s) <sup>(a)</sup>	$9.3 \pm 1$	$134 \pm 6$	$360 \pm 51$
Gastrocnemius white, no free $\beta$ II-tubulin <sup>(c)</sup>	–	–	$4.5 \pm 1.8$
Rat heart mitochondria <sup>(b)</sup>	–	–	$17.6 \pm 1$
HL-1	$1.91 \pm 0.84$	$6.1 \pm 0.2$	$16.7 \pm 2.2$
uN2a	$3.38 \pm 0.12$	$8.55 \pm 0.32$	$20 \pm 2$
dN2a	$4.07 \pm 0.46$	$8.82 \pm 0.35$	$34 \pm 4$
Rat brain synaptosomes <sup>(d)</sup>	–	$59 \pm 11$	$110 \pm 11$
Isolated rat brain mitochondria <sup>(d)</sup>	$14 \pm 4$	$36 \pm 7$	10–20
Brain mitochondria +1 $\mu\text{M}$ tubulin <sup>(d)</sup>	–	–	$169 \pm 52$

All rates of respiration were expressed as nmol O<sub>2</sub>/min/mg protein

<sup>a</sup> from (Anmann et al. 2006; Klepinin et al. 2014)

<sup>b</sup> from (Andrienko et al. 2003)

<sup>c</sup> from (Varikmaa et al. 2014)

<sup>d</sup> from (Monge et al. 2008) 2 mM malate and 5 mM glutamate served as respiratory substrates, and tubulin was in the form of  $\alpha/\beta$ -heterodimer

**Table 4** The influence of taxol and colchicine treatment on the affinity of mitochondria for exogenously-added ADP in undifferentiated (uN2a), retinoic acid differentiated (dN2a) and HL-1 tumor cells

Cells and their treatments	$K_m^{app}$ for ADP, $\mu\text{M} \pm \text{SEM}$ ; $n = 4^{(a)}$	$K_m^{app}$ for ADP, $\mu\text{M} \pm \text{SEM}$ ; $n = 4^{(b)}$
HL-1 cells, control	16.7 $\pm$ 2.2	–
HL-1, colchicine	16 $\pm$ 2	–
HL-1, taxol	25 $\pm$ 5*	–
uN2a cells, control	20 $\pm$ 2	31.7 $\pm$ 3.9
uN2a, colchicine	15 $\pm$ 2	24.6 $\pm$ 3.7
uN2a, taxol	37 $\pm$ 3*	30.4 $\pm$ 4.5
dN2a, control	–	11.0 $\pm$ 0.5
dN2a, colchicine	–	12.3 $\pm$ 1.7
dN2a, taxol	–	11.0 $\pm$ 1.1

Before respiratory studies these cells were treated for overnight<sup>(a)</sup> or for 20 min<sup>(b)</sup> with 10  $\mu\text{M}$  colchicine or 10  $\mu\text{M}$  taxol. Such prolonged (for overnight) treatment of these cells with colchicine and taxol had no effect on the number of viable cells (trypan blue exclusion assay), but was associated with a substantial (~50%) decrease in the rate of their proliferation that was estimated by MTT assay

\*- significant difference towards untreated cells;  $p < 0.05$

In the present study we noticed that the maximal rates of ADP-activated mitochondrial respiration did not change during the N2a cell differentiation (Fig. 8b), showing that RA does not influence the quantity of mitochondria; this finding is in good agreement with the recent study performed on human NB cells (Xun et al. 2012). We (see data in Table 2) as well as Xun and colleagues (2012), have demonstrated that RA-induced differentiation increases mitochondrial respiratory reserve capacity in NB cells, which is associated with their metabolism switching from aerobic glycolysis into OXPHOS. Recently Maldonado has hypothesized, that the regulation of MOM permeability for ADP, where free tubulin plays an important role, is the main switch between mitochondrial OXPHOS and glycolysis in malignant cells transformation (Maldonado 2017; Maldonado et al. 2016; Maldonado and Lemasters 2014; Maldonado et al. 2010). For both undifferentiated and differentiated N2a cell lines low apparent  $K_m$  values for ADP were registered.

The treatment of NB cells with RA also did not increase their mitochondrial respiration rate, the binding of HK-2 to VDAC and its functional coupling with OXPHOS (Figs. 7 and 8b). These results correlate with high affinity of mitochondria for ADP in uN2a and dN2a cells. Altogether, binding of HK-2 with VDAC in both N2a cell lines, as well as in HL-1 sarcoma cells, could mediate their glycolytic phenotype. It has been shown previously, that the total HK activity and the rate of glycolysis of differentiated N2a cells are substantially higher as compared with undifferentiated NB cells (Klepinin et al. 2014; Xun et al. 2012). The reason for this could be the elevated expression of HK-1, which is the predominant isoenzyme in mature neurons (Wilson 2003) and it can also bind to the mitochondrial VDAC (Pastorino and Hoek 2008). Therefore, further studies are needed to clarify the possible contribution of HK-1 to the total glycolytic capacity of NB cells.

The mitochondrial VDAC can be phosphorylated by different serine/threonine kinases in cancer cells, which can

regulate the level of the open or closed state of this channel. It has been shown that HK-2 phosphorylation by serine/threonine kinase Akt increases the HK binding to VDAC, which leads to the open state of the channel (Majewski et al. 2004).

It has been reported (Simamura et al. 2008), that cancer cells contain an increased number of VDACS per mitochondrion and, as a result, tumor mitochondria have an enhanced binding capacity for HK-2 compared to normal differentiated cells. In cancer and normal cells HK can only interact with VDAC1 isoform (Anflous-Pharayra et al. 2007; Shoshan-Barmatz et al. 2009). Maldonado and co-workers have reported that VDAC1 is also a binding partner for  $\beta$ -tubulin (Maldonado et al. 2013). Furthermore, they noticed that in HepG2 cells grown in normal conditions, another VDAC isoform VDAC2, was also occupied by  $\beta$ -tubulin and this may lead to the result by which most of VDAC channels stayed in a closed state. According to our previous work most of VDACS stay in CM in the closed state, due to their closure by  $\beta$ II tubulin (Guzun et al. 2011; Varikmaa et al. 2014).

Monge and co-workers have demonstrated that the main role of  $\beta$ II-tubulin is to regulate VDAC permeability for ADP in brain synaptosomes (Monge et al. 2008), but this is not the only function of  $\beta$ II-tubulin in neurons. A silencing study of  $\beta$ II-tubulin in NB cells revealed that  $\beta$ II-tubulin plays an important role in neurite outgrowth (Guo et al. 2010). In the current study, experiments with N2a cells revealed that although the levels of  $\beta$ II-tubulin expression in undifferentiated and RA-treated cells were almost the same, the intracellular localization was different. Olmsted et al. showed, that there are big differences between free and soluble tubulin amounts. Tubulin assembled in differentiated cells was four to five times greater than in nondifferentiated cells, constituting 48–63% and 11–16% of the total tubulin pool in the respective cell types (Olmsted 1981). In uN2a cells  $\beta$ II-tubulin is located

around the nucleus, but during differentiation with RA some part of  $\beta$ II-tubulin is incorporated in neurites in these cells (Fig. 4a). In addition, in this study, we established that both class I and III  $\beta$ -tubulin expression is significantly lower in differentiated N2a cells than in non-differentiated cells (Fig. 3). Tubulin  $\beta$ III (TUBB3) has been reported to be expressed in the mitochondrial membranes (Cicchillitti et al. 2008). It has also been found, that  $\beta$ III-tubulin is prominently expressed during the fetal and postnatal development of brain (Katsetos et al. 2003). Higher expression levels of  $\beta$ III-tubulin have been observed in malignancies like gliomas, ovarian and lung cancer cells, in those tumors increased level of  $\beta$ III-tubulin has been associated with their aggressive behavior and high proliferative rates (Kanojia et al. 2015; Kavallaris 2010; Mariani et al. 2015; McCarroll et al. 2015a; McCarroll et al. 2015b; Parker et al. 2016; Quaas et al. 2015). This isotype also regulates cellular metabolism and glucose stress response signaling to promote cell survival, proliferation in glucose starvation and decreases the reliance of cells on glycolytic metabolism (Parker et al. 2016). This tubulin isoform can be one of the candidates involved in the tubulin dimers, which regulate the mitochondrial outer membrane permeability.

The alteration of MOM permeability for ADP in cancer cells is related to the reorganization of protein supercomplex MI during carcinogens due to the changes in expression of its components (Chekulayev et al. 2015; Chevrollier et al. 2005, 2010; Kaambre et al. 2012; Willers and Cuezva 2011). The regulation of the mitochondrial outer membrane permeability may be related to the presence of post-translational modifications in  $\beta$ -tubulin, participation of other tubulin isoforms, interplay between energy transfer pathways or changes in the phosphorylation state of VDAC channels (Anmann et al. 2014; Rostovtseva and Bezrukov 2012; Sheldon et al. 2011; Tepp et al. 2014; Varikmaa et al. 2014). It has been reported that in adult rat CM(s), which have high  $K_m$  value for ADP, the spectrum of post-translational modifications of  $\beta$ -tubulin differs substantially from that in HL-1 cardiac sarcoma cells, in which mitochondria have an increased affinity for ADP (Belmadani et al. 2004). Significant differences in the profile of  $\beta$ -tubulin post-translational alterations between mature neurons and NB cells have also been observed (Song and Brady 2015). These alterations could induce a decrease in the capacity of binding of some  $\beta$ -tubulin isotypes to VDAC, and thereby loss of the cytoskeletal protein(s) role in the regulation of the mitochondrial VDAC channel permeability, which is characteristic for some oxidative muscle cells like CMs, m. soleus, and gastrocnemius red (Guzun et al. 2015; Varikmaa et al. 2014) and for mature neural cells (Monge et al. 2008). Moreover, it could be assumed that other  $\beta$ -tubulin or  $\alpha$ -tubulin isoforms could also bind to VDAC and influence its conductance (Anmann et al. 2014). At present, the levels and profiles of expression of  $\alpha$ -tubulins in malignant cells are totally uncovered and it is also unclear whether tubulin post-

translational modifications could influence the interaction of tubulin with VDAC. The permeability of VDAC may be involved in the prevalence of the energy transfer pathway(s). Differences in regulation of VDAC gating between HepG2 and N2a as well as HL-1 cells may be related to the presence of MI key enzyme mitochondrial creatine kinase (MtCK) in HepG2 cells (Uranbileg et al. 2014) and the absence of this enzyme in HL-1 cell culture (Eimre et al. 2008) and N2a cells (Klepinin et al. 2014). Thus, our results show that the regulation of the MOM permeability is more complicated than previously proposed. It has been shown that in some cancers like cardiac (Eimre et al. 2008) and skeletal muscle sarcoma (Patra et al. 2008), neuroblastoma (Klepinin et al. 2014), colorectal cancer (Kaldma et al. 2014) and prostate cancer (Amamoto et al. 2016) MtCK is downregulated. In CM with low permeability of MOM for ADP, was found, that MtCK is tightly coupled with OXPHOS due to the interaction with ANT (Timohhina et al. 2009). In CM and skeletal muscles it has been demonstrated that addition of Cr increases MOM affinity for ADP, but such an effect of Cr on MOM permeability was not observed in glycolytic muscles. This phenomenon may take place due to low expression of MtCK on fast twitching muscles (Varikmaa et al. 2014). Our current and previous studies have shown that in colorectal cancer and cardiac sarcoma cells the apparent  $K_m$  of ADP is lower as compared to their normal tissues (Eimre et al. 2008; Kaambre et al. 2012; Kaldma et al. 2014). These results correlate with the downregulation of MtCK in those cells (Eimre et al. 2008; Kaldma et al. 2014; Klepinin et al. 2014). A study on MtCK knockout mice confirms this assumption (Kaasik et al. 2001). It has been found that in the MtCK knockout heart muscle the increased permeability of MOM for ADP is 2.5 times. In previous studies on breast cancer and gastric cancer it has been shown that in those cancers MtCK coupled with OXPHOS, and in gastric cancer addition of Cr increased MOM permeability for ADP (Gruno et al. 2006; Kaambre et al. 2012). The interplay between energy transfer pathways, and different binding sites for tubulin and hexokinase to VDAC may be one of the reasons of the high metabolic plasticity of cancer cells, where the selection of metabolic phenotypes leads to growth and invasive advantages.

## Conclusion

The process of the regulation of mitochondrial outer membrane permeability is more complicated and not only based on binding between the VDAC channel and one type of a protein molecule. The current study demonstrates that the presence of mitochondrially bound HK-2 can mediate the “Warburg” behavior of murine NB(s) and cardiac sarcoma cells. Our experiments demonstrated that  $\beta$ II-tubulin plays a minor role in the regulation of energy metabolism in sarcoma cells, in contrast to cardiac and slow-twitch skeletal muscle

cells. Based on our results it can also be concluded, that the binding sites in the composition of MI for tubulin and hexokinase must be different in cancer cells. The alternations in MOM permeability for adenine nucleotides seem to be a characteristic feature of malignant tumors and understanding of this regulation still requires further work.

**Acknowledgements** This work was supported by the Estonian Ministry of Education and Research through the institutional research funding IUT23-1.

### Compliance with ethical standards

This paper does not contain any studies with animals or human participants performed by any of the authors.

**Conflict of interest** The authors declare no conflict of interest.

**Open Access** This article is distributed under the terms of the Creative Commons Attribution 4.0 International License (<http://creativecommons.org/licenses/by/4.0/>), which permits unrestricted use, distribution, and reproduction in any medium, provided you give appropriate credit to the original author(s) and the source, provide a link to the Creative Commons license, and indicate if changes were made.

### References

- Amamoto R et al (2016) The expression of ubiquitous mitochondrial Creatine kinase is downregulated as prostate Cancer progression. *J Cancer* 7:50–59. <https://doi.org/10.7150/jca.13207>
- Aminzadeh S, Vidali S, Sperl W, Kofler B, Feichtinger RG (2015) Energy metabolism in neuroblastoma and Wilms tumor. *Transl Pediatr* 4: 20–32. <https://doi.org/10.3978/j.issn.2224-4336.2015.01.04>
- Amoedo ND, Rodrigues MF, Rumjanek FD (2014) Mitochondria: are mitochondria accessory to metastasis? *Int J Biochem Cell Biol* 51: 53–57. <https://doi.org/10.1016/j.biocel.2014.03.009>
- Andrienko T et al (2003) Metabolic consequences of functional complexes of mitochondria, myofibrils and sarcoplasmic reticulum in muscle cells. *J Exp Biol* 206:2059–2072
- Anflous-Pharayra K, Cai ZJ, Craigen WJ (2007) VDAC1 serves as a mitochondrial binding site for hexokinase in oxidative muscles. *Biochim Biophys Acta* 1767:136–142. <https://doi.org/10.1016/j.bbabi.2006.11.013>
- Anmann T et al (2006) Different kinetics of the regulation of respiration in permeabilized cardiomyocytes and in HL-1 cardiac cells: Importance of cell structure/organization for respiration regulation. *Biochim Biophys Acta* 1757:1597–1606. <https://doi.org/10.1016/j.bbabi.2006.09.008>
- Anmann T et al (2014) Formation of highly organized intracellular structure and energy metabolism in cardiac muscle cells during postnatal development of rat heart. *Biochim Biophys Acta* 1837:1350–1361. <https://doi.org/10.1016/j.bbabi.2014.03.015>
- Appaix F et al (2003) Possible role of cytoskeleton in intracellular arrangement and regulation of mitochondria. *Exp Physiol* 88:175–190
- Arzoine L, Zilberberg N, Ben-Romano R, Shoshan-Barmatz V (2009) Voltage-dependent anion channel 1-based peptides interact with hexokinase to prevent its anti-apoptotic activity. *J Biol Chem* 284: 3946–3955. <https://doi.org/10.1074/jbc.M803614200>
- Belmadani S, Pous C, Fischmeister R, Mery PF (2004) Post-translational modifications of tubulin and microtubule stability in adult rat ventricular myocytes and immortalized HL-1 cardiomyocytes. *Mol Cell Biochem* 258:35–48
- Beutner G, Ruck A, Riede B, Welte W, Brdiczka D (1996) Complexes between kinases, mitochondrial porin and adenylate translocator in rat brain resemble the permeability transition pore. *FEBS Lett* 396:189–195
- Blanco V, Lopez Camelo J, Carri NG (2001) Growth inhibition, morphological differentiation and stimulation of survival in neuronal cell type (Neuro-2a) treated with trophic molecules. *Cell Biol Int* 25: 909–917. <https://doi.org/10.1006/cbir.2001.0775>
- Bryan N, Raisch KP (2015) Identification of a mitochondrial-binding site on the amino-terminal end of hexokinase II. *Biosci Rep*. <https://doi.org/10.1042/BSR20150047>
- Capetanaki Y, Bloch RJ, Kouloumenta A, Mavroidis M, Psarras S (2007) Muscle intermediate filaments and their links to membranes and membranous organelles. *Exp Cell Res* 313:2063–2076. <https://doi.org/10.1016/j.yexcr.2007.03.033>
- Carre M, Andre N, Carles G, Borghi H, Brichese L, Briand C, Braguer D (2002) Tubulin is an inherent component of mitochondrial membranes that interacts with the voltage-dependent anion channel. *J Biol Chem* 277:33664–33669. <https://doi.org/10.1074/jbc.M203834200>
- Cesar Mde C, Wilson JE (1998) Further studies on the coupling of mitochondrially bound hexokinase to intramitochondrially compartmented ATP, generated by oxidative phosphorylation. *Arch Biochem Biophys* 350:109–117
- Chekulayev V et al (2015) Metabolic remodeling in human colorectal cancer and surrounding tissues: alterations in regulation of mitochondrial respiration and metabolic fluxes. *Biochem Biophys Res* 4:111–125. <https://doi.org/10.1016/j.bbrep.2015.08.020>
- Chevrollier A, Loiseau D, Stepien G (2005) What is the specific role of ANT2 in cancer cells? *Med Sci (Paris)* 21:156–161
- Chevrollier A, Loiseau D, Stepien G, Reynier P (2010) Adenine nucleotide translocase 2 is a key. *Biochim Biophys Acta*. <https://doi.org/10.1016/j.bbabi.2010.10.008>
- Chevrollier A, Loiseau D, Reynier P, Stepien G (2011) Adenine nucleotide translocase 2 is a key mitochondrial protein in cancer metabolism. *Biochim Biophys Acta* 1807:562–567. <https://doi.org/10.1016/j.bbabi.2010.10.008>
- Cicchillitti L et al (2008) Proteomic characterization of cytoskeletal and mitochondrial class III beta-tubulin. *Mol Cancer Ther* 7:2070–2079. <https://doi.org/10.1158/1535-7163.MCT-07-2370>
- Claycomb WC, Lanson NA Jr, Stallworth BS, Egeland DB, Delcarpio JB, Bahinski A, Izzo NJ Jr (1998) HL-1 cells: a cardiac muscle cell line that contracts and retains phenotypic characteristics of the adult cardiomyocyte. *Proc Natl Acad Sci U S A* 95:2979–2984
- Diokmetzidou A et al (2016) Desmin and alphaB-crystallin interplay in the maintenance of mitochondrial homeostasis and cardiomyocyte survival. *J Cell Sci* 129:3705–3720. <https://doi.org/10.1242/jcs.192203>
- Eimre M et al (2008) Distinct organization of energy metabolism in HL-1 cardiac cell line and cardiomyocytes. *Biochim Biophys Acta* 1777: 514–524. <https://doi.org/10.1016/j.bbabi.2008.03.019>
- Gincel D, Silberberg SD, Shoshan-Barmatz V (2000) Modulation of the voltage-dependent anion channel (VDAC) by glutamate. *J Bioenerg Biomembr* 32:571–583
- Gnaiger E (2001) Oxygen solubility in experimental media OROBOROS. *Bioenerg News* 6:1–6
- Gogvadze V, Orrenius S, Zhivotovskiy B (2009) Mitochondria as targets for cancer chemotherapy. *Semin Cancer Biol* 19:57–66. <https://doi.org/10.1016/j.semcancer.2008.11.007>
- Gruno M et al (2006) Oxidative phosphorylation and its coupling to mitochondrial creatine and adenylate kinases in human gastric mucosa. *Am J Physiol Regul Integr Comp Phys* 291:R936–R946. <https://doi.org/10.1152/ajpregu.00162.2006>
- Guo J, Walss-Bass C, Luduena RF (2010) The beta isoforms of tubulin in neuronal differentiation. *Cytoskeleton (Hoboken)* 67:431–441. <https://doi.org/10.1002/cm.20455>

- Guzun R et al (2011) Mitochondria-cytoskeleton interaction: distribution of beta-tubulins in cardiomyocytes and HL-1 cells. *Biochim Biophys Acta* 1807:458–469. <https://doi.org/10.1016/j.bbabi.2011.01.010>
- Guzun R et al (2012) Regulation of respiration in muscle cells in vivo by VDAC through interaction with the cytoskeleton and MtCK within mitochondrial Interactosome. *Biochim Biophys Acta* 1818:1545–1554. <https://doi.org/10.1016/j.bbamem.2011.12.034>
- Guzun R et al (2015) Modular organization of cardiac energy metabolism: energy conversion, transfer and feedback regulation. *Acta Physiol* 213:84–106. <https://doi.org/10.1111/apha.12287>
- Hoogerheide DP, Gurnev PA, Rostovtseva TK, Bezrukov SM (2017) Mechanism of alpha-synuclein translocation through a VDAC nanopore revealed by energy landscape modeling of escape time distributions. *Nanoscale* 9:183–192. <https://doi.org/10.1039/c6nr08145b>
- Kaambre T et al (2012) Metabolic control analysis of cellular respiration in situ in intraoperative samples of human breast cancer. *J Bioenerg Biomembr* 44:539–558. <https://doi.org/10.1007/s10863-012-9457-9>
- Kaasik A, Veksler V, Boehm E, Novotova M, Minajeva A, Ventura-Clapier R (2001) Energetic crosstalk between organelles: architectural integration of energy production and utilization. *Circ Res* 89:153–159
- Kaldma A et al (2014) An in situ study of bioenergetic properties of human colorectal cancer: the regulation of mitochondrial respiration and distribution of flux control among the components of ATP synthasome. *Int J Biochem Cell Biol* 55:171–186. <https://doi.org/10.1016/j.biocel.2014.09.004>
- Kanojia D et al (2015) betaIII-tubulin regulates breast Cancer metastases to the brain. *Mol Cancer Ther* 14:1152–1161. <https://doi.org/10.1158/1535-7163.MCT-14-0950>
- Katsetos CD, Legido A, Perentes E, Mork SJ (2003) Class III beta-tubulin isotype: a key cytoskeletal protein at the crossroads of developmental neurobiology and tumor neuropathology. *J Child Neurol* 18:851–866 discussion 867
- Kavallaris M (2010) Microtubules and resistance to tubulin-binding agents. *Nat Rev Cancer* 10:194–204. <https://doi.org/10.1038/nrc2803>
- Klepinin A et al (2014) Comparative analysis of some aspects of mitochondrial metabolism in differentiated and undifferentiated neuroblastoma cells. *J Bioenerg Biomembr* 46:17–31. <https://doi.org/10.1007/s10863-013-9529-5>
- Koita A et al (2017) Mitochondrial respiration in human colorectal and breast cancer clinical material is regulated differently. *Oxid Med Cell Longev* 2017:1372640. <https://doi.org/10.1155/2017/1372640>
- Kuznetsov AV et al (1996) Striking differences between the kinetics of regulation of respiration by ADP in slow-twitch and fast-twitch muscles in vivo. *Eur J Biochem* 241:909–915
- Kuznetsov AV, Veksler V, Gellerich FN, Saks V, Margreiter R, Kunz WS (2008) Analysis of mitochondrial function in situ in permeabilized muscle fibers, tissues and cells. *Nat Protoc* 3:965–976. <https://doi.org/10.1038/nprot.2008.61>
- Lamb R, Harrison H, Hulit J, Smith DL, Lisanti MP, Sotgia F (2014) Mitochondria as new therapeutic targets for eradicating cancer stem cells: quantitative proteomics and functional validation via MCT1/2 inhibition. *Oncotarget* 5:11029–11037
- Lamb R et al (2015) Mitochondrial mass, a new metabolic biomarker for stem-like cancer cells: understanding WNT/FGF-driven anabolic signaling. *Oncotarget* 6:30453–30471. <https://doi.org/10.18632/oncotarget.5852>
- Lemeshko VV (2014) VDAC electronics: 2. A new, anaerobic mechanism of generation of the membrane potentials in mitochondria. *Biochim Biophys Acta* 1838:1801–1808. <https://doi.org/10.1016/j.bbamem.2014.02.007>
- Lu CL, Qin L, Liu HC, Candas D, Fan M, Li JJ (2015) Tumor cells switch to mitochondrial oxidative phosphorylation under radiation via mTOR-mediated hexokinase II inhibition—a Warburg-reversing effect. *PLoS One* 10:e0121046. <https://doi.org/10.1371/journal.pone.0121046>
- Majewski N et al (2004) Hexokinase-mitochondria interaction mediated by Akt is required to inhibit apoptosis in the presence or absence of Bax and Bak. *Mol Cell* 16:819–830. <https://doi.org/10.1016/j.molcel.2004.11.014>
- Maldonado EN (2017) VDAC-tubulin, an anti-Warburg pro-oxidant switch. *Front Oncol* 7:4. <https://doi.org/10.3389/fonc.2017.00004>
- Maldonado EN, Lemasters JJ (2014) ATP/ADP ratio, the missed connection between mitochondria and the Warburg effect. *Mitochondrion* 19 Pt A:78–84. <https://doi.org/10.1016/j.mito.2014.09.002>
- Maldonado EN, Patnaik J, Mullins MR, Lemasters JJ (2010) Free tubulin modulates mitochondrial membrane potential in cancer cells. *Cancer Res* 70:10192–10201. <https://doi.org/10.1158/0008-5472.CAN-10-2429>
- Maldonado EN et al (2013) Voltage-dependent anion channels modulate mitochondrial metabolism in cancer cells: regulation by free tubulin and erastin. *J Biol Chem* 288:11920–11929. <https://doi.org/10.1074/jbc.M112.433847>
- Maldonado EN, DeHart DN, Patnaik J, Klatt SC, Gooz MB, Lemasters JJ (2016) ATP/ADP turnover and import of glycolytic ATP into mitochondria in Cancer cells is independent of the adenine nucleotide translocator. *J Biol Chem* 291:19642–19650. <https://doi.org/10.1074/jbc.M116.734814>
- Mariani M et al (2015) Class III beta-tubulin in normal and cancer tissues. *Gene* 563:109–114. <https://doi.org/10.1016/j.gene.2015.03.061>
- Mathupala SP, Ko YH, Pedersen PL (2009) Hexokinase-2 bound to mitochondria: cancer's stygian link to the "Warburg effect" and a pivotal target for effective therapy. *Semin Cancer Biol* 19:17–24. <https://doi.org/10.1016/j.semcancer.2008.11.006>
- McCarroll JA et al (2015a) TUBB3/betaIII-tubulin acts through the PTEN/AKT signaling axis to promote tumorigenesis and anoikis resistance in non-small cell lung cancer. *Cancer Res* 75:415–425. <https://doi.org/10.1158/0008-5472.CAN-14-2740>
- McCarroll JA et al (2015b) betaIII-tubulin: a novel mediator of chemoresistance and metastases in pancreatic cancer. *Oncotarget* 6:2235–2249. <https://doi.org/10.18632/oncotarget.2946>
- Monge C et al (2008) Regulation of respiration in brain mitochondria and synaptosomes: restrictions of ADP diffusion in situ, roles of tubulin, and mitochondrial creatine kinase. *Mol Cell Biochem* 318:147–165. <https://doi.org/10.1007/s11010-008-9865-7>
- Moreno-Sanchez R, Rodriguez-Enriquez S, Marin-Hernandez A, Saavedra E (2007) Energy metabolism in tumor cells. *FEBS J* 274:1393–1418. <https://doi.org/10.1111/j.1742-4658.2007.05686.x>
- Nederlof R, Eerbeek O, Hollmann MW, Southworth R, Zuurbeek CJ (2014) Targeting hexokinase II to mitochondria to modulate energy metabolism and reduce ischaemia-reperfusion injury in heart. *Br J Pharmacol* 171:2067–2079. <https://doi.org/10.1111/bph.12363>
- Noskov SY, Rostovtseva TK, Bezrukov SM (2013) ATP transport through VDAC and the VDAC-tubulin complex probed by equilibrium and nonequilibrium MD simulations. *Biochemistry* 52:9246–9256. <https://doi.org/10.1021/bi4011495>
- Olmsted JB (1981) Tubulin pools in differentiating neuroblastoma cells. *J Cell Biol* 89:418–423
- Palorini R, Votta G, Balestrieri C, Monestiroli A, Olivieri S, Vento R, Chiaradonna F (2014) Energy metabolism characterization of a novel cancer stem cell-like line 3AB-OS. *J Cell Biochem* 115:368–379. <https://doi.org/10.1002/jcb.24671>
- Parker AL, Turner N, McCarroll JA, Kavallaris M (2016) betaIII-tubulin alters glucose metabolism and stress response signaling to promote cell survival and proliferation in glucose-starved non-small cell lung cancer cells. *Carcinogenesis* 37:787–798. <https://doi.org/10.1093/carcin/bgw058>
- Pastorino JG, Hoek JB (2008) Regulation of hexokinase binding to VDAC. *J Bioenerg Biomembr* 40:171–182. <https://doi.org/10.1007/s10863-008-9148-8>
- Patra S et al (2008) Progressive decrease of phosphocreatine, creatine and creatine kinase in skeletal muscle upon transformation

- to sarcoma. *FEBS J* 275:3236–3247. <https://doi.org/10.1111/j.1742-4658.2008.06475.x>
- Pedersen PL (2007a) The cancer cell's "power plants" as promising therapeutic targets: an overview. *J Bioenerg Biomembr* 39:1–12. <https://doi.org/10.1007/s10863-007-9070-5>
- Pedersen PL (2007b) Warburg, me and hexokinase 2: multiple discoveries of key molecular events underlying one of cancers' most common phenotypes, the "Warburg effect", i.E., elevated glycolysis in the presence of oxygen. *J Bioenerg Biomembr* 39:211–222. <https://doi.org/10.1007/s10863-007-9094-x>
- Pelloux S et al (2006) Non-beating HL-1 cells for confocal microscopy: application to mitochondrial functions during cardiac preconditioning. *Prog Biophys Mol Biol* 90:270–298. <https://doi.org/10.1016/j.pbiomolbio.2005.06.009>
- Quaas A et al (2015) betaIII-tubulin overexpression is linked to aggressive tumor features and shortened survival in clear cell renal cell carcinoma. *World J Urol* 33:1561–1569. <https://doi.org/10.1007/s00345-014-1463-6>
- Reipert S, Steinbock F, Fischer I, Bittner RE, Zeold A, Wiche G (1999) Association of mitochondria with plectin and desmin intermediate filaments in striated muscle. *Exp Cell Res* 252:479–491. <https://doi.org/10.1006/excr.1999.4626>. S0014-4827(99)94626-8 [pii]
- Rostovtseva TK, Bezrukov SM (2012) VDAC inhibition by tubulin and its physiological implications. *Biochim Biophys Acta* 1818:1526–1535. <https://doi.org/10.1016/j.bbame.2011.11.004>
- Rostovtseva T, Colombini M (1997) VDAC channels mediate and gate the flow of ATP: implications for the regulation of mitochondrial function. *Biophys J* 72:1954–1962. [https://doi.org/10.1016/S0006-3495\(97\)78841-6](https://doi.org/10.1016/S0006-3495(97)78841-6)
- Rostovtseva TK et al (2015) Alpha-Synuclein shows high affinity interaction with voltage-dependent Anion Channel, suggesting mechanisms of mitochondrial regulation and toxicity in Parkinson disease. *J Biol Chem* 290:18467–18477. <https://doi.org/10.1074/jbc.M115.641746>
- Saetersdal T, Greve G, Dalen H (1990) Associations between beta-tubulin and mitochondria in adult isolated heart myocytes as shown by immunofluorescence and immunoelectron microscopy. *Histochemistry* 95:1–10
- Saks VA, Aliev MK (1996) Is there the creatine kinase equilibrium in working heart cells? *Biochim Biophys Res Commun* 227:360–367. <https://doi.org/10.1006/bbrc.1996.1513>
- Saks VA, Khuchua ZA, Vasilyeva EV, Belikova O, Kuznetsov AV (1994) Metabolic compartmentation and substrate channelling in muscle cells. Role of coupled creatine kinases in *in vivo* regulation of cellular respiration—a synthesis. *Mol Cell Biochem* 133-134:155–192
- Saks V, Belikova Y, Vasilyeva E, Kuznetsov A, Fontaine E, Keriell C, Leverage X (1995) Correlation between degree of rupture of outer mitochondrial membrane and changes of kinetics of regulation of respiration by ADP in permeabilized heart and liver cells. *Biochim Biophys Res Commun* 208:919–926. <https://doi.org/10.1006/bbrc.1995.1422>
- Saks VA et al (1998) Permeabilized cell and skinned fiber techniques in studies of mitochondrial function *in vivo*. *Mol Cell Biochem* 184:81–100
- Saks V et al (2010) Structure-function relationships in feedback regulation of energy fluxes *in vivo* in health and disease: mitochondrial interactosome. *Biochim Biophys Acta* 1797:678–697. <https://doi.org/10.1016/j.bbabi.2010.01.011>
- Sheldon KL, Maldonado EN, Lemasters JJ, Rostovtseva TK, Bezrukov SM (2011) Phosphorylation of voltage-dependent anion channel by serine/threonine kinases governs its interaction with tubulin. *PLoS One* 6:e25539. <https://doi.org/10.1371/journal.pone.0025539>
- Shen J et al (2014) Alpha-Synuclein amino terminus regulates mitochondrial membrane permeability. *Brain Res* 1591:14–26. <https://doi.org/10.1016/j.brainres.2014.09.046>
- Shoshan-Barmatz V, Israelson V, Brdiczka D, Sheu SS (2006) The voltage-dependent anion channel (VDAC): function in intracellular signalling, cell life and cell death. *Curr Pharm Des* 12:2249–2270
- Shoshan-Barmatz V, Zakar M, Rosenthal K, Abu-Hamad S (2009) Key regions of VDAC1 functioning in apoptosis induction and regulation by hexokinase. *Biochim Biophys Acta* 1787:421–430. doi: S0005-2728(08)00726-3 [pii]. <https://doi.org/10.1016/j.bbabi.2008.11.009>
- Shoshan-Barmatz V, Maldonado Eduardo N, Krelin Y (2017) VDAC1 at the crossroads of cell metabolism, apoptosis and cell stress. *Cell Stress* 1:11–38. <https://doi.org/10.15698/cst2017.10.104>
- Shoshan-Barmatz V, Krelin Y, Shteinfein-Kuzmine A (2018) VDAC1 functions in ca(2+) homeostasis and cell life and death in health and disease. *Cell Calcium* 69:81–100. <https://doi.org/10.1016/j.ceca.2017.06.007>
- Simamura E, Shimada H, Hatta T, Hirai KI (2008) Mitochondrial voltage-dependent anion channels (VDACs) as novel pharmacological targets for anti-cancer agents. *J Bioenerg Biomembr* 40:213–217. <https://doi.org/10.1007/s10863-008-9158-6>
- Song Y, Brady ST (2015) Post-translational modifications of tubulin: pathways to functional diversity of microtubules. *Trends Cell Biol* 25:125–136. <https://doi.org/10.1016/j.tcb.2014.10.004>
- Tepp K et al (2011) High efficiency of energy flux controls within mitochondrial interactosome in cardiac intracellular energetic units. *BBA-Bioenergetics* 1807:1549–1561. <https://doi.org/10.1016/j.bbabi.2011.08.005>
- Tepp K et al (2014) The role of tubulin in the mitochondrial metabolism and arrangement in muscle cells. *J Bioenerg Biomembr* 46:421–434. <https://doi.org/10.1007/s10863-014-9579-3>
- Timohhina N et al (2009) Direct measurement of energy fluxes from mitochondria into cytoplasm in permeabilized cardiac cells *in situ*: some evidence for mitochondrial Interactosome. *J Bioenerg Biomembr* 41: 259–275. <https://doi.org/10.1007/s10863-009-9224-8>
- Uranbileg B et al (2014) High ubiquitous mitochondrial creatine kinase expression in hepatocellular carcinoma denotes a poor prognosis with highly malignant potential. *Int J Cancer* 134:2189–2198. <https://doi.org/10.1002/ijc.28547>
- Varikmaa M et al (2014) Role of mitochondria-cytoskeleton interactions in respiration regulation and mitochondrial organization in striated muscles. *Biochim Biophys Acta* 1837:232–245. <https://doi.org/10.1016/j.bbabi.2013.10.011>
- Willers IM, Cuezva JM (2011) Post-transcriptional regulation of the mitochondrial H(+)-ATP synthase: a key regulator of the metabolic phenotype in cancer. *Biochim Biophys Acta* 1807:543–551. <https://doi.org/10.1016/j.bbabi.2010.10.016>
- Wilson JE (2003) Isozymes of mammalian hexokinase: structure, subcellular localization and metabolic function. *J Exp Biol* 206:2049–2057. <https://doi.org/10.1242/jeb.00241>
- Winter L, Abrahamsberg C, Wiche G (2008) Plectin isoform 1b mediates mitochondrion-intermediate filament network linkage and controls organelle shape. *J Cell Biol* 181:903–911. <https://doi.org/10.1083/jcb.200710151>
- Winter L, Kuznetsov AV, Grimm M, Zeold A, Fischer I, Wiche G (2015) Plectin isoform P1b and P1d deficiencies differentially affect mitochondrial morphology and function in skeletal muscle. *Hum Mol Genet* 24:4530–4544. <https://doi.org/10.1093/hmg/ddv184>
- Xun Z, Lee DY, Lim J, Canaria CA, Barnebey A, Yanonne SM, McMurray CT (2012) Retinoic acid-induced differentiation increases the rate of oxygen consumption and enhances the spare respiratory capacity of mitochondria in SH-SY5Y cells. *Mech Ageing Dev* 133:176–185. <https://doi.org/10.1016/j.mad.2012.01.008>
- Zhang H, Liu J, Wang X, Duan C, Wang X, Yang H (2016) V63 and N65 of overexpressed alpha-synuclein are involved in mitochondrial dysfunction. *Brain Res* 1642:308–318. <https://doi.org/10.1016/j.brainres.2016.04.002>
- Zizi M, Forte M, Blachly-Dyson E, Colombini M (1994) NADH regulates the gating of VDAC, the mitochondrial outer membrane channel. *J Biol Chem* 269:1614–1616

## Appendix 3

### Publication III




E. Rebane-Klemm, L. Truu, L. Reinsalu, M. Puurand, I. Shevchuk, V. Chekulayev, N. Timohhina, K. Tepp, J. Bogovskaja, V. Afanasjev, K. Suurmaa, V. Valvere and T. Kaambre (2020). "Mitochondrial Respiration in KRAS and BRAF Mutated Colorectal Tumors and Polyps." *Cancers (Basel)* 12(4).





Article

# Mitochondrial Respiration in *KRAS* and *BRAF* Mutated Colorectal Tumors and Polyps

Egle Rebane-Klemm <sup>1,2,†,\*</sup>, Laura Truu <sup>1,2,†</sup>, Leenu Reinsalu <sup>1,2</sup>, Marju Puurand <sup>1</sup>, Igor Shevchuk <sup>1</sup>, Vladimir Chekulayev <sup>1</sup>, Natalja Timohhina <sup>1</sup>, Kersti Tepp <sup>1</sup>, Jelena Bogovskaja <sup>3</sup>, Vladimir Afanasjev <sup>4</sup>, Külliki Suurmaa <sup>5</sup>, Vahur Valvere <sup>6</sup> and Tuuli Kaambre <sup>1</sup>

<sup>1</sup> Laboratory of Chemical Biology, National Institute of Chemical Physics and Biophysics, Akadeemia tee 23, 12618 Tallinn, Estonia; laura.truu@gmail.com (L.T.); leenu.reinsalu@gmail.com (L.R.); marju.puurand@kbfi.ee (M.P.); igor@chemnet.ee (I.S.); vladimir@chemnet.ee (V.C.); natalja.timohhina@kbfi.ee (N.T.); kersti.tepp@kbfi.ee (K.T.); tuuli.kaambre@kbfi.ee (T.K.)

<sup>2</sup> Department of Chemistry and Biotechnology, School of Science, Tallinn University of Technology, Ehitajate tee 5, 12618 Tallinn, Estonia

<sup>3</sup> Clinic of Diagnostics at the North Estonia Medical Centre, J. Sütiste tee 19, 13419 Tallinn, Estonia; jelena.bogovskaja@regionaalhaigla.ee

<sup>4</sup> Clinic of Surgery at the North Estonia Medical Centre, J. Sütiste tee 19, 13419 Tallinn, Estonia; Vladimir.Afanasjev2@regionaalhaigla.ee

<sup>5</sup> Department of Gastroenterology, the West Tallinn Central Hospital, Paldiski mnt 68, 10617 Tallinn, Estonia; kulliki.suurmaa@keskhaigla.ee

<sup>6</sup> Oncology and Haematology Clinic at the North Estonia Medical Centre, J. Sütiste tee 19, 13419 Tallinn, Estonia; vahur.valvere@regionaalhaigla.ee

\* Correspondence: egle.rebane@gmail.com

† These authors contributed equally to this work.

Received: 14 February 2020; Accepted: 27 March 2020; Published: 28 March 2020



**Abstract:** This study aimed to characterize the ATP-synthesis by oxidative phosphorylation in colorectal cancer (CRC) and premalignant colon polyps in relation to molecular biomarkers *KRAS* and *BRAF*. This prospective study included 48 patients. Resected colorectal polyps and postoperative CRC tissue with adjacent normal tissue (control) were collected. Patients with polyps and CRC were divided into three molecular groups: *KRAS* mutated, *BRAF* mutated and *KRAS/BRAF* wild-type. Mitochondrial respiration in permeabilized tissue samples was observed using high resolution respirometry. ADP-activated respiration rate ( $V_{max}$ ) and an apparent affinity of mitochondria to ADP, which is related to mitochondrial outer membrane (MOM) permeability, were determined. Clear differences were present between molecular groups. *KRAS* mutated CRC group had lower  $V_{max}$  values compared to wild-type; however, the  $V_{max}$  value was higher than in the control group, while MOM permeability did not change. This suggests that *KRAS* mutation status might be involved in acquiring oxidative phenotype. *KRAS* mutated polyps had higher  $V_{max}$  values and elevated MOM permeability as compared to the control. *BRAF* mutated CRC and polyps had reduced respiration and altered MOM permeability, indicating a glycolytic phenotype. To conclude, prognostic biomarkers *KRAS* and *BRAF* are likely related to the metabolic phenotype in CRC and polyps. Assessment of the tumor mitochondrial ATP synthesis could be a potential component of patient risk stratification.

**Keywords:** energy metabolism; colorectal cancer; colorectal polyps; mitochondria; oxidative phosphorylation; *KRAS*; *BRAF*

## 1. Introduction

Colorectal cancer (CRC) is the leading cause of premature cancer death worldwide, prompting the urgent need to develop more effective treatment strategies. CRC is a heterogeneous disease and presents distinct subtypes with different molecular and pathological features. The majority of sporadic CRC typically develops progressively from premalignant precursor lesions, known as polyps, to malignant tumors. Most colorectal polyps are harmless, but some can develop (by not fully understood mechanisms) into malignant invasive adenocarcinomas. According to modern concepts, CRC is triggered by various molecular events in several proto-oncogenes (such as the *PIK3CA*, *p53*, *KRAS*, *BRAF* and *c-MYC* genes) and tumor suppressor genes (such as the *APC*, *PTEN*, *SMAD4* genes) [1–3]. The malignant transformation of cells, including colon epithelium, is accompanied by strong alterations (reprogramming) of metabolic pathways involved in energy production and biosynthesis that promote tumor growth and metastasis [4–6]. A better understanding of the pathogenesis of CRC, the metabolic heterogeneity of emerging polyps and potential drivers is very important to develop new prognostic markers and successful agents for the prevention and treatment of this disease.

Transcriptome-based classification has been used in CRC as it can better describe the behavior of the tumors. The international CRC Subtyping Consortium classifies CRC into four consensus molecular subtypes (CMSs), each with distinct features: CMS1 (hypermethylated, microsatellite instability (MSI), *BRAF* mutation, and immune infiltration and activation); CMS2 (epithelial, WNT and MYC signaling pathway activation); CMS3 (metabolic dysregulation, *KRAS* mutations); and CMS4 (transforming growth factor beta activation, stromal invasion, TGF $\beta$  activation, and angiogenesis) [7]. Although transcriptome profiles are not associated with specific mutations, the frequency of *KRAS* mutation varies among the CRC subtypes (23% in CMS1, 28% in CMS2, 68% in CMS3, and 38% in CMS4), these data suggest mutations may drive distinct programs of metabolism gene expression [7]. Mutations in *KRAS* or *BRAF* genes appear to play an important role in the regulation of metabolic reprogramming in multiple cancers, including CRC [8–11]. In this study, two established and common prognostic biomarkers in CRC were investigated: *KRAS* and *BRAF* mutation status. Mutation in *BRAF* codon 600 of exon 15 (V600E) is associated with unfavorable prognosis [12]. Activating *KRAS* mutations in codon 12 and 13 of exon 2, which is common in CRC (30–50% of tumors), are associated with poorer survival and response to chemotherapeutics [13,14]. Our study aims to contribute to understanding how prognostic biomarkers *KRAS* and *BRAF* are correlating to cellular metabolic phenotypes in the course of CRC carcinogenesis.

The metabolism of cancer cells is specially adapted to meet their needs to survive and proliferate in both well oxygenated and hypoxic microenvironments. To date, transcriptomics and metabolomics studies have shown the coexistence of three distinct cellular metabolic phenotypes that exist in cancer cells, which are characterized by the following predominant states: glycolytic (aerobic glycolysis, so called Warburg phenotype [15]), oxidative (energy production relying mainly on oxidative phosphorylation, OXPHOS), and hybrid (both OXPHOS and glycolysis can be active simultaneously). Normal cells exhibit only glycolytic and oxidative states [16–18]. Premalignant polyps and arising adenocarcinomas are still regarded as highly glycolytic tumors of the Warburg phenotype [19–21]. Previous studies indicate that although polyps have higher inclination to aerobic glycolysis, the metastatic carcinomas maintain high rates of O<sub>2</sub> consumption (much more than adjacent normal tissues) and exhibit obvious signs of stimulated mitochondrial biogenesis [6,22–24]. In this regard, we assume that upon malignant transformation, there is a selection of specific cell clones that have stimulated mitochondrial biogenesis and, as a result, have elevated aggressiveness. Among patients with CRC, a high level of mitochondrial respiration of tumor samples have been found to be associated with reduced survival [25].

As part of cancer bioenergetic studies, analysis of OXPHOS with high-resolution respirometry can be applied to study the mechanisms of this key element in cellular bioenergetics. Investigating the dependency of adenosine diphosphate (ADP)-dependent respiration rate on ADP concentration in tissue samples can provide two fundamental characteristics for OXPHOS: a maximal ADP-activated

respiration rate ( $V_{\max}$ ), and an apparent affinity of mitochondria for exogenous ADP expressed as apparent Michaelis–Menten constant  $K_m$  ( $K_m(\text{ADP})$ ). Our previous experiments showed that the  $V_{\max}$  value for CRC cells is significantly higher than in cells in healthy colorectal control tissue showing more active ATP-synthesis by OXPHOS. This finding corresponds well with differences in the content of mitochondria in these cells (the number of mitochondria in CRC is almost two times higher than in healthy tissue) [6,25]. The changes in  $K_m(\text{ADP})$  show changes in tissue-specific intracellular complexity in terms of energy transport and regulation of mitochondrial outer membrane (MOM) permeability. For the operation of OXPHOS, the flux of respiratory substrates, ATP, ADP and Pi through MOM is regulated by the voltage-dependent anion channel (VDAC) permeability control. In the closed state, VDAC is impermeable to adenine nucleotides [26,27]. Several studies have shown that during carcinogenesis the VDAC permeability for ADP is altered [22,28–30]. The cell-specific differences in  $K_m(\text{ADP})$  are likely due to specific structural and functional organization of energy metabolism. For example, cells with a low  $K_m(\text{ADP})$  value ( $\sim 10 \mu\text{M}$ ) like glycolytic muscle, possess less structural and functional obstacles for movement ADP/ATP through MOM as compared to the oxidative muscles ( $\sim 300 \mu\text{M}$ ) [31]. Known  $K_m(\text{ADP})$  values for CRC measured for tumor tissue are about  $100 \mu\text{M}$  [22,25], implying existence of some restrictions for ADP passing VDAC. The sensitivity of the mitochondrial respiration for exogenous ADP in cell cultures is very high (low  $K_m(\text{ADP})$  values) and is similar to isolated mitochondria [25,28,32–34], which suggests the need to investigate cancer energy metabolism directly in fresh clinical material. To our knowledge, there is no data on the rate of OXPHOS and its regulation in colon polyps. Assessment of OXPHOS status of this pathology enhances our understanding of colon carcinogenesis.

Thus, the main goal of our study was to characterize the functional activity of mitochondrial OXPHOS among premalignant polyps and CRC, taking into account their *KRAS* and *BRAF* mutation status. To date, it has been shown that *KRAS* and *BRAF* mutations increase the glycolytic capacity of tumor cells and their glutaminolysis [8,35]. In our work, the function of the OXPHOS system was analyzed by means of high-resolution respirometry using freshly prepared postoperative tissue samples.

## 2. Results and Discussion

Cancer metabolism profoundly differs from normal cellular metabolism, and interrelated connections between cancer mitochondrial respiration and oncogenic driver genes like *KRAS* and *BRAF* are relatively unexplored. Somatic mutations involving the GTP-ase RAS protein family and its downstream serine/threonine-protein kinase *BRAF* lead to loss of cell cycle regulation at key checkpoints and are the main driver mutations for colorectal carcinogenesis [36]. *KRAS* mutations are detected in approximately 40% of all CRC patients, suggesting the importance of *KRAS* in tumor development [37]. The *KRAS* mutation is an early event in CRC and most *KRAS* mutations are located in codons 12 and 13. However, at least 5–10% of CRCs are believed to initiate via acquiring activating mutations in the *BRAF* oncogene [38]. Mutations of *KRAS* and *BRAF* are usually mutually exclusive. Although the existence of intertumoral heterogeneity in CRC is well established and illustrated by molecular subtyping [7], pure genome or transcriptome data are not sufficient to describe the final in situ modifications and the final outcomes of pathways or cellular processes [25]. The purpose of this study was to determine the activity of ATP production by OXPHOS in human tissues during the development of CRC from normal colon tissue to polyps and cancer, depending on the status of *BRAF* and *KRAS* mutations.

To characterize ATP-synthesis by OXPHOS during CRC carcinogenesis we used high resolution respirometry to measure the rate of maximal ADP-activated respiration ( $V_{\max}$ ). We also used apparent  $K_m$  values for exogenously added ADP ( $K_m(\text{ADP})$ ) using permeabilized postoperative tissue (CRC, colon polyps and normal colon tissue). Our previous studies showed that OXPHOS can be a significant supplier of ATP in CRC because its  $V_{\max}$  values (corresponding to the number of mitochondria) were almost two times higher than in surrounding normal tissues [6,39,40]. Among all the studied groups, the wild-type tumor showed the highest  $V_{\max}$ , while these values measured for *BRAF* or *KRAS* mutated

tumors were significantly lower (Figure 1A, Tables S1 and S2). This reveals involvement of oncogenic *KRAS* and *BRAF* in metabolic reprogramming of colon mucosa and confirms their role in shifting CRC metabolism to a more glycolytic type. Furthermore, in contrast to the results from an in vitro study conducted by Yun et al.—done with CRC cell cultures where oxygen consumption in cells with mutant *KRAS* or *BRAF* alleles was similar to that in cells with wild type alleles of these genes [41]—we saw a difference in  $V_{\max}$  values between *BRAF* mutated and *KRAS* mutated tumors (Figure 1A, Tables S1 and S2). Interestingly, the  $V_{\max}$  of *BRAF* mutated tumors was similar to that in control tissues. These results suggest a distinct role of mutated *KRAS* and *BRAF* in affecting mitochondrial biogenesis and likely tissue differentiation as well.

In colorectal polyps, the  $V_{\max}$  pattern largely followed that of the respective tumors. The respiration rates in polyps in *KRAS* mutated and wild-type molecular groups showed remarkably higher  $V_{\max}$  values than the control tissue ( $V_{\max}$  values  $2.19 \pm 0.19$  and  $1.95 \pm 0.28$  for *KRAS* mutated and wild-type group, respectively,  $p < 0.001$  and  $p = 0.004$  as compared to the control group (Tables S1 and S2). Polyps that had acquired the *BRAF* mutation showed a tendency to have lower OXPHOS rates ( $V_{\max}$   $1.41 \pm 0.27$ ) than in mutated *KRAS* and wild-type groups. Similar to the *BRAF* tumor group, polyps with mutated *BRAF* did not show a difference with the control tissue (Figure 1, Tables S1 and S2). This suggests that alterations in mitochondrial biogenesis is a very early event and already happens in the pre-malignant stage.

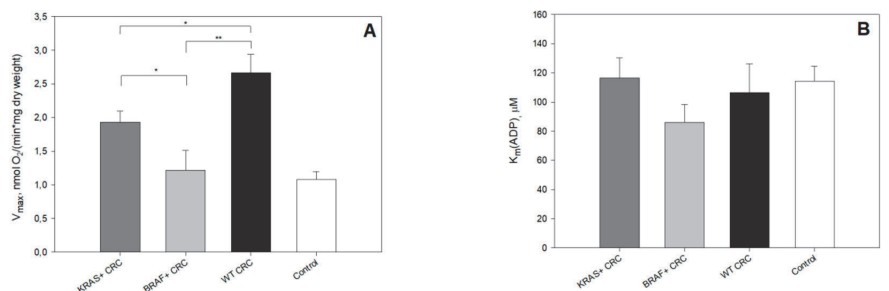


**Figure 1.** Regulation of mitochondrial respiration in *KRAS*+, *BRAF*+ and wild-type tumors and control. (A) Comparative analysis of maximal ADP-activated respiratory rate ( $V_{\max}$ ) and (B) the apparent Michaelis–Menten constant ( $K_m$ (ADP)) values for ADP. *KRAS*+: *KRAS* mutated; *BRAF*+: *BRAF* mutated; WT: wild type; CRC: colorectal cancer; Control: control tissue. \*  $p < 0.05$ ; \*\*  $p < 0.01$ .

Maintaining high functional activity of OXPHOS may be necessary because cancer cells with a very low respiration rate cannot form tumors [42]. At the same time, a certain reduction in respiration may be useful for the functioning of signaling molecules, the synthesis of anabolic precursors and other typical aspects of cancer phenotypes [43]. Thus, functional OXPHOS is important in both proliferating and non-proliferating cells, but each situation will emphasize its unique functional aspects [42]. It has been shown that the metabolic profile of cancer cells in culture can have significant variations as a consequence of the culture conditions [25]. In general, cells growing in a glucose-free medium display relatively high rates of oxygen consumption, whereas cultivation in a high-glucose medium results in hyperglycolytic cells together with declined respiratory flux [44–48]. Therefore, for the study of OXPHOS in human tumors, the use of postoperative tissue material is likely to be a more suitable approach.

To investigate possible regulatory alterations affecting OXPHOS during carcinogenesis, we estimated apparent affinity mitochondria for ADP. In all CRC and polyp groups, the corresponding  $K_m$ (ADP) value was determined and the measured values (Figure 1B, Tables S1 and S2) were found to be 4 to 8 times higher than in isolated mitochondria (15  $\mu$ M, measured by Chance and Williams [49,50]). This finding points to the existence of restrictions for the movement of ADP through mitochondrial membranes. The OXPHOS system is located in the inner mitochondrial membrane

and the ADP/ATP carrier has the function of crossing the adenine nucleotides through the membrane into the mitochondrial matrix. In our previous study, we applied metabolic control analysis on ATP-synthasome which consisted of the respiratory system, ATP-synthase, ATP/ADP carrier and Pi transporter, all in CRC tissue. In the framework of metabolic control analysis and by using specific inhibitors, the rate of effect each enzyme has in a pathway (flux control coefficients) can be determined. This analysis showed that the main control over ATP-synthesis by OXPHOS (the highest flux control coefficients) in CRC relied on respiratory complexes I and III and Pi transporter. Inhibition of the ADP/ATP carrier had no major rate-limiting effect on ATP synthesis by OXPHOS [26]. Thus, we assumed that the considerable control over ability of exogenous ADP to influence respiration was mainly dependent on ADP passage through MOM in CRC. The comparison of  $K_m(\text{ADP})$  values for *KRAS* mutated, *BRAF* mutated and wild-type tumors did not reveal any substantial differences. In all CRC groups the  $K_m(\text{ADP})$  values for tumor and control tissue were similar. Our previous study showed that we can distinguish two different populations of mitochondria in control tissue—what we believe could be a mucosal population with lower  $K_m(\text{ADP})$  ( $75 \pm 4 \mu\text{M}$ ), and the smooth muscle population with a much higher  $K_m(\text{ADP})$  value ( $362 \pm 60 \mu\text{M}$ ) [25]. This is in good agreement with our preliminary results obtained from separately measured colon smooth muscle and mucosa ( $259 \pm 35 \mu\text{M}$  and  $118 \pm 11 \mu\text{M}$ , respectively). To estimate the percentage of mitochondria with highly regulated (oxidative) and unregulated (glycolytic) MOM permeability, we applied the mathematical model used for muscle cells and adapted it to tissues studied by us. According to the model proposed earlier [51], the hypothetical percentage of low oxidative capacity mitochondria in tissue is calculated from the  $K_m(\text{ADP})$  value as an inverse asymptotic dependence. Percent of low oxidative capacity of mitochondrion demonstrates the metabolic shift to glycolytic state in all colon polyps, but not in *KRAS* mutated and wild-type tumors compared to control tissue (Table 1, Tables S1 and S2). The changes in glycolytic markers have been observed in the early premalignant colorectal mucosal field and these changes would be expected to promote increased glycolysis [19]. The  $K_m(\text{ADP})$  values in polyp molecular groups were  $55.3 \pm 7.4 \mu\text{M}$ ,  $52.5 \pm 4.7 \mu\text{M}$  and  $60.1 \pm 6.3 \mu\text{M}$  for *KRAS* mutated, *BRAF* mutated and wild-type group, respectively. These were lower than in control tissue (Tables S1 and S2), which indicates significant changes in regulation MOM permeability. Interestingly, despite the similar  $V_{\text{max}}$  values in *KRAS* mutated polyp and CRC groups, the difference in  $K_m(\text{ADP})$  between these groups was significant,  $p = 0.014$  (Tables S1, S2 and Figure S1). Our findings of the relatively low  $K_m$  value for ADP for colorectal polyps suggest an early metabolic reprogramming towards the glycolytic phenotype with functional OXPHOS.

**Table 1.** Modelled percentage of low oxidative capacity of mitochondrion in *KRAS*+, *BRAF*+ and wild-type tumors and controls.

Sample	% of Low Oxidative Capacity of Mitochondrion
<i>KRAS</i> tumors	28.1
<i>KRAS</i> polyps	65.9
<i>BRAF</i> tumors	43.0
<i>BRAF</i> polyps	68.6
Wild-type tumors	32.4
Wild-type polyps	61.7
All controls	29.0

The results of the current study confirm our previous findings, indicating that in cancer tissues, the regulation of MOM permeability to adenine nucleotides is different from that in normal cells [25,28,29]. Proteins that could regulate the VDAC permeability for adenine nucleotides in colonocytes and corresponding cancer cells are still unknown. There are two possible mechanisms proposed for this regulation. According to the first model, cancer cells due to overexpression of

mitochondrially-bound hexokinase 2 support high permeability of the VDAC to adenine nucleotides and direct the ATP formed in mitochondria to the glycolytic pathway. As a consequence, the aerobic glycolysis is facilitated and malignant metabolic reprogramming occurs [52,53]. The second model involves the inhibition of VDAC by free tubulin to limit mitochondrial metabolism in cancer cells [30,54]. The possible candidates are  $\beta$ III-tubulin and  $\gamma$ -tubulin.  $\beta$ III-tubulin acts as a marker of cancer aggressiveness, and  $\gamma$ -tubulin formed meshwork has been shown to be associated with mitochondrial membranes [29,55,56]. However, the regulation of energy metabolism through control over metabolites and energy fluxes that pass through the MOM is only one aspect of the possible role of VDAC influencing carcinogenesis. VDAC1—the major mitochondrial protein expressed in mammals and functions in metabolism,  $\text{Ca}^{2+}$  homeostasis, apoptosis and other activities—is regulated via its interaction with many proteins associated with cell survival and cellular death pathways. VDAC1 is overexpressed in many cancers and represents a promising cancer drug target (reviewed in [57,58]). The mechanistic understanding behind the changes in  $K_m(\text{ADP})$  during CRC carcinogenesis observed in the current study and connections with other functions of VDAC require further investigation.

Further, we analyzed whether the observed changes in  $V_{\text{max}}$  and  $K_m(\text{ADP})$  values are related to tumor location. CRC is more frequently observed in the distal colon (left colon, from splenic flexure to rectum) than in the proximal side (right colon, from the cecum to transverse colon [59]). In the current study, the distal and proximal tumors were presented almost equally—20 and 24 samples, respectively. Studies have shown that tumors arising from the left and right colon are distinct in their epidemiology, biology, histology and microbial diversity [59,60]. In the current study, comparing all the distal and proximal tumors showed differences in  $K_m(\text{ADP})$  but not in  $V_{\text{max}}$  values (Figure 2A). A study including 57,847 patients showed proximal patients had better outcomes than those with distal CRC in several subgroups including stage II disease, patients aged >70 years and mucinous adenocarcinoma [61]. Inside the *KRAS* mutated group, proximal and distal tumors were compared to see the potential effect of cancer location on metabolic changes. No statistically significant difference between  $V_{\text{max}}$  and  $K_m(\text{ADP})$  values comparing proximal and distal tumors in the *KRAS* mutated group (Figure 2B) was seen. The location of a tumor did not have an effect on the mitochondrial respiration in the *KRAS* mutated group and all observed alterations were related to the *KRAS* status of the tumor. All *BRAF* mutated tumors were located in the proximal side.

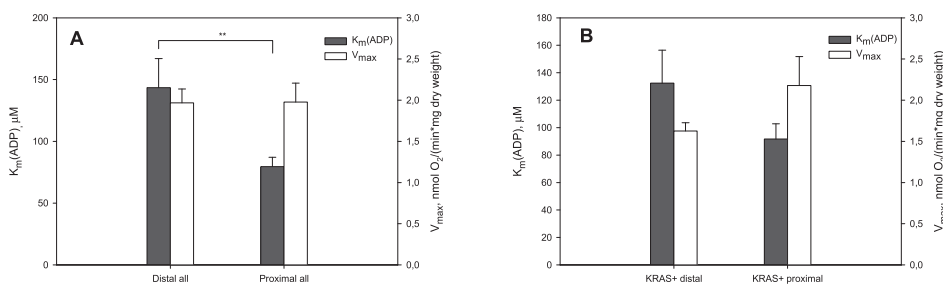


**Figure 2.** (A) In the current study, a comparison of all distal and proximal tumors showed a difference in  $K_m(\text{ADP})$  values, but not in  $V_{\text{max}}$ . (B)  $V_{\text{max}}$  and  $K_m(\text{ADP})$  values comparing proximal and distal tumors in the *KRAS* mutated group. \*\* Significant difference,  $p < 0.01$ .

All together, we found that colon polyps and colon tumors had higher rates of maximal ADP-activated respiration (a marker of mitochondrial mass) than normal colon tissue (Figure 1A, Tables S1 and S2). *BRAF* mutant tumors and polyps exhibited lower  $V_{\text{max}}$  values than *KRAS* mutated lesions and they had a relatively high percentage of mitochondria with low control over the movement adenine nucleotides through MOM (Table 1). Therefore, it is most likely that lesions with *BRAF* mutations have higher glycolytic activity, which is confirmed by some published data [62]. In contrast to the *BRAF* mutated lesions, *KRAS* mutated polyps showed signs of stimulated mitochondrial

biogenesis and upon progression could give highly metastatic malignant tumors (i.e., polyps with this energetic phenotype can be more prone to tumor formation). This was unexpected, since the transformed cells carrying the *KRAS* gene mutations were characterized by an increased glycolytic flow associated with the over-expression of glucose transporter 1 (GLUT1) and hexokinase 2 and reduced oxygen consumption due to mitochondrial dysfunction in cell cultures [41,63,64]. Our previous studies demonstrated that the oxygen consumption in vitro significantly differed compared to what occurred in vivo [25]. Moreover, the rate of oxidative ATP production of the tumor seems to be a prognostic marker for cancer survival and metastatic potential [22]. The estimation of *KRAS* or *BRAF* mutation status in colorectal pre- and neoplastic lesions could be a predictor of their response to drugs affecting the OXPHOS. Recently, a new class of anticancer drugs called “mitocans” was proposed. These affect different mitochondrial-associated activities including ATP/ADP carrier, hexokinase, electron transport/respiratory chain inhibitors, and others [65].

### 3. Materials and Methods

#### 3.1. Reagents

Unless otherwise indicated, all chemicals were purchased from Sigma-Aldrich Chemical Com. (St. Louis, MO, USA) and were used directly without further purification.

#### 3.2. Clinical Material

All tumor patients examined ( $n = 33$  with ages ranging from 38 to 91 years) had local or locally advanced disease (T2-4 N0-1, M0-1). The patients in the study had not received prior radiation or chemotherapy (Table 2). All subjects gave their informed consent for inclusion before they participated in the study. The study was conducted in accordance with the Declaration of Helsinki, and the protocol was approved by the Medical Research Ethics Committee (National Institute for Health Development, Tallinn, Estonia) of nr.1728.

**Table 2.** Clinicopathological patient characteristics of the colon cancer and polyps cohort.

Characteristics	<i>n</i>
Total patients	48
Females	19
Males	29
Age at diagnosis	
Mean	72
Median	74
Range	38–91
Stage of tumor	
I-II	15
III-IV	9
Unknown	9
Molecular subtype of tumor	
<i>KRAS</i> mutated	13
<i>BRAF</i> mutated	6
<i>KRAS</i> and <i>BRAF</i> wild-type	14
Molecular subtypes of polyps	
<i>KRAS</i> mutated	4
<i>BRAF</i> mutated	2
<i>KRAS</i> and <i>BRAF</i> wild-type	9



CRC post operational and normal tissue samples (0.1–0.5 g) were provided by the Oncology and Hematologic Clinic at the North Estonia Medical Centre (NEMC, Tallinn, Estonia). Pathology reports were obtained by the NEMC for each tissue sample. Only primary tumor samples were examined. All investigations were approved by the Medical Research Ethics Committee (National Institute for Health Development, Tallinn, Estonia) and were in accordance with Helsinki Declaration and Convention of the Council of Europe on Human Rights and Biomedicine.

Normal tissue samples were taken from the same location at sites distant from the tumor and they were evaluated for presence of malignant cells. The adjacent control tissues consisted of colonocytes and smooth muscle cells.

Patients with colorectal polyps ( $n = 15$ ) (Table 2) were consecutive patients undergoing a colonoscopy for resection of the polyps at the West Tallinn Central Hospital. After removal, tissue samples were immediately placed in medium B, which consisted of the following: 0.5 mM EGTA, 3 mM  $MgCl_2$ , 60 mM K-lactobionate, 20 mM taurine, 3 mM  $KH_2PO_4$ , 110 mM sucrose, 0.5 mM dithiothreitol, 20 mM HEPES, 5  $\mu$ M leupeptin, 2 mg/mL fatty acids free bovine serum albumin (BSA), pH 7.1. All polyps were analyzed immediately after the colonoscopy with quick cancer tests. Only part of the cancer negative polyps was subjected to further analysis for OXPHOS. Due to the limited amount of fresh tissue, *KRAS* and *BRAF* mutation analyses were performed using Formalin-Fixed Paraffin-Embedded (FFPE) samples.

### 3.3. Preparation of Skinned Tumor Fibers and Permeabilization Procedure

Immediately after the surgery, the tissue samples were placed into pre-cooled (4 °C) medium A, which consisted of 20 mM imidazole, 3 mM  $KH_2PO_4$ , 0.5 mM dithiothreitol, 20 mM taurine, 4 mM  $MgCl_2$ , 100 mM 2-morpholinoethanesulfonic acid, 2.74 mM  $K_2Ca$ -EGTA, 4.72 mM  $K_2$ -EGTA, 5  $\mu$ M leupeptin and 2 mg/mL BSA [39]. The samples were dissected into small fiber bundles (10–20 mg) and permeabilized in the same medium with 50  $\mu$ g/mL of saponin. They were mildly stirred for 30 min at 4 °C [39,66]. The obtained permeabilized (skinned) fibers were then washed three times for 5 min in pre-cooled medium B (without leupeptin). After that, samples were kept in medium B at 4 °C until use. The typical dimension of skinned fibers was about  $2 \times 2 \times 2$  mm, and one of these pieces was used in oxygraphic experiments.

### 3.4. Oxygraphic Measurements

Mitochondrial respiration of permeabilized tissue samples was measured at 25 °C in medium B supplemented with 5 mM glutamate, 2 mM malate and 10 mM succinate, with respiratory substrates using a high-resolution respirometer Oxygraph-2k (Oroboros Instruments, Innsbruck, Austria) as described previously [66,67]. The solubility of oxygen at 25 °C was taken as 240 nmol/mL [68]. All respiration rates were normalized per mg dry weight of tissue. To determine the apparent affinity of mitochondria to exogenous ADP ( $K_m(ADP)$ ), the dependence of respiration rate on exogenous ADP was measured (Figure 3A). The obtained data were plotted as rates of  $O_2$  consumption (the basal respiration rate of respiration was subtracted) versus ADP concentration and  $K_m(ADP)$  and  $V_{max}$  values were calculated from these plots by nonlinear regression using Michaelis–Menten equation [69,70] (Figure 3B). Additionally, plotting the data to double reciprocal plot gives information about presence of different mitochondrial populations with differently regulated MOM.

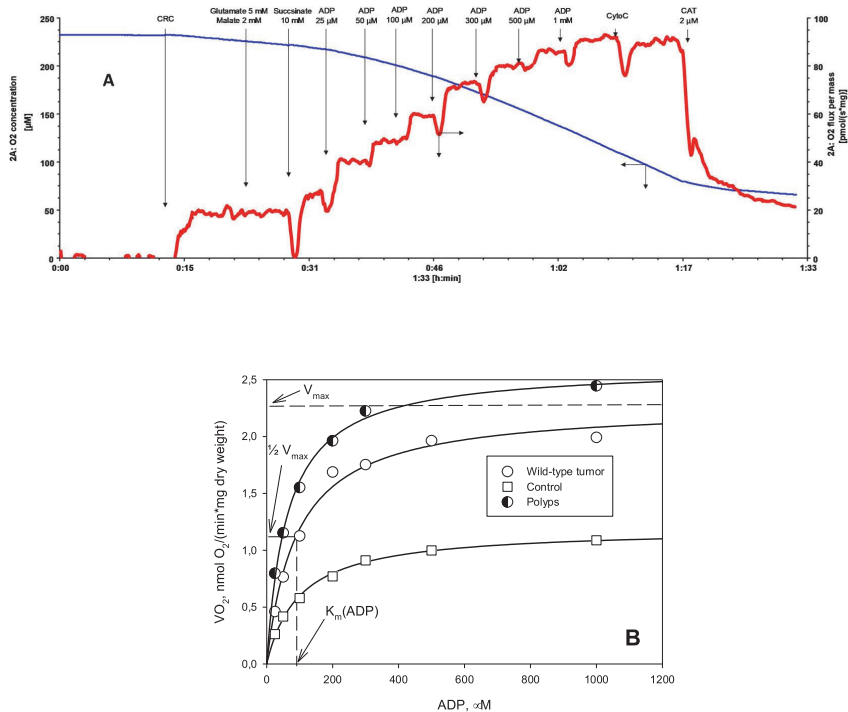


**Figure 3.** Different kinetics of regulation of mitochondrial respiration by exogenous ADP in colon tissue. **(A)** Recording of original traces of O<sub>2</sub> consumption by permeabilized colorectal cancer (CRC) tissue upon additions of increasing concentrations of ADP. CAT stands for carboxyatractylsoid; CyoC stands for cytochrome C. **(B)** The measured respiration rates were plotted vs ADP concentrations, and from this plot corresponding V<sub>max</sub> and K<sub>m</sub>(ADP) values were calculated by nonlinear regression using Michaelis–Menten equation. There was a marked difference in ADP kinetics between wild-type CRC, colon polyps and normal colon tissue (control).

### 3.5. DNA Extraction

DNA from formalin-fixed paraffin-embedded tissue (FFPE) samples was extracted using ZYMO Quick-DNA™ FFPE Kit (Zymo Research, Irvine, CA, USA) according to the manufacturer’s instructions. DNA concentrations and quality were measured using the NanoDrop 2000 spectrophotometer (Thermo Scientific, Waltham, MA, USA).

### 3.6. KRAS and BRAF Mutation Analysis

Mutations in *BRAF* codon 600 of exon 15 (V600E) and *KRAS* codon 12 and 13 of exon 2 were screened using High-Resolution Melt (HRM) analysis. Briefly, a 10 μl reaction mix contained 1x HOT FIREPol® EvaGreen® HRM Mix (Solis BioDyne, Estonia), 250 nM of sense and antisense primers (*KRAS*-antisense, 5'- AAATGACTGAATATAAACTTGTGGTAGT-3'; *KRAS*-sense, 5'- TGAATTAGCTGTATCGTCAAGGCACT-3'; *BRAF*-antisense wild-type, 5'-cgccgcgcgccAAAATAGGTGATTTTGGTCT-3'; *BRAF*-antisense mutation, 5'-TAAAAATAGGTGATTTTGGTCTAGCTACA-3'; *BRAF*-sense, 5'- CCACAAAATGGATCCAGAC AACTG 3') and 100x dilution of PCR amplification product. PCR amplification and HRM analysis were performed with Rotor-Gene 6000 (QIAGEN) and consisted of an initial 15 min denaturation step at 95 °C, followed by 45 cycles at 95 °C for 10 s, 54 °C for 10 s and 72 °C for 15 s, with a final extension at 72 °C for 3 min. The resulting PCR products were heated at 95 °C for 1 min and cooled to 40 °C to facilitate heteroduplex formation. HRM analysis was

performed from 62 °C to 92 °C with a 0.1 °C step. The results were analyzed using Rotor-Gene 6000 software and unknown samples were compared to control samples with known genotypes.

### 3.7. Data Analysis

Data in the text, tables and figures are presented as mean  $\pm$  standard error (SEM). Results were analyzed by Student's *t*-test and *p*-values < 0.05 were considered statistically significant. Apparent  $K_m$  values for ADP were measured by fitting experimental data to a non-linear regression (according to a Michaelis–Menten model equation, as shown in Figure 3).

## 4. Conclusions

While many studies have characterized the metabolic phenotype of CRC cell lines, it is important to understand the metabolic reprogramming in clinical material. Our findings confirm that early changes in mitochondria respiration occur in CRC carcinogenesis and precede the development of pre-cancerous lesions. Mitochondrial respiration differs in *KRAS*, *BRAF* mutated and wild-type tumor groups, confirming that oncogenes may affect the metabolic requirements of cancer cells. In common polyps, it still remains unclear whether the specific metabolic requirement of tumor cells is dictated by oncogenes or if they change dynamically during tumor evolution. Mitochondrial biogenesis, involved in mitochondrial respiration rate, may be developed to be the prognostic marker for cancer prognosis. As there are profound differences in mitochondrial respiration, the assessment of the metabolic profile of CRC polyps and tumors has the potential to become a component of patient risk stratification.

**Supplementary Materials:** The following are available online at <http://www.mdpi.com/2072-6694/12/4/815/s1>, Figure S1: Regulation of mitochondrial respiration in *KRAS*+, *BRAF*+ and wild-type tumors and controls, Table S1: The maximal ADP-activated respiration rates ( $V_{max}$ ) comparison by molecular groups. Respiration rates are given in nmol O<sub>2</sub>/(min×mg dry weight), Table S2:  $K_m$  comparison by molecular groups.

**Author Contributions:** Conceptualization, E.R.-K., L.T. and T.K.; data curation, I.S.; formal analysis, E.R.-K., L.T., L.R. and I.S.; funding acquisition, T.K.; investigation, E.R.-K., L.T., L.R., M.P., V.C., N.T. and K.T.; methodology, E.R.-K., L.T. and T.K.; project administration, K.S., V.V. and T.K.; resources, J.B., V.A., K.S. and V.V.; supervision, T.K.; visualization, L.R. and I.S.; writing—original draft, E.R.-K., L.T. and M.P.; writing—review & editing, I.S., V.C. and T.K. All authors have read and agreed to the published version of the manuscript.

**Funding:** This work was supported by institutional research funding IUT23-1 of the Estonian Ministry of Education and Research.

**Conflicts of Interest:** The authors declare no conflict of interest. The funders had no role in the design of the study; in the collection, analyses, or interpretation of data; in the writing of the manuscript; or in the decision to publish the results.

## Abbreviations

ADP	adenosine diphosphate
CMS	consensus molecular subtype
CRC	colorectal cancer
$K_m$	Michaelis–Menten constant
$K_m$ (ADP)	apparent affinity of mitochondria for exogenous ADP
OXPHOS	oxidative phosphorylation
MOM	outer mitochondrial membrane
VDAC	voltage-dependent anion channel
$V_{max}$	maximal-ADP-activated respiration rate

## References

1. Vogelstein, B.; Kinzler, K.W. Cancer genes and the pathways they control. *Nat. Med.* **2004**, *10*, 789–799. [[CrossRef](#)]
2. Boutin, A.T.; Liao, W.T.; Wang, M.; Hwang, S.S.; Karpinets, T.V.; Cheung, H.; Chu, G.C.; Jiang, S.; Hu, J.; Chang, K.; et al. Oncogenic *kras* drives invasion and maintains metastases in colorectal cancer. *Genes Dev.* **2017**, *31*, 370–382. [[CrossRef](#)]

3. Hao, Y.; Samuels, Y.; Li, Q.; Krokowski, D.; Guan, B.J.; Wang, C.; Jin, Z.; Dong, B.; Cao, B.; Feng, X.; et al. Oncogenic pik3ca mutations reprogram glutamine metabolism in colorectal cancer. *Nat. Commun.* **2016**, *7*, 11971. [[CrossRef](#)]
4. Hanahan, D.; Weinberg, R.A. Hallmarks of cancer: The next generation. *Cell* **2011**, *144*, 646–674. [[CrossRef](#)]
5. Schwitalla, S. Tumor cell plasticity: The challenge to catch a moving target. *J. Gastroenterol.* **2014**, *49*, 618–627. [[CrossRef](#)]
6. Kaldma, A.; Klepinin, A.; Chekulayev, V.; Mado, K.; Shevchuk, I.; Timohhina, N.; Tepp, K.; Kandashvili, M.; Varikmaa, M.; Koit, A.; et al. An in situ study of bioenergetic properties of human colorectal cancer: The regulation of mitochondrial respiration and distribution of flux control among the components of atp synthasome. *Int. J. Biochem. Cell Biol.* **2014**, *55*, 171–186. [[CrossRef](#)]
7. Guinney, J.; Dienstmann, R.; Wang, X.; de Reynies, A.; Schlicker, A.; Soneson, C.; Marisa, L.; Roepman, P.; Nyamundanda, G.; Angelino, P.; et al. The consensus molecular subtypes of colorectal cancer. *Nat. Med.* **2015**, *21*, 1350–1356. [[CrossRef](#)]
8. Hutton, J.E.; Wang, X.; Zimmerman, L.J.; Slebos, R.J.; Trenary, I.A.; Young, J.D.; Li, M.; Liebler, D.C. Oncogenic kras and braf drive metabolic reprogramming in colorectal cancer. *Mol. Cell. Proteom.* **2016**, *15*, 2924–2938. [[CrossRef](#)]
9. Corazao-Rozas, P.; Guerreschi, P.; Andre, F.; Gabert, P.E.; Lancel, S.; Dekioux, S.; Fontaine, D.; Tardivel, M.; Savina, A.; Quesnel, B.; et al. Mitochondrial oxidative phosphorylation controls cancer cell's life and death decisions upon exposure to mapk inhibitors. *Oncotarget* **2016**, *7*, 39473–39485. [[CrossRef](#)]
10. Ruocco, M.R.; Avagliano, A.; Granato, G.; Vigliar, E.; Masone, S.; Montagnani, S.; Arcucci, A. Metabolic flexibility in melanoma: A potential therapeutic target. *Semin. Cancer Biol.* **2019**, *59*, 187–207. [[CrossRef](#)]
11. Pupo, E.; Avanzato, D.; Middonti, E.; Bussolino, F.; Lanzetti, L. Kras-driven metabolic rewiring reveals novel actionable targets in cancer. *Front. Oncol.* **2019**, *9*, 848. [[CrossRef](#)] [[PubMed](#)]
12. Yokota, T.; Ura, T.; Shibata, N.; Takahari, D.; Shitara, K.; Nomura, M.; Kondo, C.; Mizota, A.; Utsunomiya, S.; Muro, K.; et al. Braf mutation is a powerful prognostic factor in advanced and recurrent colorectal cancer. *Br. J. Cancer* **2011**, *104*, 856–862. [[CrossRef](#)] [[PubMed](#)]
13. Phipps, A.I.; Buchanan, D.D.; Makar, K.W.; Win, A.K.; Baron, J.A.; Lindor, N.M.; Potter, J.D.; Newcomb, P.A. Kras-mutation status in relation to colorectal cancer survival: The joint impact of correlated tumour markers. *Br. J. Cancer* **2013**, *108*, 1757–1764. [[CrossRef](#)]
14. De Roock, W.; Claes, B.; Bernasconi, D.; De Schutter, J.; Biesmans, B.; Fountzilias, G.; Kalogeras, K.T.; Kotoula, V.; Papamichael, D.; Laurent-Puig, P.; et al. Effects of kras, braf, nras, and pik3ca mutations on the efficacy of cetuximab plus chemotherapy in chemotherapy-refractory metastatic colorectal cancer: A retrospective consortium analysis. *Lancet Oncol.* **2010**, *11*, 753–762. [[CrossRef](#)]
15. Warburg, O. On the origin of cancer cells. *Science* **1956**, *123*, 309–314. [[CrossRef](#)] [[PubMed](#)]
16. Paudel, B.B.; Quaranta, V. Metabolic plasticity meets gene regulation. *Proc. Natl. Acad. Sci. USA* **2019**, *116*, 3370–3372. [[CrossRef](#)]
17. Jia, D.; Lu, M.; Jung, K.H.; Park, J.H.; Yu, L.; Onuchic, J.N.; Kaiparettu, B.A.; Levine, H. Elucidating cancer metabolic plasticity by coupling gene regulation with metabolic pathways. *Proc. Natl. Acad. Sci. USA* **2019**, *116*, 3909–3918. [[CrossRef](#)]
18. Yu, L.; Lu, M.; Jia, D.; Ma, J.; Ben-Jacob, E.; Levine, H.; Kaiparettu, B.A.; Onuchic, J.N. Modeling the genetic regulation of cancer metabolism: Interplay between glycolysis and oxidative phosphorylation. *Cancer Res.* **2017**, *77*, 1564–1574. [[CrossRef](#)]
19. Cruz, M.D.; Ledbetter, S.; Chowdhury, S.; Tiwari, A.K.; Momi, N.; Wali, R.K.; Bliss, C.; Huang, C.; Lichtenstein, D.; Bhattacharya, S.; et al. Metabolic reprogramming of the premalignant colonic mucosa is an early event in carcinogenesis. *Oncotarget* **2017**, *8*, 20543–20557. [[CrossRef](#)]
20. Grassetto, G.; Capirci, C.; Marzola, M.C.; Rampin, L.; Chondrogiannis, S.; Musto, A.; Crepaldi, G.; Minicozzi, A.M.; Massaro, A.; Rubello, D. Colorectal cancer: Prognostic role of 18f-fdg-pet/ct. *Abdom. Imaging* **2012**, *37*, 575–579. [[CrossRef](#)]
21. Graziano, F.; Ruzzo, A.; Giacomini, E.; Ricciardi, T.; Aprile, G.; Loupakis, F.; Lorenzini, P.; Ongaro, E.; Zoratto, F.; Catalano, V.; et al. Glycolysis gene expression analysis and selective metabolic advantage in the clinical progression of colorectal cancer. *Pharm. J.* **2017**, *17*, 258–264. [[CrossRef](#)] [[PubMed](#)]

22. Chekulayev, V.; Mado, K.; Shevchuk, I.; Koit, A.; Kaldma, A.; Klepinin, A.; Timohhina, N.; Tepp, K.; Kandashvili, M.; Ounpuu, L.; et al. Metabolic remodeling in human colorectal cancer and surrounding tissues: Alterations in regulation of mitochondrial respiration and metabolic fluxes. *Biochem. Biophys. Rep.* **2015**, *4*, 111–125. [[CrossRef](#)]
23. Ou, J.; Miao, H.; Ma, Y.; Guo, F.; Deng, J.; Wei, X.; Zhou, J.; Xie, G.; Shi, H.; Xue, B.; et al. Loss of abhd5 promotes colorectal tumor development and progression by inducing aerobic glycolysis and epithelial-mesenchymal transition. *Cell Rep.* **2014**, *9*, 1798–1811. [[CrossRef](#)] [[PubMed](#)]
24. Ounpuu, L.; Truu, L.; Shevchuk, I.; Chekulayev, V.; Klepinin, A.; Koit, A.; Tepp, K.; Puurand, M.; Rebane-Klemm, E.; Kaambre, T. Comparative analysis of the bioenergetics of human adenocarcinoma caco-2 cell line and postoperative tissue samples from colorectal cancer patients. *Biochim. Biol. Cell.* **2018**, *96*, 808–817. [[CrossRef](#)] [[PubMed](#)]
25. Koit, A.; Shevchuk, I.; Ounpuu, L.; Klepinin, A.; Chekulayev, V.; Timohhina, N.; Tepp, K.; Puurand, M.; Truu, L.; Heck, K.; et al. Mitochondrial respiration in human colorectal and breast cancer clinical material is regulated differently. *Oxid. Med. Cell. Longev.* **2017**, *2017*, 1372640. [[CrossRef](#)]
26. Colombini, M. The vdc channel: Molecular basis for selectivity. *Biochim. Biophys. Acta (BBA) Mol. Cell Res.* **2016**, *1863*, 2498–2502. [[CrossRef](#)]
27. Noskov, S.Y.; Rostovtseva, T.K.; Chamberlin, A.C.; Tejjido, O.; Jiang, W.; Bezrukov, S.M. Current state of theoretical and experimental studies of the voltage-dependent anion channel (vdac). *Biochim. Biophys. Acta* **2016**, *1858*, 1778–1790. [[CrossRef](#)]
28. Klepinin, A.; Ounpuu, L.; Mado, K.; Truu, L.; Chekulayev, V.; Puurand, M.; Shevchuk, I.; Tepp, K.; Planken, A.; Kaambre, T. The complexity of mitochondrial outer membrane permeability and vdc regulation by associated proteins. *J. Bioenerg. Biomembr.* **2018**, *50*, 339–354. [[CrossRef](#)]
29. Puurand, M.; Tepp, K.; Timohhina, N.; Aid, J.; Shevchuk, I.; Chekulayev, V.; Kaambre, T. Tubulin betaii and betaiiii isoforms as the regulators of vdc channel permeability in health and disease. *Cells* **2019**, *8*, 239. [[CrossRef](#)]
30. Maldonado, E.N.; Sheldon, K.L.; DeHart, D.N.; Patnaik, J.; Manevich, Y.; Townsend, D.M.; Bezrukov, S.M.; Rostovtseva, T.K.; Lemasters, J.J. Voltage-dependent anion channels modulate mitochondrial metabolism in cancer cells: Regulation by free tubulin and erastin. *J. Biol. Chem.* **2013**, *288*, 11920–11929. [[CrossRef](#)]
31. Varikmaa, M.; Bagur, R.; Kaambre, T.; Grichine, A.; Timohhina, N.; Tepp, K.; Shevchuk, I.; Chekulayev, V.; Metsis, M.; Boucher, F.; et al. Role of mitochondria-cytoskeleton interactions in respiration regulation and mitochondrial organization in striated muscles. *Biochim. Biophys. Acta* **2014**, *1837*, 232–245. [[CrossRef](#)] [[PubMed](#)]
32. Anmann, T.; Guzun, R.; Beraud, N.; Pelloux, S.; Kuznetsov, A.V.; Kogerman, L.; Kaambre, T.; Sikk, P.; Paju, K.; Peet, N.; et al. Different kinetics of the regulation of respiration in permeabilized cardiomyocytes and in hl-1 cardiac cells. Importance of cell structure/organization for respiration regulation. *Biochim. Biophys. Acta* **2006**, *1757*, 1597–1606. [[CrossRef](#)] [[PubMed](#)]
33. Monge, C.; Beraud, N.; Tepp, K.; Pelloux, S.; Chahboun, S.; Kaambre, T.; Kadaja, L.; Roosimaa, M.; Piirsoo, A.; Tourneur, Y.; et al. Comparative analysis of the bioenergetics of adult cardiomyocytes and nonbeating hl-1 cells: Respiratory chain activities, glycolytic enzyme profiles, and metabolic fluxes. *Can. J. Physiol. Pharmacol.* **2009**, *87*, 318–326. [[CrossRef](#)] [[PubMed](#)]
34. Klepinin, A.; Chekulayev, V.; Timohhina, N.; Shevchuk, I.; Tepp, K.; Kaldma, A.; Koit, A.; Saks, V.; Kaambre, T. Comparative analysis of some aspects of mitochondrial metabolism in differentiated and undifferentiated neuroblastoma cells. *J. Bioenerg. Biomembr.* **2014**, *46*, 17–31. [[CrossRef](#)]
35. Kawada, K.; Toda, K.; Sakai, Y. Targeting metabolic reprogramming in kras-driven cancers. *Int. J. Clin. Oncol.* **2017**, *22*, 651–659. [[CrossRef](#)]
36. Oikonomou, E.; Koustas, E.; Goulielmaki, M.; Pintzas, A. Braf vs ras oncogenes: Are mutations of the same pathway equal? Differential signalling and therapeutic implications. *Oncotarget* **2014**, *5*, 11752–11777. [[CrossRef](#)]
37. Vaughn, C.P.; Zobell, S.D.; Furtado, L.V.; Baker, C.L.; Samowitz, W.S. Frequency of kras, braf, and nras mutations in colorectal cancer. *Genes Chromosomes Cancer* **2011**, *50*, 307–312. [[CrossRef](#)]
38. Lai, E.; Pretta, A.; Impera, V.; Mariani, S.; Giampieri, R.; Casula, L.; Pusceddu, V.; Coni, P.; Fanni, D.; Puzzone, M.; et al. Braf-mutant colorectal cancer, a different breed evolving. *Expert Rev. Mol. Diagn.* **2018**, *18*, 499–512. [[CrossRef](#)]

39. Kaambre, T.; Chekulayev, V.; Shevchuk, I.; Karu-Varikmaa, M.; Timohhina, N.; Tepp, K.; Bogovskaja, J.; Kutner, R.; Valvere, V.; Saks, V. Metabolic control analysis of cellular respiration in situ in intraoperational samples of human breast cancer. *J. Bioenerg. Biomembr.* **2012**, *44*, 539–558. [[CrossRef](#)]
40. Kaambre, T.; Chekulayev, V.; Shevchuk, I.; Tepp, K.; Timohhina, N.; Varikmaa, M.; Bagur, R.; Klepinin, A.; Anmann, T.; Koit, A.; et al. Metabolic control analysis of respiration in human cancer tissue. *Front. Physiol.* **2013**, *4*, 151. [[CrossRef](#)]
41. Yun, J.; Rago, C.; Cheong, I.; Pagliarini, R.; Angenendt, P.; Rajagopalan, H.; Schmidt, K.; Willson, J.K.; Markowitz, S.; Zhou, S.; et al. Glucose deprivation contributes to the development of kras pathway mutations in tumor cells. *Science* **2009**, *325*, 1555–1559. [[CrossRef](#)]
42. Hubackova, S.; Magalhaes Novais, S.; Davidova, E.; Neuzil, J.; Rohlena, J. Mitochondria-driven elimination of cancer and senescent cells. *Biol. Chem.* **2019**, *400*, 141–148. [[CrossRef](#)]
43. Lu, J.; Tan, M.; Cai, Q. The warburg effect in tumor progression: Mitochondrial oxidative metabolism as an anti-metastasis mechanism. *Cancer Lett.* **2015**, *356*, 156–164. [[CrossRef](#)]
44. Gnaiger, E.; Kemp, R.B. Anaerobic metabolism in aerobic mammalian cells: Information from the ratio of calorimetric heat flux and respirometric oxygen flux. *Biochim. Biophys. Acta* **1990**, *1016*, 328–332. [[CrossRef](#)]
45. Gstraunthaler, G.; Seppi, T.; Pfaller, W. Impact of culture conditions, culture media volumes, and glucose content on metabolic properties of renal epithelial cell cultures. Are renal cells in tissue culture hypoxic? *Cell Physiol. Biochem.* **1999**, *9*, 150–172. [[CrossRef](#)]
46. Sherr, C.J.; DePinho, R.A. Cellular senescence: Mitotic clock or culture shock? *Cell* **2000**, *102*, 407–410. [[CrossRef](#)]
47. Jose, C.; Rossignol, R. Rationale for mitochondria-targeting strategies in cancer bioenergetic therapies. *Int. J. Biochem. Cell Biol.* **2013**, *45*, 123–129. [[CrossRef](#)]
48. Swerdlow, R.H.; Lezi, E.; Aires, D.; Lu, J. Glycolysis-respiration relationships in a neuroblastoma cell line. *Biochim. Biophys. Acta* **2013**, *1830*, 2891–2898. [[CrossRef](#)]
49. Chance, B.; Williams, G.R. Respiratory enzymes in oxidative phosphorylation. Ii. Difference spectra. *J. Biol. Chem.* **1955**, *217*, 395–407.
50. Chance, B.; Williams, G.R. Respiratory enzymes in oxidative phosphorylation. Vi. The effects of adenosine diphosphate on azide-treated mitochondria. *J. Biol. Chem.* **1956**, *221*, 477–489.
51. Saks, V.A.; Veksler, V.I.; Kuznetsov, A.V.; Kay, L.; Sikk, P.; Tiivel, T.; Tranqui, L.; Olivares, J.; Winkler, K.; Wiedemann, F.; et al. Permeabilized cell and skinned fiber techniques in studies of mitochondrial function in vivo. *Mol. Cell. Biochem.* **1998**, *184*, 81–100. [[CrossRef](#)]
52. Mathupala, S.P.; Ko, Y.H.; Pedersen, P.L. Hexokinase-2 bound to mitochondria: Cancer’s stygian link to the “warburg effect” and a pivotal target for effective therapy. *Semin. Cancer Biol.* **2009**, *19*, 17–24. [[CrossRef](#)]
53. Pedersen, P.L. Warburg, me and hexokinase 2: Multiple discoveries of key molecular events underlying one of cancers’ most common phenotypes, the “warburg effect”, i.e., elevated glycolysis in the presence of oxygen. *J. Bioenerg. Biomembr.* **2007**, *39*, 211–222. [[CrossRef](#)]
54. Maldonado, E.N.; Patnaik, J.; Mullins, M.R.; Lemasters, J.J. Free tubulin modulates mitochondrial membrane potential in cancer cells. *Cancer Res.* **2010**, *70*, 10192–10201. [[CrossRef](#)]
55. Draberova, E.; Sulimenko, V.; Vinopal, S.; Sulimenko, T.; Sladkova, V.; D’Agostino, L.; Sobol, M.; Hozak, P.; Kren, L.; Katsetos, C.D.; et al. Differential expression of human gamma-tubulin isoforms during neuronal development and oxidative stress points to a gamma-tubulin-2 prosurvival function. *FASEB J. Off. Publ. Fed. Am. Soc. Exp. Biol.* **2017**, *31*, 1828–1846. [[CrossRef](#)]
56. Lindstrom, L.; Li, T.; Malycheva, D.; Kancharla, A.; Nilsson, H.; Vishnu, N.; Mulder, H.; Johansson, M.; Rossello, C.A.; Alvarado-Kristensson, M. The gtpase domain of gamma-tubulin is required for normal mitochondrial function and spatial organization. *Commun. Biol.* **2018**, *1*, 37. [[CrossRef](#)]
57. Shoshan-Barmatz, V.; Krelin, Y.; Shteinfein-Kuzmine, A.; Arif, T. Voltage-dependent anion channel 1 as an emerging drug target for novel anti-cancer therapeutics. *Front. Oncol.* **2017**, *7*, 154. [[CrossRef](#)]
58. Shoshan-Barmatz, V.; Maldonado, E.N.; Krelin, Y. Vdac1 at the crossroads of cell metabolism, apoptosis and cell stress. *Cell Stress* **2017**, *1*, 11–36. [[CrossRef](#)]
59. Missiaglia, E.; Jacobs, B.; D’Ario, G.; Di Narzo, A.F.; Soneson, C.; Budinska, E.; Popovici, V.; Vecchione, L.; Gerster, S.; Yan, P.; et al. Distal and proximal colon cancers differ in terms of molecular, pathological, and clinical features. *Ann. Oncol.* **2014**, *25*, 1995–2001. [[CrossRef](#)]

60. Drewes, J.L.; Housseau, F.; Sears, C.L. Sporadic colorectal cancer: Microbial contributors to disease prevention, development and therapy. *Br. J. Cancer* **2016**, *115*, 273–280. [[CrossRef](#)]
61. De Palma, F.D.E.; D’Argenio, V.; Pol, J.; Kroemer, G.; Maiuri, M.C.; Salvatore, F. The molecular hallmarks of the serrated pathway in colorectal cancer. *Cancers (Basel)* **2019**, *11*, 1017. [[CrossRef](#)]
62. Fang, S.; Fang, X. Advances in glucose metabolism research in colorectal cancer. *Biomed. Rep.* **2016**, *5*, 289–295. [[CrossRef](#)]
63. Iwamoto, M.; Kawada, K.; Nakamoto, Y.; Itatani, Y.; Inamoto, S.; Toda, K.; Kimura, H.; Sasazuki, T.; Shirasawa, S.; Okuyama, H.; et al. Regulation of 18f-fdg accumulation in colorectal cancer cells with mutated kras. *J. Nucl. Med.* **2014**, *55*, 2038–2044. [[CrossRef](#)]
64. Wang, P.; Song, M.; Zeng, Z.L.; Zhu, C.F.; Lu, W.H.; Yang, J.; Ma, M.Z.; Huang, A.M.; Hu, Y.; Huang, P. Identification of ndufaf1 in mediating k-ras induced mitochondrial dysfunction by a proteomic screening approach. *Oncotarget* **2015**, *6*, 3947–3962. [[CrossRef](#)]
65. Ralph, S.J.; Low, P.; Dong, L.; Lawen, A.; Neuzil, J. Mitocans: Mitochondrial targeted anti-cancer drugs as improved therapies and related patent documents. *Recent Pat. Anticancer Drug Discov.* **2006**, *1*, 327–346. [[CrossRef](#)]
66. Kuznetsov, A.V.; Veksler, V.; Gellerich, F.N.; Saks, V.; Margreiter, R.; Kunz, W.S. Analysis of mitochondrial function in situ in permeabilized muscle fibers, tissues and cells. *Nat. Protoc.* **2008**, *3*, 965–976. [[CrossRef](#)]
67. Kuznetsov, A.V.; Tiivel, T.; Sikk, P.; Kaambre, T.; Kay, L.; Daneshrad, Z.; Rossi, A.; Kadaja, L.; Peet, N.; Seppet, E.; et al. Striking differences between the kinetics of regulation of respiration by adp in slow-twitch and fast-twitch muscles in vivo. *Eur. J. Biochem.* **1996**, *241*, 909–915. [[CrossRef](#)]
68. Gnaiger, E. Oxygen solubility in experimental media. *OROBOROS Bioenerg. News* **2001**, *6*, 1–6.
69. Puurand, M.; Tepp, K.; Klepinin, A.; Klepinina, L.; Shevchuk, I.; Kaambre, T. Intracellular energy-transfer networks and high-resolution respirometry: A convenient approach for studying their function. *Int. J. Mol. Sci.* **2018**, *19*, 2933. [[CrossRef](#)]
70. Timohhina, N.; Guzun, R.; Tepp, K.; Monge, C.; Varikmaa, M.; Vija, H.; Sikk, P.; Kaambre, T.; Sackett, D.; Saks, V. Direct measurement of energy fluxes from mitochondria into cytoplasm in permeabilized cardiac cells in situ: Some evidence for mitochondrial interactosome. *J. Bioenerg. Biomembr.* **2009**, *41*, 259–275. [[CrossRef](#)]



## ***Curriculum vitae***

Name	Laura Truu
Date of birth	23.06.1991
E-mail	laura.truu@gmail.com

### **Institutions and positions**

01.09.2022–...	SYNLAB Eesti OÜ, Head of Production (1,00)
2021–2022	SYNLAB Eesti OÜ, Head of Molecular Biology Department (1,00)
2019–2021	SYNLAB Eesti OÜ, Laboratory specialist (1,00)
2016–31.08.2016	National Institute of Chemical Physics and Biophysics, Engineer (1,00)
09.09.2015–28.01.2016	Boğaziçi University, Laboratory of Genome Regulation, Junior Researcher (0,25)
2013–2015	Competence Center for Cancer Research, Junior Researcher (0,50)

### **Language skills**

Estonian	Native language
English	Advanced
Finnish	Mid-range
Russian	Beginner

### **Academic degrees**

Laura Truu, Master's Degree, 2016, (sup) Anu Planken; Andres Valkna, Molekulaar-bioenergeetiline vaatenurk kasvajaliste protsesside mõistmisel (Molecular- bioenergetic perspective in understanding oncogenic processes), Tallinn University of Technology.



## Education

2016–...	Tallinn University of Technology , Department of Gene Technology, PhD student
11.09.2015–31.01.2016	Boğaziçi University, Istanbul, Turkey. Exchange student
2013–2016	Tallinn University of Technology, M.Sc (Gene Technology), diploma cum laude
2010–2013	University of Tartu, B.Sc. (Biology)
2002–2010	Kuristiku Gymnasium of Tallinn
1998–2002	Lilleküla Gymnasium of Tallinn

## Publications

Kaup, Karl Kristjan; Toom, Lauri; Truu, Laura; Miller, Sten; Puurand, Marju; Tepp, Kersti; Käämbre Tuuli; Reile, Indrek (2021). A line-broadening free real-time <sup>31</sup>P Pure Shift NMR method for phosphometabolomic analysis. *The Analyst*, 146 (18), 5502–5507. DOI: 10.1039/d1an01198g.

Rebane-Klemm, Egle; Truu, Laura; Reinsalu, Leenu; Puurand, Marju; Shevchuk, Igor; Chekulayev, Vladimir; Timohhina, Natalja; Tepp, Kersti; Bogovskaja, Jelena; Afanasjev, Vladimir; Suurmaa, Külliki; Valvere, Vahur; Käämbre, Tuuli (2020). Mitochondrial Respiration in KRAS and BRAF Mutated Colorectal Tumors and Polyps. *Cancers*, 12 (4), ARTN 815. DOI: 10.3390/cancers12040815.

Koit, Andre; Timohhina, Natalja; Truu, Laura; Chekulayev, Vladimir; Gudlawar, Shivakumar; Shevchuk, Igor; Lepik, Katrin; Mallo, Lea; Kutner, Riina; Valvere, Vahur; Kaambre, Tuuli (2020). Metabolic and OXPHOS Activities Quantified by Temporalex vivo Analysis Display Patient-Specific Metabolic Vulnerabilities in Human Breast Cancers. *Frontiers in Oncology*, 10, ARTN 1053. DOI: 10.3389/fonc.2020.01053.

Gnaiger, E; Aasander, Frostner, E; Abumrad, NA; Acuna-Castroviejo, D; Adams, SH; Ahn, B; Ali, SS; Alves, MG; Amati, F; Amoedo, ND; Andreadou, I; Arago, Belenguer, M; Aral, C; Arandarcikaite, O; Armand, AS; Arnould, T; Avram, VF; Bailey, DM; Bajpeyi, S; Bajzikova, M ... Zvejniece, L (2019). Mitochondrial respiratory states and rates: Building blocks of mitochondrial physiology. 1–40. DOI: 10.26124/mitofit:190001.v6.

Ounpuu, Lyudmila; Truu, Laura; Shevchuk, Igor; Chekulayev, Vladimir; Klepinin, Aleksandr; Koit, Andre; Tepp, Kersti; Puurand, Marju; Rebane-Klemm, Egle; Käämbre, Tuuli (2018). Comparative analysis of the bioenergetics of human adenocarcinoma Caco-2 cell line and postoperative tissue samples from colorectal cancer patients. *Biochemistry and Cell Biology*. DOI: 10.1139/bcb-2018-0076.

Klepinin, Aleksandr; Ounpuu, Lyudmila; Mado, Kati; Truu, Laura; Chekulayev, Vladimir; Puurand, Marju; Shevchuk, Igor; Tepp, Kersti; Planken, Anu; Kaambre, Tuuli (2018). The complexity of mitochondrial outer membrane permeability and VDAC regulation by associated proteins. *Journal of Bioenergetics and Biomembranes*. DOI: 10.1007/s10863-018-9765-9.

Koit, Andre; Shevchuk, Igor; Ounpuu, Lyudmila; Klepinin, Aleksandr; Chekulayev, Vladimir; Timohhina, Natalja; Tepp, Kersti; Puurand, Marju; Truu, Laura; Heck, Karoliina; Valvere, Vahur; Guzun, Rita; Kaambre, Tuuli (2017). Mitochondrial Respiration in Human Colorectal and Breast Cancer Clinical Material Is Regulated Differently. *Oxidative Medicine and Cellular Longevity*, 2017 (1372640), 1–16. DOI: 10.1155/2017/1372640.

Tepp, Kersti; Puurand, Marju; Timohhina, Natalja; Adamson, Jesper; Klepinin, Aleksandr; Truu, Laura; Shevchuk, Igor; Chekulayev, Vladimir; Kaambre, Tuuli. (2017). Changes in the mitochondrial function and in the efficiency of energy transfer pathways during cardiomyocyte aging. *Molecular and Cellular Biochemistry*, 432 (1-2), 141–158. DOI: 10.1007/s11010-017-3005-1.

Chekulayev, Vladimir; Mado, Kati; Shevchuk, Igor; Koit, Andre; Kaldma, Andrus; Klepinin, Aleksandr; Timohhina, Natalja; Tepp, Kersti; Kandashvili, Manana; Ounpuu, Lyudmila; Heck, Karoliina; Truu, Laura; Planken, Anu; Valvere, Vahur; Kaambre, Tuuli (2015). Metabolic remodeling in human colorectal cancer and surrounding tissues: alterations in regulation of mitochondrial respiration and metabolic fluxes. *Biochemistry and Biophysics Reports*, 4, 111–125.

Kaldma, Andrus; Klepinin, Aleksandr; Chekulayev, Vladimir; Mado, Kati; Shevchuk, Igor; Timohhina, Natalja; Tepp, Kersti; Kandashvili, Manana; Varikmaa, Minna; Koit, Andre; Planken, Margus; Heck, Karoliina; Truu, Laura; Planken, Anu; Valvere, Vahur; Rebane, Egle; Kaambre, Tuuli. (2014). An in situ study of bioenergetic properties of human colorectal cancer: The regulation of mitochondrial respiration and distribution of flux control among the components of ATP synthasome. *The International Journal of Biochemistry & Cell Biology*, 55, 171–186. DOI: 10.1016/j.biocel.2014.09.004.

Tekko, Triin; Lilleväli, Kersti; Luuk, Hendrik; Sütt, Silva; Truu, Laura; Örd, Tiit; Möls, Märt; Vasar, Eero (2014). Initiation and developmental dynamics of Wfs1 expression in the context of neural differentiation and ER stress in mouse forebrain. *International Journal of Developmental Neuroscience*, 35C, 80–88. DOI: 10.1016/j.ijdevneu.2014.03.009.

## Elulookirjeldus

Nimi Laura Truu  
Sünniaeg 23.06.1991  
E-post laura.truu@gmail.com

### Keelteoskus

Eesti keel Emakeel  
Inglise keel Kõrgtase  
Soome keel Keskase  
Vene keel Algtase

### Töökohad ja ametid

01.09.2022–... SYNLAB Eesti OÜ, Tootmisjuht (1,00)  
2021–2022 SYNLAB Eesti OÜ, Vastutav laborispetsialist (1,00)  
2019–2021 SYNLAB Eesti OÜ, Laborispetsialist (1,00)  
2016–31.08.2016 National Institute of Chemical Physics and Biophysics, insener (1,00)  
09.09.2015–28.01.2016 Boğaziçi University, Laboratory of Genome Regulation, Nooremteadur (0,25)  
2013–2015 Vähiuuringute Tehnoloogia Arenduskeskus AS, Nooremteadur (0,50)

### Teaduskraadid

Laura Truu, magistrikraad, 2016, (juh) Anu Planken; Andres Valkna, Molekulaar-bioenergeetiline vaatenurk kasvajaliste protsesside mõistmisel, Tallinna Tehnikaülikool.

### Haridustee

2016–... Tallinna Tehnikaülikool, Geenitehnoloogia instituut, doktorant  
11.09.2015–31.01.2016 Boğaziçi University, Istanbul, Türgi. Vahetusüliõpilane

2013–2016	Tallinna Tehnikaülikool, M.Sc (Geenitehnoloogia), diplom cum laude
2010–2013	Tartu Ülikool, B.Sc (Bioloogia)
2002–2010	Tallinna Kuristiku Gümnaasium
1998–2002	Tallinna Lilleküla Gümnaasium

## Publikatsioonid

Kaup, Karl Kristjan; Toom, Lauri; Truu, Laura; Miller, Sten; Puurand, Marju; Tepp, Kersti; Käämbre Tuuli; Reile, Indrek (2021). A line-broadening free real-time <sup>31</sup>P Pure Shift NMR method for phosphometabolomic analysis. *The Analyst*, 146 (18), 5502–5507. DOI: 10.1039/d1an01198g.

Rebane-Klemm, Egle; Truu, Laura; Reinsalu, Leenu; Puurand, Marju; Shevchuk, Igor; Chekulayev, Vladimir; Timohhina, Natalja; Tepp, Kersti; Bogovskaja, Jelena; Afanasjev, Vladimir; Suurmaa, Külliki; Valvere, Vahur; Käämbre, Tuuli (2020). Mitochondrial Respiration in KRAS and BRAF Mutated Colorectal Tumors and Polyps. *Cancers*, 12 (4), ARTN 815. DOI: 10.3390/cancers12040815.

Koit, Andre; Timohhina, Natalja; Truu, Laura; Chekulayev, Vladimir; Gudlawar, Shivakumar; Shevchuk, Igor; Lepik, Katrin; Mallo, Lea; Kutner, Riina; Valvere, Vahur; Kaambre, Tuuli (2020). Metabolic and OXPHOS Activities Quantified by Temporalex vivo Analysis Display Patient-Specific Metabolic Vulnerabilities in Human Breast Cancers. *Frontiers in Oncology*, 10, ARTN 1053. DOI: 10.3389/fonc.2020.01053.

Gnaiger, E; Aasander, Frostner, E; Abumrad, NA; Acuna-Castroviejo, D; Adams, SH; Ahn, B; Ali, SS; Alves, MG; Amati, F; Amoedo, ND; Andreadou, I; Arago, Belenguer, M; Aral, C; Arandarcikaite, O; Armand, AS; Arnould, T; Avram, VF; Bailey, DM; Bajpeyi, S; Bajzikova, M ... Zvejniece, L (2019). Mitochondrial respiratory states and rates: Building blocks of mitochondrial physiology. 1–40. DOI: 10.26124/mitofit:190001.v6.

Ounpuu, Lyudmila; Truu, Laura; Shevchuk, Igor; Chekulayev, Vladimir; Klepinin, Aleksandr; Koit, Andre; Tepp, Kersti; Puurand, Marju; Rebane-Klemm, Egle; Käämbre, Tuuli (2018). Comparative analysis of the bioenergetics of human adenocarcinoma Caco-2 cell line and postoperative tissue samples from colorectal cancer patients. *Biochemistry and Cell Biology*. DOI: 10.1139/bcb-2018-0076.

Klepinin, Aleksandr; Ounpuu, Lyudmila; Mado, Kati; Truu, Laura; Chekulayev, Vladimir; Puurand, Marju; Shevchuk, Igor; Tepp, Kersti; Planken, Anu; Kaambre, Tuuli (2018). The complexity of mitochondrial outer membrane permeability and VDAC regulation by associated proteins. *Journal of Bioenergetics and Biomembranes*. DOI: 10.1007/s10863-018-9765-9.

Koit, Andre; Shevchuk, Igor; Ounpuu, Lyudmila; Klepinin, Aleksandr; Chekulayev, Vladimir; Timohhina, Natalja; Tepp, Kersti; Puurand, Marju; Truu, Laura; Heck, Karoliina; Valvere, Vahur; Guzun, Rita; Kaambre, Tuuli (2017). Mitochondrial Respiration in Human Colorectal and Breast Cancer Clinical Material Is Regulated Differently. *Oxidative Medicine and Cellular Longevity*, 2017 (1372640), 1–16. DOI: 10.1155/2017/1372640.

Tepp, Kersti; Puurand, Marju; Timohhina, Natalja; Adamson, Jesper; Klepinin, Aleksandr; Truu, Laura; Shevchuk, Igor; Chekulayev, Vladimir; Kaambre, Tuuli. (2017). Changes in the mitochondrial function and in the efficiency of energy transfer pathways during cardiomyocyte aging. *Molecular and Cellular Biochemistry*, 432 (1-2), 141–158. DOI: 10.1007/s11010-017-3005-1.

Chekulayev, Vladimir; Mado, Kati; Shevchuk, Igor; Koit, Andre; Kaldma, Andrus; Klepinin, Aleksandr; Timohhina, Natalja; Tepp, Kersti; Kandashvili, Manana; Ounpuu, Lyudmila; Heck, Karoliina; Truu, Laura; Planken, Anu; Valvere, Vahur; Kaambre, Tuuli (2015). Metabolic remodeling in human colorectal cancer and surrounding tissues: alterations in regulation of mitochondrial respiration and metabolic fluxes. *Biochemistry and Biophysics Reports*, 4, 111–125.

Kaldma, Andrus; Klepinin, Aleksandr; Chekulayev, Vladimir; Mado, Kati; Shevchuk, Igor; Timohhina, Natalja; Tepp, Kersti; Kandashvili, Manana; Varikmaa, Minna; Koit, Andre; Planken, Margus; Heck, Karoliina; Truu, Laura; Planken, Anu; Valvere, Vahur; Rebane, Egle; Kaambre, Tuuli. (2014). An in situ study of bioenergetic properties of human colorectal cancer: The regulation of mitochondrial respiration and distribution of flux control among the components of ATP synthasome. *The International Journal of Biochemistry & Cell Biology*, 55, 171–186. DOI: 10.1016/j.biocel.2014.09.004.

Tekko, Triin; Lilleväli, Kersti; Luuk, Hendrik; Sütt, Silva; Truu, Laura; Örd, Tiit; Möls, Märt; Vasar, Eero (2014). Initiation and developmental dynamics of *Wfs1* expression in the context of neural differentiation and ER stress in mouse forebrain. *International Journal of Developmental Neuroscience*, 35C, 80–88. DOI: 10.1016/j.ijdevneu.2014.03.009.

ISSN 2585-6901 (PDF)  
ISBN 978-9916-80-135-2 (PDF)